LOW TEMPERATURE PERFORMANCE OF ASPHALT CONCRETE UNDER DIRECT TENSION LOADING

A THESIS SUBMITTED TO
THE GRADUATE SCHOOL OF NATURAL AND APPLIED SCIENCES
OF
MIDDLE EAST TECHNICAL UNIVERSITY

BY

YALÇIN KARAKAYA

IN PARTIAL FULFILLMENT OF THE REQUIREMENTS
FOR
THE DEGREE OF MASTER OF SCIENCE
IN
CIVIL ENGINEERING

JUNE 2015

Approval of the Thesis:

LOW TEMPERATURE PERFORMANCE OF ASPHALT CONCRETE UNDER DIRECT TENSION LOADING

Submitted by **YALÇIN KARAKAYA** in partial fulfillment of the requirements for the degree of **Master of Science in Civil Engineering Department, Middle East Technical University** by,

Prof. Dr. Gülbin Dural Ünver
Dean, Graduate School of **Natural and Applied Sciences** _____

Prof. Dr. Ahmet Cevdet Yalçıner
Head of Department, **Civil Engineering** _____

Prof. Dr. Murat Güler
Supervisor, **Civil Engineering Dept., METU** _____

Examining Committee Members

Prof. Dr. İsmail Özgür Yaman
Civil Engineering Dept., METU _____

Prof. Dr. Murat Güler
Civil Engineering Dept., METU _____

Asst. Prof. Dr. Hande Işık Öztürk
Civil Engineering Dept., METU _____

Asst. Prof. Dr. Onur Pekcan
Civil Engineering Dept., METU _____

Asst. Prof. Dr. Mustafa Kürşat Çubuk
Civil Engineering Dept., Gazi University _____

Date: June 30, 2015

I hereby declare that all information in this document has been obtained and presented in accordance with academic rules and ethical conduct. I also declare that, as required by these rules and conduct, I have fully cited and referenced all material and results that are not original to this work.

Name, Last name: Yalçın Karakaya

Signature :

ABSTRACT

LOW TEMPERATURE PERFORMANCE OF ASPHALT CONCRETE UNDER DIRECT TENSION LOADING

Karakaya, Yalçın
M. S., Department of Civil Engineering
Supervisor: Prof. Dr. Murat Güler

June 2015, 114 pages

Thermal cracking is one of the major distresses in asphalt pavements and has been a serious concern especially in cold regions. There are two different mechanisms for temperature cracking in the field: Low temperature cracking associated with severe temperature drops and thermal fatigue cracking in reaction to repeated temperature cycles. In this study, in order to investigate the thermal tensile properties of asphalt concrete, Direct Tension Test (DTT) is utilized in a TSRST experimental setup. Naturally-aged asphalt concrete specimens including varying design variables of aggregate type, gradation, asphalt grade, and asphalt content is fabricated based on the Superpave method of mixture design. For each specimen the toughness and the peak stresses are calculated from the DTT test results. Then, using the statistical analysis of variance the effects of input parameters on the two output responses are investigated. Finally, the DTT results are compared with previous low temperature and thermal fatigue test results to check if any correlations exist between different methods of testing procedure.

The statistical analyses indicate that while gradation, asphalt grade and asphalt content significantly affect the peak tensile stress, for toughness aggregate type and gradation seem to be the significant factors. The results of this study have shown that DTT does not correlate with the results of low temperature cracking test, nor with thermal fatigue cracking test.

Keywords: Thermal Cracking, Asphalt Concrete, Direct Tension Test, Toughness, Peak Stress

ÖZ

ASFALT BETONUN DOĞRUDAN ÇEKME GERİLMESİ ALTINDAKİ DÜŞÜK SICAKLIK PERFORMANSI

Karakaya, Yalçın
Yüksek Lisans, İnşaat Mühendisliği Bölümü
Tez Yöneticisi: Prof. Dr. Murat Güler

Haziran 2015, 114 Sayfa

Sıcaklık çatlakları asfalt kaplamalarda görülen ana bozulmalardan birisidir ve özellikle soğuk iklimler için ciddi sorun teşkil eder. Saha içi sıcaklık çatlaklarının iki farklı mekanizması vardır: Şiddetli sıcaklık düşmelerinden kaynaklanan düşük sıcaklık çatlakları ve termal salınımlar sonucu oluşan termal yorulma çatlamaları. Bu çalışmada, asfalt betonun düşük sıcaklık çekme özelliklerinin incelenmesi amacıyla, bir TSRST deney düzeneğini içinde Doğrudan Çekme Deneyleri uygulanmıştır. Doğal yoldan yaşlanmış asfalt beton numuneleri, Superpave karışım dizayn metodu ile dizayn edilmiş olup, agrega türü, gradasyonu, asfalt sınıfı, ve asfalt miktarı dahil olmak üzere bir çok karışım dizayn değişkeni içermektedir. Her bir numune için tokluk ve maksimum gerilme değerleri, deney sonuçlarından hesaplandı. Sonra, istatistiksel varyans analizi kullanılarak girdi parametrelerinin, iki analiz çıktıları üzerindeki etkisi incelendi. Son olarak, Doğrudan Çekme Deney sonuçları, daha önceki düşük sıcaklık ve termal yorulma deney sonuçları ile kıyaslanarak aralarındaki ilişki arandı.

İstatistiksel varyans analizi sonunda, maksimum çekme dayanımı sonuçları üzerinde gradasyon, asfalt sıfı ve asfalt miktarı etkili olurken, tokluk sonuçları açısından önemli etkiye agrega türü ve gradasyon sahiptir. Bu çalışmanın sonuçları göstermiştir ki Doğrudan Çekme Deneyi ne düşük sıcaklık çatlamaları deneyleri ne de termal yorulma deneyleri ile bir bağlantı göstermemektedir.

Anahtar Kelimeler: Termal Çatlama, Asfalt Betonu, Doğrudan Çekme Deneyi, Tokluk, Maksimum Gerilme Dayanımı

To my parents

ACKNOWLEDGEMENTS

There are a number of people without whom this thesis might not have been written, and to whom I owe deepest gratitude.

Foremost, I would like to express my deep gratitude to my advisor Prof. Dr. Murat Güler for his guidance, advice, patient and wisdom throughout the research.

I take this opportunity to record my sincere thanks to Adnan Qadir, Ali Arabzadeh and Ahmet Sağlam for the devoted work they have done.

To my dear friends Pınar Karataş, Meltem Tangüler, Can Ceylan, and Ayhan Öner Yücel for their continuous support and all the fun we have had and to my friend Sertaç Günay for his vision and mission.

The last but not the least, I would like to thank my family: my parents Ayşen Karakaya and Ali Karakaya, and my sister Gonca Karakaya for supporting me throughout my life.

TABLE OF CONTENTS

LIST OF TABLES

TABLES

LIST OF FIGUERS

FIGURES

LIST OF ABBREVIATIONS

ANOVA: Analysis of Variance

α_g: Thermal coefficient after glass transition temperature

α_l: Thermal coefficient before glass transition temperature

B: Basalt Aggregate

C: Coarse Gradation

DTT: Direct Tension Test

F: Fine Gradation

FHWA: Federal Highway Administration

HMA: Hot Mix Asphalt

L: Limestone Aggregate

LCPC: Laboratire Central des Ponts et Chaussees

LVDT: Linear Variable Displacement Transducer

O-: Optimum Asphalt Content - 0.5%

O+: Optimum Asphalt Content + 0.5%

PG: Performance Grade

RTD: Resistance Temperature Detectors

S: SBS Modification

SBS: Styrene Butadiene Styrene

Superpave: Superior Performing Asphalt Pavements

TGDH: Turkish General Directorate of Highways

TSRST: Thermal Stress Restrained Specimen Tests

Z: Neat or non-modified asphalt

CHAPTER 1

INTRODUCTION

1.1 Background

In Turkey, asphalt concrete is the main surface paving material for motorways and state highways with an approximate length of 20,000 km.
It is known that necessity of annual maintenance, rehabilitation or even re-construction of asphalt concrete pavements against deteriorations cost millions of dollars for the responsible authorities. There are three major types of distress for asphalt concrete pavements: permanent deformation, fatigue cracking, and thermal cracking, being one of the most detrimental factor for pavement structure and serviceability performance. Not only the thermal cracks cause serious structural problems in pavement but also they jeopardize the safety of the roadway users.

Cracks in asphalt pavements occur for various reasons. Some cracks develop as a result of traffic loading. Others such as transverse cracks are formed from temperature fluctuations in the field. There are two different mechanisms for thermal related cracks: In severe climates conditions when the air temperature reaches to extremely low points, low temperature cracking occurs. On the other hand, in moderate climates or during spring times the air temperature does not drop too much, it fluctuates instead and leads to thermal fatigue cracking.

Asphalt concrete like all materials, tends to contract with a decrease in ambient air temperature. This contraction behavior results in a tensile stress known as thermally induced stress. If this thermally induced stress exceeds the tensile

strength of the asphalt pavement, cracks will occur at the surface of the pavement and the temperature at which cracking occurs is known as fracture temperature. The reason for the induction of thermal stress is the friction between the surface layer and the underlying layer. Additionally, in some cases the air temperature simply cannot reach the fracture temperature but instead fluctuates for a period of time and eventually causes thermal fatigue cracking.

While low temperature cracking typically occurs at temperatures below -7ºC (20ºF), the temperature for fatigue cracking is somewhat between -7ºC (20ºF) and 21ºC (70ºF). Since the asphalt mixture is a viscoelastic material above the fatigue region the thermal stresses are dissipated through the viscous behavior.

Regardless of their mechanism, the treatment for thermally induced cracks have to be applied quickly once these cracks initiated. If not done so, rainfall waters may penetrate through the cracks into the subgrade and cause serious structural failures. Also the infiltration of water into the pavement may lead to formation of ice lenses, which can produce heaving on the surface or strength loss due to thawing cycles. Pumping which is a direct consequence of water infiltration is also one of the serious consequence of thermal cracks. Rainfall water makes granular base, subbase and subgrade saturated and these saturated fines would pumped out through the cracks every time a vehicle tire moves over. Additionally, the loss of these fines create air voids around the crack region, thereby leading to loss of support beneath the pavement layer that promotes cracking. The treatments for sealing this cracks are expensive and time consuming process for the highway agencies. Moreover, even with an overlaid layer, these cracks can reflect through the new pavement, costing more money and rehabilitation time. Over the years because of their widespread occurrence and crucial impacts on pavement performance, investigating and understanding the thermal cracks remains as an important topic for the researchers.

Several techniques to simulate the thermal behavior of asphalt concrete in the laboratory have been carried out over the years, thermal stress restrained specimen test (TSRST) is one of the common methods of testing used by many researchers. It is a well-known fact that thermal cracking performance of asphalt concrete can be evaluated well by conducting TSRST. But there are a few of drawbacks of this testing procedure. For instance when it is used for thermal fatigue cracking, the overall time for the experiment is very long because of the large number of cycles to develop fatigue cracking. The sample preparation is also difficult and time-consuming for the experimenters and needs high level of skill for specimen gluing and centering to the testing platens. However, apart from its disadvantages, TSRST provides a good estimation of the field performance of asphalt concrete behavior under thermal variations. The test setup can also be used to simulate various cooling rates and even measure the glass transition temperature of mixtures without any revisions to the test setup.

Direct tension tests is a rather fast and easy way to evaluate the low temperature properties of asphalt concrete. Asphalt specimen placed into a loading compartment is subjected to tension loading under a constant rate of strain until it breaks or a peak stress is observed during testing. The displacements and stresses are recorded in order to obtain the stress versus strain diagram from which several important data about the mixture can be gathered.

Qadir (2010) have prepared and evaluated the low temperature cracking of asphalt mixtures in METU Transportation laboratory. A portion of the remaining specimen set was also tested for thermal fatigue cracking by Arabzadeh (2015). In this study, direct tension tests were conducted on laboratory samples that were also used by Qadir (2010) and Arabzadeh (2015). The main objective of this study is to test the strength of asphalt concrete specimen using TSRST apparatus and compare the results in order to prove if there is any correlation between the results of direct tension tests, thermal fatigue tests and low temperature cracking tests.

1.2 Research Objectives

The objective of this research is summarized as follows:

(1) Setup a testing procedure in order to carry out direct tension tests in Thermal Stress Restrained Specimen Testing (TSRST) condition.

(2) Identify the significant mixture variables for tensile strength of asphalt concrete using statistical design of experiments.

(3) Compare the direct tension test results with the ones from previous thermal tests, i.e., low temperature cracking (Qadir, 2010) and thermal fatigue cracking (Arabzadeh, 2015) in order to prove the correlations.

Based on the findings of this study, it is expected that the mixture properties that are significant for direct tension test will be identified. By comparing the test results it is anticipated that there is a correlation between direct tension tests, low temperature cracking tests and thermal fatigue tests.

1.3 Scope

Three main steps of this research study is as follows:

(1) Developing a testing procedure for the direct tension tests of asphalt concrete specimens.

(2) Developing an experimental model for the testing program and testing the laboratory prepared asphalt beam specimens.

(3) Analyzing the test results, identifying the significant mixture parameters and comparing the test results based on the statistical analysis of variance.

A modified version of TSRST equipment is used in order to apply direct tension loads on the asphalt concrete specimens. Although the previous studies have used TSRST to measure the thermal strength of asphalt concrete, in this study the TSRST device is utilized to apply tension loads at a constant rate of strain to determine various engineering properties of asphalt concrete specimens.

1.4 Outline of Research

In Chapter 2, a brief literature review about the thermal behavior of asphalt mixtures and previous efforts are presented. A summary of the test methods used by the previous researchers to simulate thermal cracking, along with the effective mixture properties and environmental conditions are also discussed in this chapter.

Chapter 3 explains all testing and mixture variables, test setup and the method used while conducting the direct tension tests. The specimen preparation is also described in details in this chapter.

In Chapter 4, the experimental results from the direct tension tests, along with their statistical analyses and comparison with other results are presented.

Last but not least, conclusions and recommendations for future studies are also given in Chapter 5.

CHAPTER 2

LITERATURE REVIEW

2.1 Introduction

In this chapter, the thermal fatigue phenomenon in asphalt concrete pavements is explained in detail. The factors behind the thermal fatigue cracking together with the numerous studies over the years constitute the main theme of this chapter. In additionally the testing methods for thermal cracking are presented.

2.2 Thermal cracking of asphalt concrete pavements

There are three major distresses for asphalt pavements: permanent deformation, fatigue cracking, and thermal cracking. The performance and service life of asphalt pavements mainly depend on these distresses. Permanent deformation, such as rutting, is resulted from repetition of heavy axle loads. It depends on the shear strength of the mixture which decreases at high temperatures where asphalt binder becomes soft and loses its elasticity. The deterioration is downward and lateral movement of asphalt mixtures. Fatigue cracking or also referred to as alligator cracking is the failure of the surface layer due to repeated traffic loading or aging. These cracks are developed in longitudinal direction with respect to the centerline of roadways. The thermal cracks on the other hand are evenly spaced, non-load related and transverse to the direction of the pavement.

Asphalt concrete, like all engineering materials, shrinks when the air temperature drops and expands when it increases. As the air temperature drops thermal stresses are generated in the asphalt concrete layer because of the fact that surface layer is a continuous structure and it is restrained by the friction between the underlying layers. It is known that the reduction in air temperature increases the stiffness of

asphalt mixture, which facilitates the brittle fracture of the surface course when the tensile stresses exceed the ultimate strength of the layer (Figure 2.1). These thermal cracks can result from a single drop to a critical point or from fluctuations, yielding two common modes of thermal distresses: Low temperature cracking and thermal fatigue cracking.

Thermal cracks associated with a single temperature drop is referred to as low temperature cracking. When the environmental temperature drops to extreme points, the thermally induced tensile stresses, which are generated because of the friction between the AC layer and underlying layer, exceed the strength of the asphalt concrete layer, thereby resulting in low temperature cracking in the pavement (Kliewer et al., 1996). This type of cracking is common especially in cold regions.

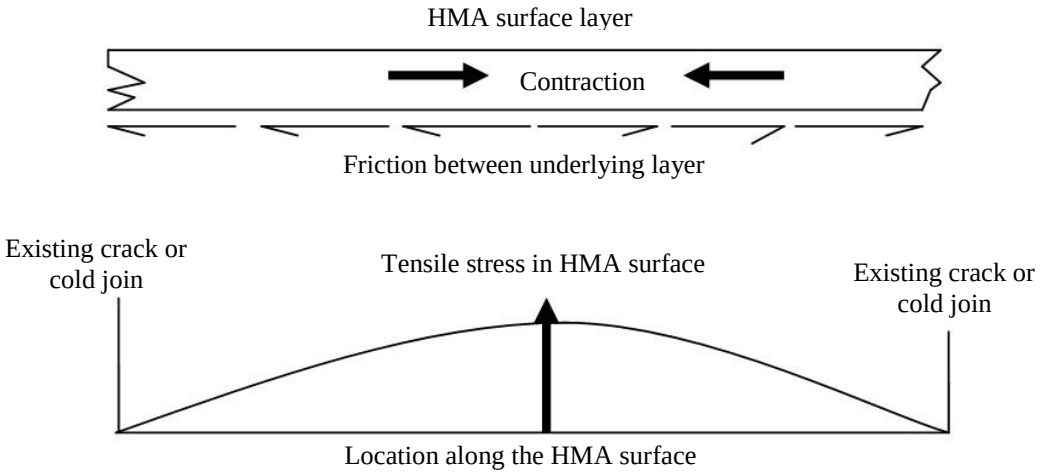

Figure 2.1 Mechanism of low temperature cracking in AC pavement (FHWA courses, 1998).

Thermal fatigue cracking, on the other hand, is associated with daily temperature changes. The temperature drops at night and rises during daytime, thus generates stress cycles. Vinson et al. (1989) stated that these temperature cycles are higher than those required for low temperature cracking, and therefore the generated stresses are far smaller than the strength of the mixture. Thus, the failure doesn't happen immediately but develops over a period of time. This type of failure is called thermal fatigue cracking and usually happens in relatively moderate climates. It should be noted that the time required for developing thermal fatigue is similar to that of load related fatigue cracking.

The temperature ranges for both modes of thermal cracking can be seen from Figure 2.2 (Carpenter, 1983). While low temperature cracking typically occurs at temperatures below -7ºC (20ºF), the thermal fatigue cracking region is between -7ºC (20ºF) and 21ºC (70ºF). It should be noted that above the fatigue region there is no thermal stress due to relaxation (Carpenter, 1983).

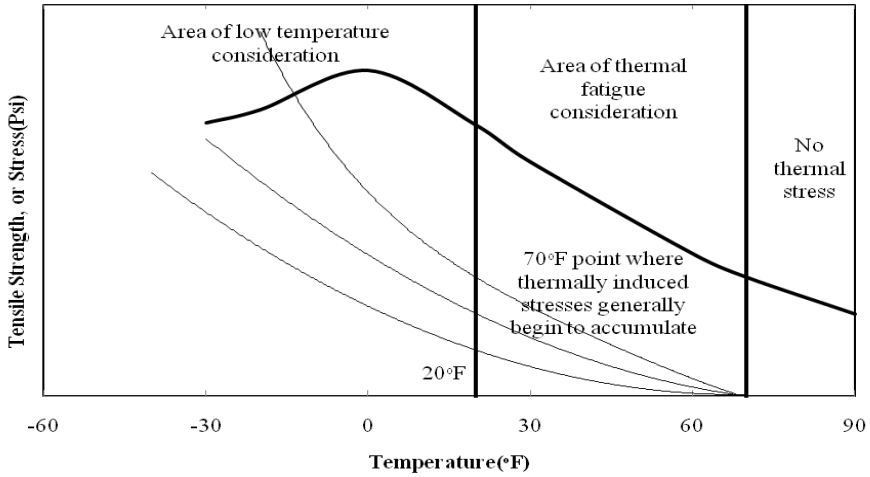

Figure 2.2 Approximate temperature ranges of thermal cracks (Carpenter, 1983).

Thermal crack initiation starts from the surface where the cooling starts first and then gradually propagates through the layer (Vinson et al., 1989). As it can be seen from the Figure 2.3 both the temperature gradient and thermally induced tension stresses reach to their peak values at the surface and decrease gradually through the thickness.

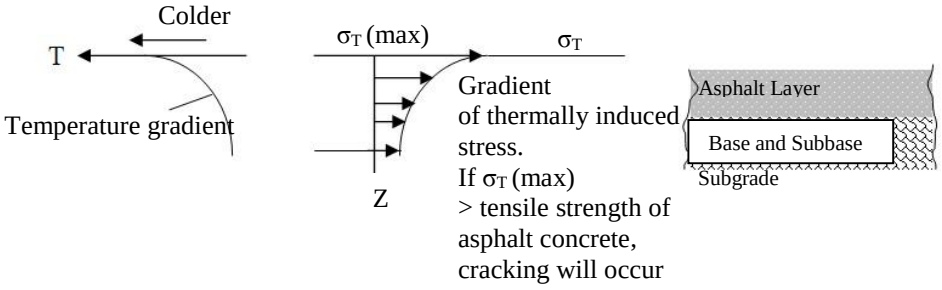

Figure 2.3 Temperature and thermal stress gradients (Haas et al., 1987).

2.3 Significance of thermal cracks in asphalt concrete pavements

It is a well-known fact that thermal cracks develop transverse to the direction of traffic, often perpendicular to the road axis (Figure 2.4). The length of the pavement is quite longer compared to its width, causing shrinkage in its length more than in its width, and therefore transverse cracks rather than being longitudinal are generated in the field conditions. But according to Vinson et al. (1989), in some cases if the spacing between these transverse cracks is less than the width of the pavement longitudinal thermal cracking may occur instead. Another unique characteristic of these cracks is that the crack spacing will be evenly distributed due to the tensile stresses generated almost equally along the pavement length at a given temperature drop (Wysong, 2004).

Regardless of their mechanism, these cracks cause serious problems for both the highway users and the pavement structure. The most important problem in these cracks is that they allow water and fine aggregates infiltration into the pavement foundation. Although the modulus of bituminous layers is weak to temperature variations, the variation of moisture content is the main factor influencing the

modulus of unbound materials. Infiltration of rainfall water may cause the base, subbase and subgrade saturated depending on the drainage conditions. When this saturated fines are subjected to the confinement effect by the wheel loads, soil particles along with water may pumped out through the cracks, also called pumping phenomenon (Figure 2.5). The air voids as a result of pumping lead to loss of support beneath the pavement layer, and thus additional cracks may develop around thermal cracks upon loading.

Figure 2.4 An example of thermal cracks in asphalt concrete pavement.

Another problem is the frost heave phenomenon. The water beneath the pavement freeze during winter, resulting in the formation of ice lens, which can produce heaving on the roadway surface due to the increase in volume (Figure 2.6). The heaving can be up to 20 cm, and bends the pavement layer, resulting in even more cracks to appeal. In spring period, melting of these ice lenses ends up softening the subgrade and thus strength loss. Thaw weakening contributes to the gradual appearance of potholes, fatigue cracks and rutting.

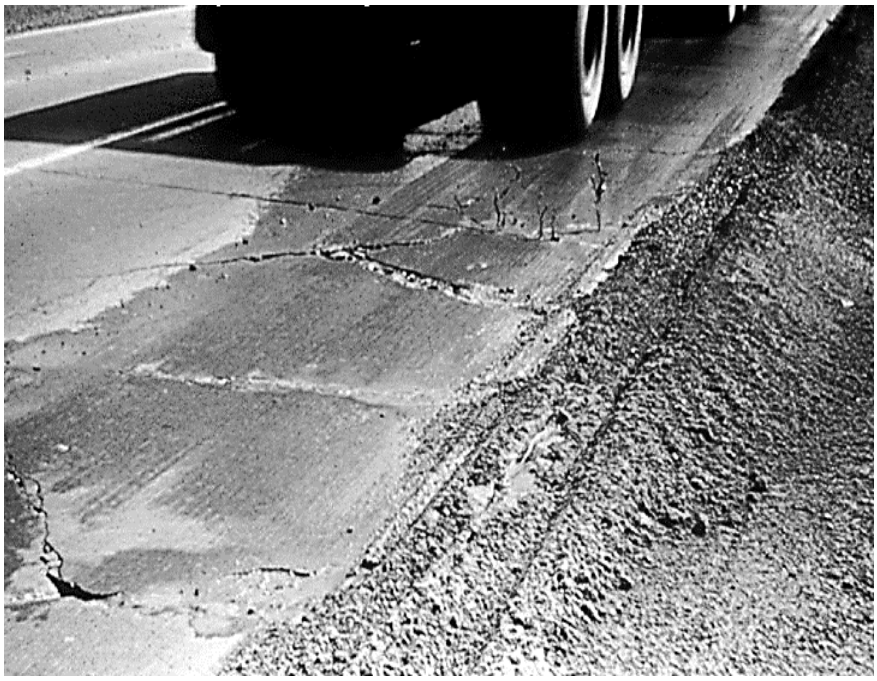

Figure 2.5 Pumping of fines through cracks.

Figure 2.6 The effect of frost heave on roads.

In addition to frost heave and thaw weakening, moisture penetration may also lead to reduction of adhesion between the asphalt binder and aggregate, namely stripping, which leads to various forms of distress including rutting and fatigue cracking.

All of these distresses lead to reduction in pavement serviceability, structural performance, and riding quality, thus increasing potential risks in driving safety and maintenance costs. The treatment of these cracks are generally expensive and requires time consuming applications. Moreover, when an overlay is used on an existing AC pavement, these cracks can easily reflect to the new layer, costing more money and time. Therefore, understanding the behavior of thermally induced cracks has been one of the important topics for researches.

2.4 Low temperature cracking

Low temperature cracking is associated with the volumetric contraction of asphalt concrete surface. When materials are exposed to a temperature drop, they tend to shrink. This is not a problem if the material is unrestrained, and it would shorten freely. But if the material is restrained by the friction between the underlying layers, as in the case of asphalt surface course, the tendency to shorten generates thermal stresses. These stresses are easily dissipated at warm temperatures in which asphalt concrete considered as viscoelastic material due to stress relaxation, but if in a low temperature range, asphalt concrete behaves as an elastic material making impossible to disperse these stresses (Vinson et al., 1989). When these thermal stresses reach the strength of the pavement mixture, low temperature cracking occurs (Figure 2.7). The temperature at which thermal stresses are equal to the tensile strength, is described as the fracture temperature. For new pavements, cracks generally occur at 30+ meters (100+ ft) spacing, as the pavement ages and/or undergoes extreme temperature drops, the crack spacing decreases to 3-6 meters (10-20 ft) (Vinson et al., 1989).

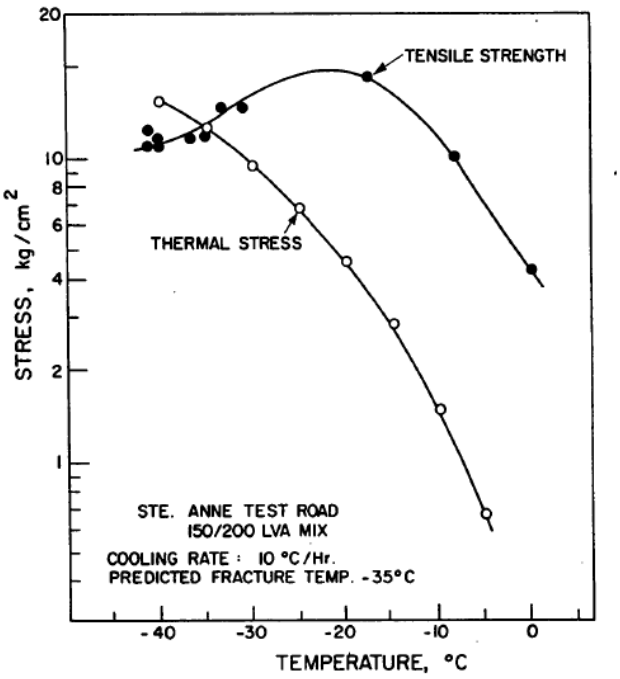

Figure 2.7 Prediction of fracture temperature for a restrained strip of asphalt concrete (Vinson & Janoo, 1989).

2.5 Thermal fatigue cracking

Although thermal cracks have been investigating since 1960's, it was not clear that the thermal fatigue might be the cause of transverse cracks until early 70's (Al-Qadi et al., 2005). In 1970's, severe transverse cracking were noticed in western Texas although the pavements were not exposed to extreme low temperatures. The main reason for the development of these cracks were associated with thermal fatigue (Carpenter et al., 1974). Later studies suggested that there might be other factors behind severe thermal cracks (Carpenter & Lytton, 1977; Anderson & Epps, 1983).

Many researchers still believe that the thermal fluctuations above the fracture temperature could not induce enough damage to cause instant cracking, as the thermal fatigue develops at very slow loading as compared to load-associated fatigue. However, in 1980's, Sugawara and Morioshi (1984) found that the fatigue life of asphalt concrete is much shorter in the thermal mode than in the traffic-associated fatigue because of the fact that thermal fatigue occurs at a relatively high stress level.

Later on, laboratory studies by Gerritsen and Jongeneel (1988) showed that traffic-load associated fatigue could also be formed in asphalt concrete by low frequency loading, similar to the cycling load induced by thermal fluctuations. Al-Qadi et al. (2005) worked on strain magnitude associated with thermal fatigue. Results of their experimental program showed that the high stress/strain levels in each cycle were critical for thermal fatigue rather than the frequency of the loading cycles.

Jackson and Vinson (1996) evaluated the possibility of the occurrence of the thermal fatigue cracking and found that the thermal fatigue distress is not a valid mode of distress but instead a special form of low temperature cracking. Despite their effort, other researchers, such as Shahin and McCullough (1972), Vinson et al. (1989), Epps (1999) and Al-Qadi et al. (2005) considered that thermal fatigue cracking due to temperature fluctuations at relatively low temperatures is a different type of thermal cracking.

Epps (1999) conducted slow frequency beam fatigue tests for measuring the mixture resistance. She used controlled strain modes to simulate thermal stress levels. The test results showed that the transverse cracking in pavements may be the result of thermal fatigue (Epps, 1999).

The other studies also pointed out the thermal fluctuations and traffic loading were the responsible mechanism for fatigue failures in asphalt concrete pavements. In traffic induced fatigue, failure occurs because of the repeated traffic loads, and starts from the bottom of the pavement and progresses to the surface, while the thermally induced fatigue cracking initiates on the surface and then progresses through depth, until it reaches to the bottom (Gerritsen & Jongeneel, 1988).

2.5.1 Factors effecting low temperature cracking

Many researchers categorized the factors influencing low temperature cracking differently. For example, in their summary report conducted as part of the Strategic Highway Research Program (SHRP), Vinson et al. (1989) have considered these factors as: Material, environmental, pavement structure, and geometry. A rather different approach was made by Haas et al. (1987), who have categorized the factors as: Asphalt mixture characteristics, design and construction of pavements, age of pavement, and weathering effect of traffic.

For thermal fatigue, on the other hand, evaluating these factors is not easy since there is no standard or established testing procedure. In the literature, the common approach given in the literature is consider these factors altogether because of definite similarities between them (Jackson, 1992; Vinson et al., 1989; Arabzadeh, 2015).

The factors influencing both thermal fatigue and low temperature cracking will be categorized under environmental, material and asphalt mixture properties in the following sections.

2.5.1.1 Environmental Factors

While low temperature cracking occurs in cold regions, where the temperature can drop to extreme levels at winter, fatigue cracking usually dominates in the desert climates where the temperature differences are fairly high between day and night.

When it comes to the thermal cracking, temperature, rate of cooling and aging are the main factors in the terms of climate.

a) Temperature

The most important factor is the ambient temperature because the pavement temperature is directly affected by the environmental conditions (Wysong, 2004). Regardless of the reason, as the air temperature drops thermal stresses are generated inside the pavement because of the tendency of shortening. When the temperature goes beneath -7^{o}C low temperature cracks occurs, if it cannot reach -7^{o}C, fluctuates above it (-7^{o}C and 21^{o}C) thermal fatigue would be considered, and if it is more than 21^{o}C there are still concerns about pavement but thermal stresses are dissipated through relaxation (Carpenter, 1983).

Evaluating thermal cracks in the laboratory is rather a challenging work. Some researchers prefer to apply these thermally induced stresses directly. In their effort to analyze thermal fatigue cracking, Jackson and Vinson (1996) applied cooling cycles directly to the specimens in a controlled environmental, i.e. used TSRTS machine. However, the experiments took quite a long time. One of the problems was that cooling rates had to be slow enough, e.g. much less than 10^{o}C/h, due to the low thermal conductivity of asphalt concrete. Others have used mechanical loads to simulate thermally induced stresses instead. For instance, Epps (1999 simulated the stresses caused by field temperature fluctuations with strain levels while keeping the test temperature constant. She have concluded that if the strain levels were selected carefully, a controlled strain mode could be used to measure mixture resistance to thermal fatigue (Epps, 1999).

b) Rate of cooling

Thermal cracks occur at fracture temperature at which the thermally induced stresses reach the strength of asphalt concrete. The magnitude of the incremented stresses are highly effected by the rate of cooling. Because the rate of cooling effects the loading time, it can influence the stress-relaxation behavior of asphalt

mixture (Nam, 2005). At faster cooling rates, asphalt mixture has less time to react and mitigate the stress, thus it may break at rather higher temperatures. Jung and Vinson (1994) have studied the cooling rate effect among the other factors on low temperature cracking and have found that slower cooling rate allows more stress relaxation, consequently leads to fracture at colder temperatures and lower stress levels.

Although the cooling rates in the field are much slower, varying from 0.5^{o}C/h to 2.7^{o}C/h, in the laboratory it ranges between 3 to 30^{o}C/h (Jung & Vinson, 1994). In most of the studies, 10^{o}C/h was selected to reduce the testing time.

Certain studies found little or no effect of cooling rates on fracture temperature and tensile strength of asphalt concrete if the cooling rates were to be equal or greater than 5^{o}C/h (Fabb, 1974; Sugawara et al., 1982). In their semianalytical model by Shen and Kirkener (2001), they proved that the effect of cooling rate on thermal stresses is important. Apeagyei et al. (2008) also worked on the effect of cooling rate on the accumulation of thermal stresses in asphalt pavements and stated that the thermal cracking performance of asphalt concrete pavements highly depend on the rate of cooling. A study for the effect of cooling rate on the fracture strength and temperature was also conducted by the Minnesota Department of Transportation in 2007 and found no significant difference between 2^{o}C/h and 10^{o}C/h (Marasteanu et al., 2007).

c) Pavement aging

Among the environmental factors effecting thermal cracking, aging of pavement, also referred to as age hardening, is also important as it causes stiffening of asphalt concrete as time elapses because of changes in its chemical composition. Between mixing and final placement, at which asphalt mixture losses volatiles, i.e., oxidation, is the first stage of aging called short-term aging (Kliewer et al., 1996). Additionally, this oxidation continues through the life of pavement, which makes long-term aging. There is a large influence of age hardening on the performance of AC pavements. It is a well-known fact that as the pavement gets older, it becomes stiffer, and behaves as brittle material, losing its ability to dissipate stress through viscous flow.

Strategic Highway Research Program (SHRP) emphasized two aging procedures for asphalt concrete pavements: The rolling thin film oven test (RTFOT) to simulate the short term oxidation of asphalt binder, and the pressure-aging vessel (PAV) to simulate oxidative hardening. While the RTFOT aging provides the hardening conditions during mixture production, in the PAV aging method, where the asphalt binder is subjected to high air pressure and temperature, in-situ aging of asphalt binder is simulated.

Jung and Vinson (1994) showed that asphalt concrete mixtures could be more susceptible to low temperature cracking with increased aging, and confirmed that the most effective factor influencing fracture temperature was the degree of aging. Kliewer et al. (1996) also investigated the effect of aging temperature and duration of aging on the thermal cracking performance of AC mixtures, and found a strong correlation between aging temperature and fracture properties.

Jackson and Vinson (1996) reported that the occurrence of thermal fatigue failure is not possible without aging. Moreover, Epps (1999) stated that both short-term and long-term aging of the asphalt concrete increases the level of thermally induced stresses upon cooling. Similar conclusions were also made by several authors for the effect of aging on thermal cracking (Seebaaly et al., 2002; Lee et al., 2009; Nam & Bahia, 2009).

2.5.1.2 Component material properties

Asphalt concrete which is a heterogeneous material contains aggregate, asphalt cement as binder and optionally modifiers. Size, shape, type and gradation of aggregates, and stiffness of asphalt binder are the main material properties that are controlled by engineers during mix design phase to reduce the detrimental effects of environment and traffic loading.

a) Aggregate

Being the major volumetric portion of asphalt mixture, mineral aggregates constitutes the backbone of asphalt mixtures. In the past, despite some efforts, it is stated by some researchers that aggregates with high absorption rate reduce the low temperature strength of asphalt concrete because there will be less asphalt cement available in the mixture for coating aggregate particles (Vinson & Janoo, 1989). However, other researchers believed that thermal cracks had nothing to do with aggregate in spite of several studies disproving the sole effect of asphalt cement properties on thermal cracking.

Jun and Vinson (1994) studied the effect of aggregate type using TSRST setup and found that aggregate type has a substantial influence on the low temperature cracking resistance of asphalt concrete. In another study conducted by Epss (1999) showed that for asphalt mixtures fabricated with gap-graded aggregate resulted in greater number of thermal cycles prior to failure as compared to those with dense-graded aggregate. . In a pooled study by the Minnesota Department of Highways (2007) investigated the fracture toughness of mixtures with two

different aggregate types and concluded that limestone aggregate type gives lowest toughness values.

Moreover, Xinjun et al. (2010) reported the effect of aggregate type on fracture resistance by their semi-circular bending fracture test. The effect of asphalt gradation combined with asphalt grade were investigated by Zhaohui et al. (2014), and their findings proved a correlation between aggregate gradation and the low temperature performance of asphalt mixtures.

The effect of aggregate gradation on tensile strength of asphalt mixture was also studied by Huang et al. (2003). They conducted a series of direct tension tests for the tensile strength of asphalt concrete at low temperatures, and found that mixtures with the dense-graded aggregates had higher tensile strength (Huang et al., 2003).

b) Asphalt binder

Although the role of aggregate was investigated by several researchers, the importance of selecting a proper asphalt binder for the thermal behavior of asphalt mixtures has always been considered by many researchers. The behavior of asphalt binder depend on its stiffness, thermal properties and modification, which are discussed in the following sections.

1- Asphalt cement stiffness

There is a general acceptance that the single most important factor affecting the degree of low temperature cracking in an asphalt concrete is the temperature-stiffness relationship of asphalt cement (Vinson et al., 1989). Stiffness (S) is the rigidity of an object, which determines the degree of resistance to deformation under an induced force and it can be represented as the stress (σ) divided by the strain (ε) as a function of time (t) and temperature (T) (Equation 2.1; Van der Poel, 1954).

$$|S(t,T)| = \frac{\sigma}{\varepsilon} \quad (2.1)$$

Under fast loading or at low temperatures it is completely independent of time, which means it behaves like an elastic solid, i.e., approaches to the modulus of elasticity E, on the other hand, under slow loading or at high temperatures, asphalt cement acts like a viscous liquid (Wysong, 2004). Furthermore, on an average loading speed the behavior of asphalt concrete contains both elastic behavior, in which it deforms under loading and returns to its initial state on removal of loads, and viscous behavior, in which it deforms permanently under loading.

All of these time dependencies classify asphalt cement as a visco-elastic material. Figure 2.8 illustrates the relationship between asphalt stiffness and time. The stiffness of asphalt concrete mainly depends on the stiffness of asphalt cement, and thus the binders with low stiffness perform better against low temperature cracking (Robert et al., 1996).

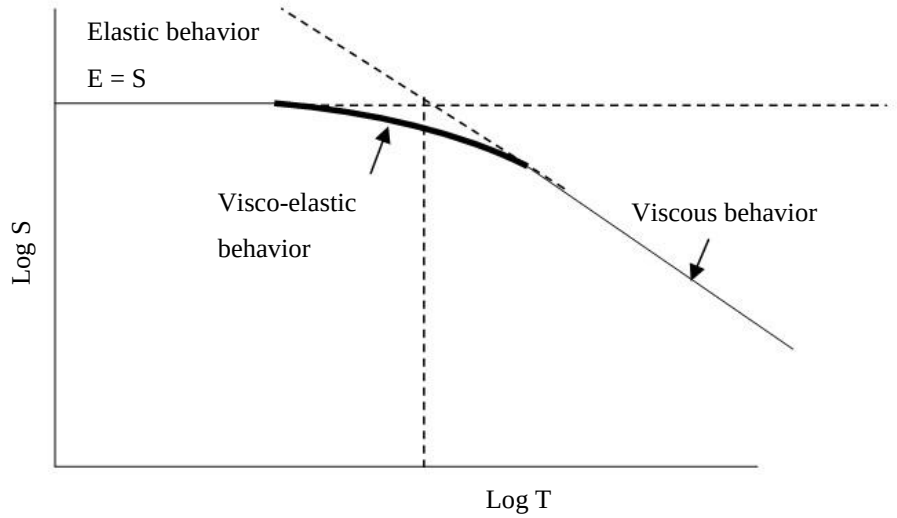

Figure 2.8 Stiffness behavior of asphalt binder (Robert et al., 1996).

2- Asphalt cement thermal properties

One of the important factors affecting the thermal behavior of asphalt concrete is the thermal properties of asphalt cement. Asphalt cement behavior, in a sufficient range of temperature, has three different stages: liquid, rubbery and glassy (Breen & Stephens, 1967). As it is illustrated in Figure 2.9, the temperature at which asphalt concrete goes from visco-elastic state to elastic state or vice versa called the glass transition temperature T_g. At the rubbery state, large amount of delayed elasticity and drastic changes in the stiffness occur as the temperature or loading time is altered (Wysong, 2004).

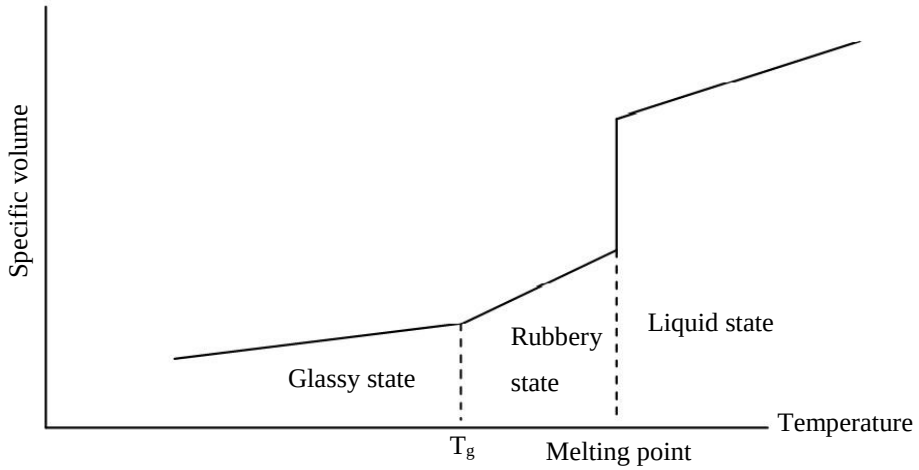

Figure 2.9 Behavior of asphalt cement according to temperature (Breen & Stephens, 1967).

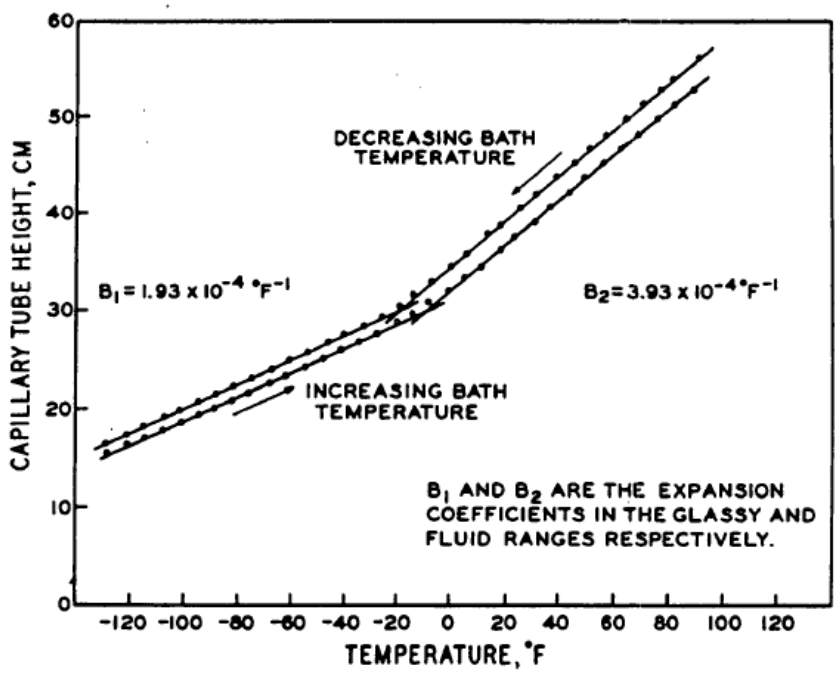

Figure 2.10 Typical expansion of asphalt concrete with temperature change (Schmidt & Santucci, 1996).

The glass transition temperature is generally determined by measuring the changes in volume, which are induced by the change in temperature. A similar study made by Schmidt and Santucci (1966) resulted in having T_g values from -36 to -15^{o}C with an average of -26^{o}C (Figure 2.10). In their study, two different slopes in the volume change corresponding to temperature change indicated two different thermal coefficients, which were separated by the glass transition temperature.

3- Asphalt cement modification

Over the years asphalt cement modifiers have been increasingly popular to achieve some specific purposes. Softening binders at low temperatures by additives for instance improves the relaxation properties and strain tolerances in order to avoid thermal cracking (Roberts et al., 1996).

There are several ways of modifying the asphalt binder such as crumb rubber, mineral filler and polymers. Polymers are one of the most common additives used

for asphalt modification, and categorized into two types: elastomers and plastomers. While elastomers are being used for flexibility and elastic recovery, plastomers provide higher strength under heavy loads.

The effect of modification on thermal cracks have been studied by many researchers. Different types of polymer-modified asphalt were studied with TSRST procedure with regard to low temperature cracking by Isacsson and Zeng (1996). Their findings indicated an influence between polymer type and low temperature properties of asphalt mixtures. Epps (1999) have examined the mixture resistance to thermal fatigue with and without crumb-rubber modification (CRM), and her findings resulted in an improved mixture resistance to thermal fatigue with CRM modification. In addition to thermo-volumetric properties, the failure properties of asphalt with modifiers in a wide temperature range were investigated by Nam and Bahia (2009), and they found significant effects of modification on thermal cracking temperatures. Another study regarding the effect of EVA polymer modification on thermal fatigue was performed by Glaoui et al. (2011). According to their results, polymer modification increased the rigidity and the elasticity, by which the behavior was improved in terms of permanent deformation resistance. Apart from these studies, Qadir (2010) found no significant influence between SBS modification and low temperature cracking of asphalt concrete. Similarly, Arabzadeh (2015) did not see any evidence of the effect of SBS modification on measured thermal coefficient nor on the thermal fatigue behavior. It is worth to mention that the mixture design variables of Qadir (2010) and Arabzadeh (2015) were the same as for this study.

2.5.1.3 Asphalt mixture properties

Asphalt mixture, while heterogeneous material, consists mainly of three components: aggregate, asphalt cement and air voids as illustrated in Figure 2.11. Despite being asphalt cement's itself as the most important factor in thermal

cracking, the mixture properties are also important for the thermal behavior of asphalt concrete. In following chapters, the importance of asphalt mixture properties on thermal cracking is discussed.

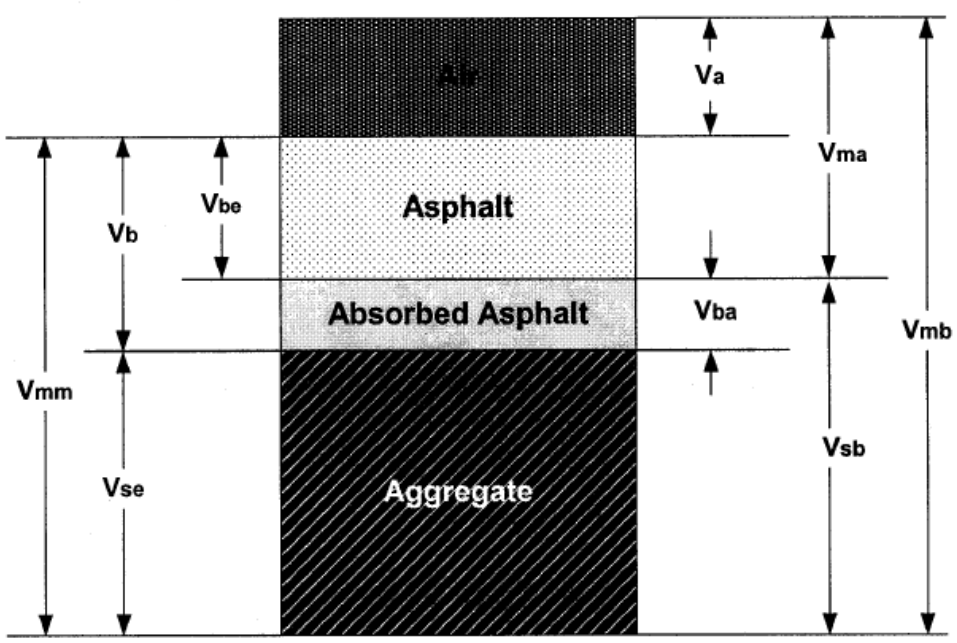

where,

V_{mb}	=	Total volume of asphalt mixture (including air)
V_{mm}	=	Voidless volume of asphalt mixture (no air)
V_b	=	Volume of asphalt binder
V_{sb}	=	Volume of effective aggregate (by bulk S.G.)
V_{be}	=	Volume of effective asphalt binder
V_{ba}	=	Volume of absorbed asphalt binder
V_{ma}	=	Volume of void in mineral aggregate
V_{se}	=	Volume of effective aggregate
V_a	=	Volume of air voids

Figure 2.11 Schematic of asphalt mixture volumetric components (Nam, 2005).

a) Stiffness of asphalt mixture

When considering the resistance of a pavement against load related or temperature related deteriorations, stiffness of the asphalt mixture has a great impact on service performance of the pavement. It is a well-known fact that mixtures with high stiffness values can withstand against low temperature cracking longer than

mixtures with low stiffness. Pellinen and Xiao (2006) stated that mixtures having shear stiffness |G*|, measured by Simple Shear Tester (SST) at 40^{o}C with 10 Hz frequency, higher than 250 MPa are adequate to stay functional long enough, which has been considered as a rule of thumb over the years.

In the literature there are several ways to measure mixture resistance in terms of both test equipment and methods. One method is to use the nomograph shown in Figure 2.12 developed by Bonnaure et al. (1997). The nomograph takes three factors as the stiffness modulus of bitumen, the percent volume of bitumen and the percent volume of aggregate and returns the stiffness of the mixture by extrapolation.

Apart from theoretical methods, much research has been conducted to determine the asphalt mixture stiffness empirically either from field cores or laboratory prepared specimens. Indirect tensile creep test, dynamic modulus test, shear dynamic modulus test are among the test methods used to measure mixture stiffness.

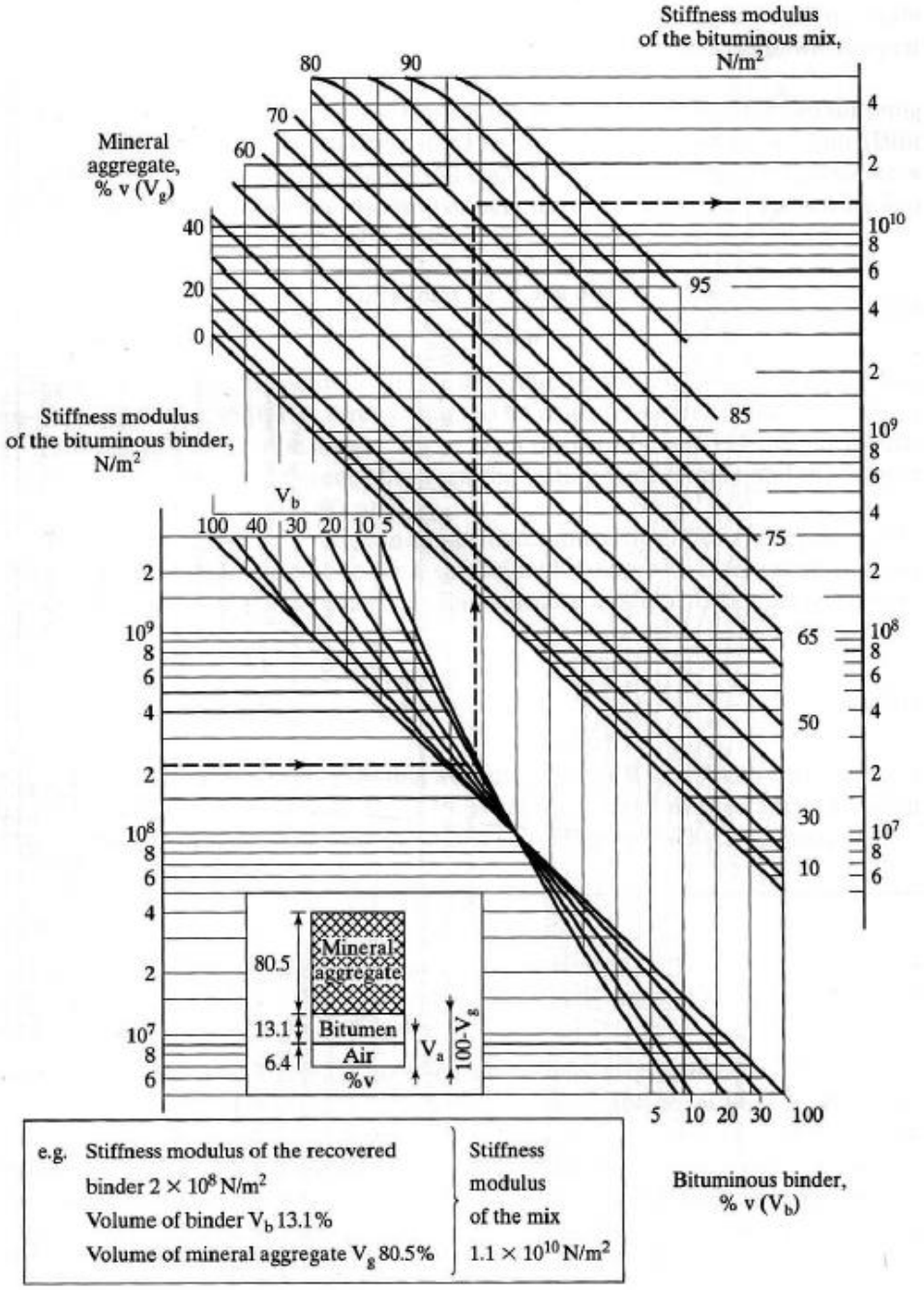

Figure 2.12 Nomograph for stiffness modulus of asphalt mixtures (Huang, 2004).

b) Thermal properties of asphalt mixture

The glass transition temperature and the coefficient of contraction are the two properties related with the volume change of asphalt mixture by temperature. In general, materials contract and expand under temperature fluctuations with regard to the thermal coefficient of expansion-contraction. However, in pavement engineering due to the fact that contracting is the main concern, the coefficient of contraction becomes prominent. The average value of the volumetric thermal coefficient of contraction (β) defined over a temperature decrease (ΔT) is expressed by Vinson et al. (1989):

$$\beta=\frac{\Delta V}{\Delta T V_o} \tag{2.2}$$

where

β = volumetric coefficient of thermal contraction

V_o = volume at some reference temperature

ΔV = chance in volume because of temperature change ΔT from reference temperature

Similarly, the relative decrease in length of a material with decreasing temperature expressed by the linear thermal coefficient of contraction:

$$\alpha = \frac{\Delta L}{\Delta T L_o} \tag{2.3}$$

where

α = linear thermal coefficient of contraction

L_0 = length at some reference temperature

ΔL = change in length because of temperature change ΔT from the reference temperature

Materials with the same thermal contraction in every direction described as isotropic and the linear thermal coefficient of contraction is equal to:

$$\alpha = \beta/3 \tag{2.4}$$

The glassy and the fluid coefficients are the two coefficients of thermal contraction of asphalt cement that are separated by the glass transition temperature (T_g). At temperatures below the T_g, asphalt exhibits glassy coefficient of contraction. At temperatures above the T_g, asphalt exhibits fluid coefficient of contraction. For simplicity, some researchers prefer to avoid glass transition temperature while calculating the linear coefficient of contraction and use assumptions as suggested by Jonas et al. (1968):

$$B_{mix} = \frac{WMA \times B_{AC} + V_{AGG} \times B_{AGG}}{3 \times V_{TOTAL}} \tag{2.5}$$

where:

B_{mix} = linear coefficient of thermal contraction of asphalt mixture (1/^{o}C),

B_{AC} = volumetric coefficient of thermal contraction of asphalt binder in the solid state (1/^{o}C). Average value of 3.45 x 10^{-4} 1/^{o}C is used.

B_{AGG} = volumetric coefficient of thermal contraction of aggregate (1/^{o}C).

VMA = percent volume of voids in mineral aggregate (air voids + volume of effective asphalt).

V_{AGG} = percent of volume of aggregate in the mixture.

V_{TOTAL} = the total volume = 100 percent.

Apart from their effort, Bahia et al. (1993) suggested Equation 2.6 for calculating the thermal coefficient before and after the glass transition temperature by fitting a five-parameter curve to the data of volume chance versus temperature change:

$$v = C_v + \alpha_g(T - T_g) + R(\alpha_l - \alpha_g)\ln\left[1 + \exp\left(\frac{T - T_g}{R}\right)\right] \quad (2.6)$$

where:

v = specific volume at temperature T,

C_v = volume at a given temperature,

T_g = glass transition temperature,

R = constant defining the curvature,

α_l = thermal coefficient for $T > T_g$, and

α_g = thermal coefficient for $T < T_g$.

c) Air void content and asphalt content

Air void content is a physical property that affects the performance of asphalt pavements and plays an important role in low temperature cracking. (Nam, 2005). Jung and Vinson (1994) reported that specimens with low air voids had greater fracture strengths. Xinjun et al. (2010) studied the influence of air voids content on low temperature cracking, and showed that apart from aggregate type, fracture resistance is highly affected by the specimens' air void content.

In addition to air voids, asphalt content in a mixture also plays an important role in thermal resistance of asphalt concrete. Xinjun et al. (2010) have found that asphalt content is one of the significant factors for fracture energy, but not so for fracture toughness. Arabzadeh (2015) found that both thermal coefficient and thermal fatigue resistance of asphalt mixtures are affected by asphalt content. Similar to his work, Qadir (2010) studied several effects on low temperature cracking and found a strong influence of the asphalt content on thermal strength of asphalt concrete. Based upon their study, it can be said that the performance of mixtures with the optimum asphalt content can reach to its peak strength values.

2.6 Test methods and systems for evaluating thermal cracks

Various tests have been used by researchers to understand the behavior of asphalt mixtures under temperature changes. In the next chapters, the methods of testing mixtures against both low temperature and thermal fatigue cracking are explained.

2.6.1 Thermal stress restrained specimen test (TSRST)

Although different models in previous studies contributed to the development of the TSRST, it was first introduced first by the Strategic Highway Research Program (SHRP) to simulate low temperature cracking of asphalt concrete. In the current test procedures, rectangular or cylindrical AC specimens are prepared and mounted into a temperature controlled chamber by resistance temperature detectors (RTDs) and then deformations are measured with linear variable displacement transducers (LVDTs).

While it is used for testing low temperature behavior of asphalt concrete, TSRST setup can provide satisfactory results for low temperature cracking and thermal fatigue test. For the thermal fatigue tests, simulating field temperature variations in the test setup is quite time consuming. Another disadvantage of TSRST is long time required for preparing test samples. Rectangular or cylindrical specimens can be used in the laboratory, however, this requires a slab compactor and diamond saw machine. Also aligning these specimens into the machine is very critical in order to prevent eccentricity between the test sample and the platens. Apart from its disadvantages, TSRST provides, however, a good estimation of low temperature performance of asphalt concrete. Using this setup, it is also possible to achieve faster cooling rates using liquid nitrogen, which can significantly shorten the testing time. Jung and Vinson (1994) recommended TSRST to be used in evaluating the low temperature cracking of asphalt concrete. Sebaaly et al. (2002) also stated that the TSRST provides the best conditions for evaluating the low temperature properties of HMA mixtures.

2.6.2 Indirect tensile test

The indirect tensile test (IDT) was first introduced in 1950's to measure the tensile strength of Portland cement concrete, and then improved by the Strategic Highway Research Program (SHRP) for low temperature cracking of asphalt concrete samples. It is a well-known fact that the critical cracking temperature at low temperatures can be analyzed from the indirect tensile strength and creep compliance properties of asphalt concrete. Although both the tensile strength and the creep are measured from cylindrical specimens with 50 mm thickness, the creep compliance is determined from measuring the time dependent deformation, which results from a constant compressive load across the vertical diameter. Samples for IDT can be prepared easily in the laboratory with gyratory compactor they can be obtained from the field cores. The modulus of test samples are measured by tension loading and the test results are used to rate mixture performance for low temperature cracking and fatigue performance.

2.6.3 Direct tension test

Direct tension test (DTT) which evaluates the low temperature tensile properties of asphalt concrete, was developed by Haas (1973) in an effort to overcome some problems of the indirect tensile test. After applying a constant rate of extension with a uniaxial tensile load to rectangular AC beams, he concluded that DTT test simulates the thermal distress of asphalt concrete pavements better. In their report SHRP-A-306 Vinson et al. (1989) evaluated several test systems and methods for thermal fatigue cracking and suggested four different method of testing, one of which was the direct tension-constant rate of extension test.

In the DTT, an asphalt specimen is placed into the loading compartment which is mounted to the gripping system by its ends. While one end is being restrained, a uniform displacement rate is applied to the other moving end in a temperature controlled chamber. While LVDTs are used for measuring the elongation of the specimen as it is pulled by the uniaxial load, the loads itself are also measured by a load cell. Elongations and stresses are recorded until the breakage occurs by a data acquisition system. The tensile strength, stiffness or limiting strain of an asphalt mixture then can be measured from the DTT results. This testing procedure is simples and completed short time durations. However, sample preparation task is time consuming as in the TSRTST test and requires careful specimen alignment during sample preparation.

From a typical stress versus strain diagram obtained from DTT (Figure 2.13; Haas, 1973) several important data about the pavement can be gathered including strength, deformation and energy properties. Toughness which is the area under the stress-strain curve, represents the failure energy of a material. High toughness levels are desirable for specimens indicating a better performance of asphalt concrete under thermal variations in the field. Elastic modulus commonly referred to as Young's modulus is the slope of the stress-strain plot within the elastic region, and indicates material's stiffness and resistance to elongation during service conditions. When material exhibits high strain values, from the Young's

modulus become less accurate. Secant modulus which is the stress-strain ratio at a specific designated extension is used where the stress-strain curve deviates from linearity (Ho & Zanzotto, 2005).

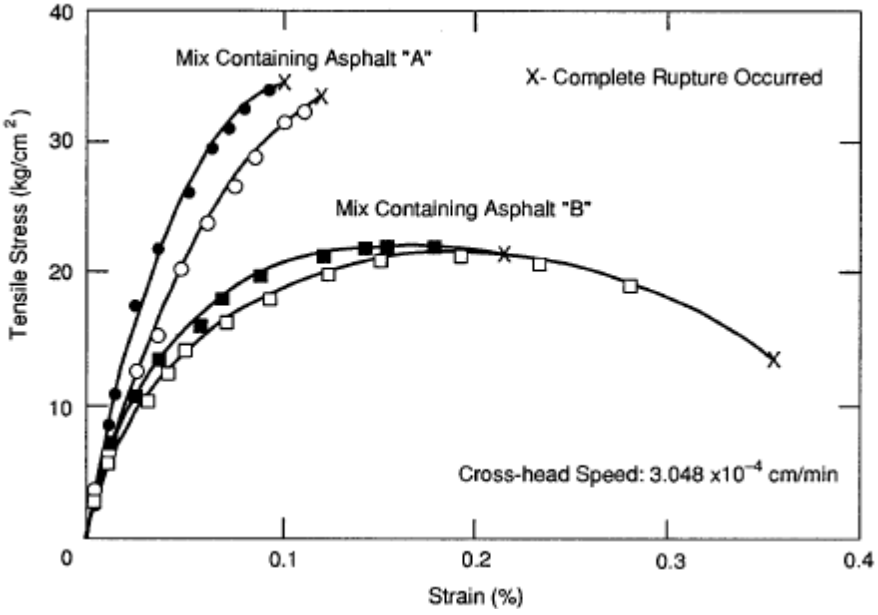

Figure 2.13 Stress-strain curves at -18ºC from constant rate extension test (Haas, 1973).

The controlling parameters of DTT are the rate of extension and temperature. Roberts et al. (1996) stated that typical temperature range for measuring the low temperature ultimate tensile strain of asphalt binders in DTT is 0º to -46ºC. Since failure occurs in a brittle manner at low temperatures, DTT is not valid at high temperatures at which asphalt exhibits ductile failure (AASHTO, 1996). Besides, the deformation rate must be carefully selected during DTT testing. While low temperature shrinkage fracture occurs under slow buildup of tensile stresses, inadequate slow rates lead to stress relaxation of mixture. Haas (1973) suggested a range from 2.4 to 12 cm/s of extension to be used in DTT. Table 2.1 shows various temperature and deformation rates reported in the literature.

Table 2.1 Temperature ranges and strain rates used in DTT by different authors.

Researchers	Temperature range (ºC)	Strain rate
Jackson, 1992	-17.8 and -34.4	8.5e-6 cm/s
Jung & Vinson, 1996	-30 to +5	1.0 mm/min
Huang et al., 2003	-12 and 0	N.A.
Gonzalez et al., 2006	+8.3 and +20	1 to 0.0057 mm/min
Mun & Lee, 2010	-10 and +5	0,001 ε/s
Wang et al., 2011	-35 to -10	N.A.
Lee et al., 2011	5	2.1e-5 to 5.5e-5 ε/s
Xie et al., 2011	15 and 25	0.1 to 18 mm/min
Lee et al., 2012	5	N.A.
Forough et al., 2013	-7 to +21	1.27 mm/min
Underwood & Kim, 2013	10	0.6902 ε/s
Yoo & Al-Qadi, 2013	25	0.02 mm/s
Hamzah et al., 2013	15	25.4 mm/min
Zeng et al., 2014	5	5 mm/min
Yoo & Kim, 2014	20	0.02 mm/s

CHAPTER 3

METHODOLOGY

3.1 Introduction

This chapter describes the method used in this research. A thorough explanation of experimental design of samples, material characterization, programming and calibrating the apparatus, testing conditions, cutting and preparation of samples for testing is given in the following chapters.

3.2 Experimental testing machine

Although the TSRST device has been used in numerous thermal cracking study, lack of specific standards procreated variety between studies. That being said over the years successful experiments have been conducted despite the fact that different test setups and procedures have been used by different researchers in their work. Hereby, in this thesis work a TSRST machine is used with direct tension test method.

3.2.1 Design and fabrication

The TSRST machine used in this study consisted of three main parts: temperature-controlled cabinet, a servo motor for loading and a compressor unit for cooling. Apart from these main parts, a computer and a data acquisition system is used in order to control and gather the data (Figure 3.1 and 3.2).

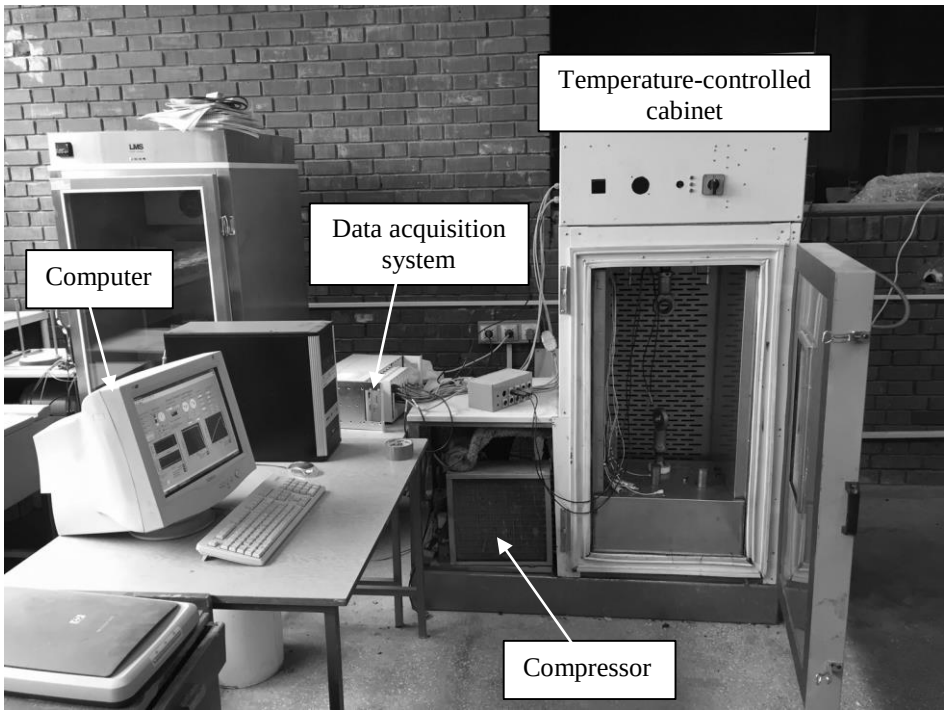

Figure 3.1 TSRST machine used for direct tension tests.

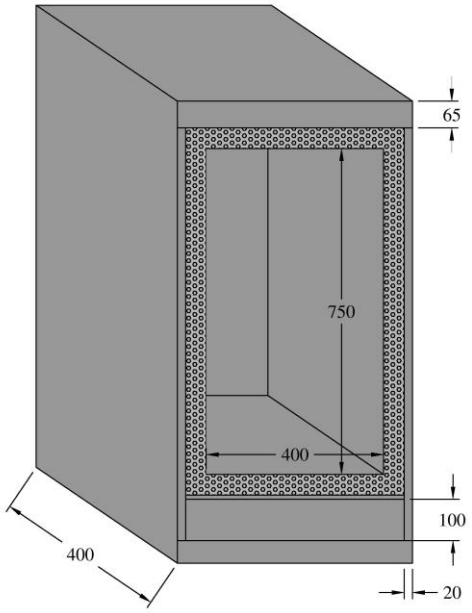

Figure 3.2 Details of the temperature-controlled cabinet.

The temperature-controlled chamber has two layers. An external steel frame for structural purposes and an internal foam layer for insulation. As it can be seen from Figure 3.2, steel plates with 65 mm at the top, 100 mm at the bottom and 20 mm thicknesses on the sides were welded together to support the system. The internal layer on the other hand made of foam for insulation purposes. With 170 mm thickness, this foam layer helps maintaining target temperatures during testing and prevents heat transformation from outside the chamber.

At the bottom of the cabinet beneath the foam layer, a load cell is used for measuring the load. The test device also has a servo-controlled motor at the top. This electrical motor drives the mechanical actuator to create axial tension or compression loads in a straight line. A computer with Labview® software combined with a data acquisition system is used for operating the machine, conducting the tests and collecting the data. With the help of foam layer, a compressor is used to control the temperature inside the chamber. The machine is also capable of achieving extremely low temperatures with the help of liquid nitrogen. For the same device, Qadir (2010) have used liquid nitrogen with a tank to test samples for low temperature cracking and achieved drastic temperature drops. He was the first person ever to use this machine, so before starting the tests he needed to verify the rigidity of the steel frame. After modeling the steel frame in a finite element analysis, he confirmed that the test results would not be effected by the deflections on the steel frame due to loading (Qadir, 2010). The main components of the chamber is illustrated in Figure 3.3. In this study direct tension tests were applied on the specimens with pre-determined constant strain rate at a constant temperature. Tests were conducted at 5^{o}C which was achieved easily by compressor. Thus the requirement for liquid nitrogen was not needed. It is worth mentioning that the load levels in regard to strain levels are provided by the servo motor which has a capacity of 50 kN.

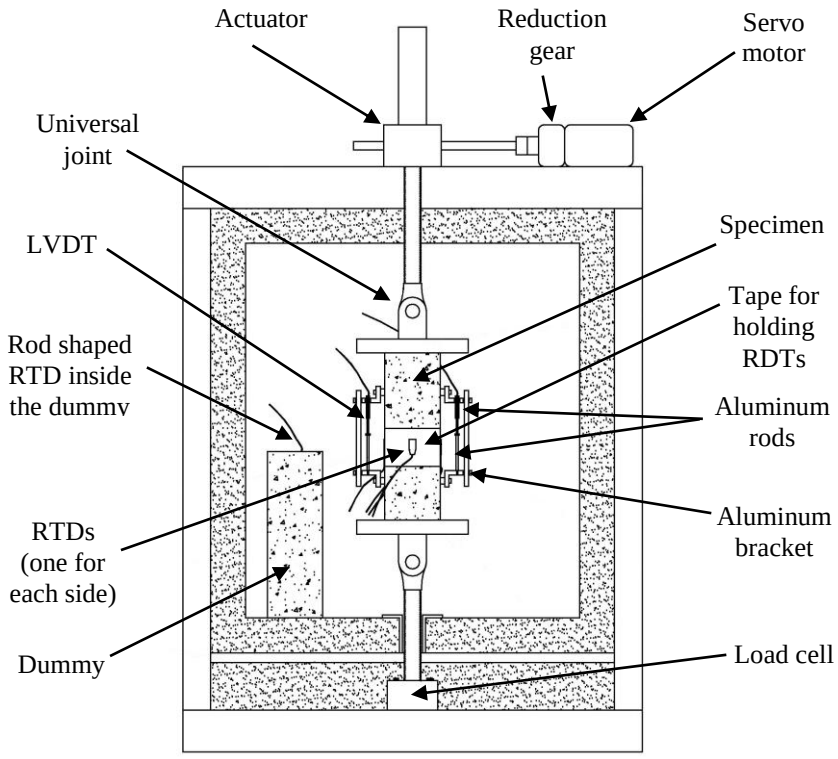

Figure 3.3 General schematic of inside the temperature-controlled cabinet.

The elongation readings from the LVDTs, temperature readings from the RTDs and the load readings from the load cell are gathered and used by a personal computer and a data acquisition in order to control the machine. For example a 100 μs/min of strain rate is maintained by the motor through the direct tension tests in response to the electrical signals coming from the LVDTs located on the opposite sides of the specimens. While the LVDTs are capturing the elongation, constant strain rate is achieved by the servo motor by adjusting the load through the entire testing period.

Two LVDTs are attached to the narrow sides of the specimens with aluminum fixtures (Figure 3.4). The fixtures have a template, so that the LVDTs can be fixed from the top platen and their tips are touched to the short aluminum rods which are fixed to the bottom platen. Long rods are used for keeping the LVDTs in a straight line. While these long rods are fixed to the same top platen as the LVDTs, at the bottom platen they are free for vertical movement. In this way, they allow the LVDTs to freely move in the vertical direction while preventing them to deviate from the other axis.

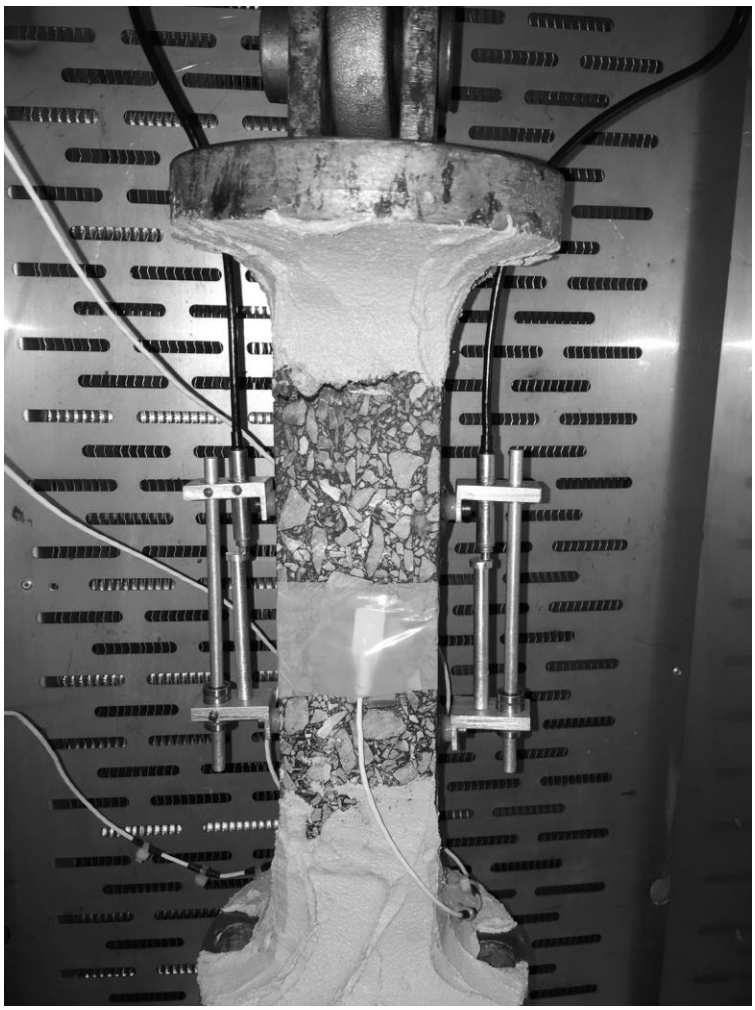

Figure 3.4 A testing sample with LVDTs and RTDs.

On the each side of the specimen RTDs are attached with a tape to monitor the temperature. Another rod shaped RTD is put inside a dummy specimen, which is vertically placed inside the chamber along with the specimen that is being tested. The system takes the average of four surface and one core readings and regulates the temperature inside the chamber to desirable levels.

3.2.2 Programing

In this thesis work Labview® software is used for programing. The program used in direct tension tests processes the electrical signals coming from the LVDTs, the RTDs and the load cell through the data acquisition system and stores the data in the computer for further analyses. The data acquisition system consists of transducer signal conditioners and a data acquisition card. A user interface software is written in graphical programming language with Labview® (Figure 3.5). A full detailed procedure for using this software interface is explained in the appendices.

The program starts with the pre-conditioning phase. This phase is simply for maintaining target temperature within the specimen that being tested. Then the direct tensile test procedure is initiated. The axial deformations and stresses are recorded by the program while the specimens are pulled. As it can be seen from the Figure 3.5 the interface has two major parts: input section is at the top and output section is at the bottom. The input section is divided into six: system control, motor control, test control mode, displacement control, load control and temperature control. Deformation, rate of deformation, load and temperature changes in time are plotted in the output section.

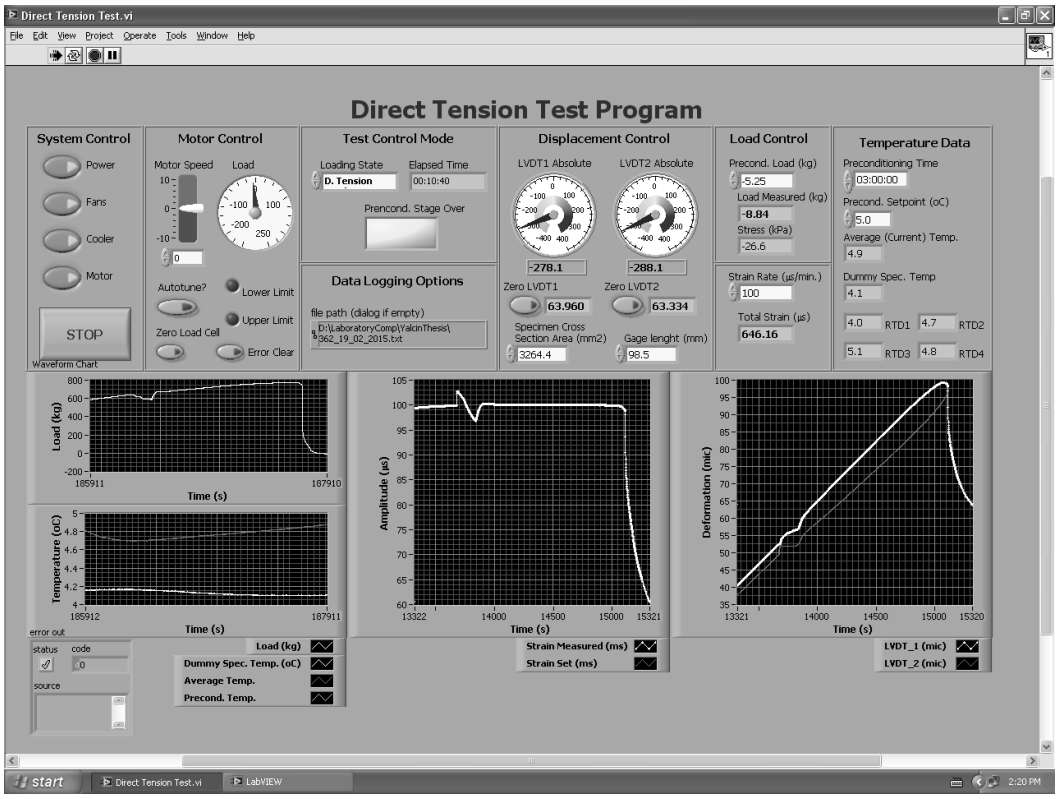

Figure 3.5 The software interface of the direct tension test.

3.2.2.1 The system control

The system control section has four buttons for turning on and off the power, the fans, the cooler and the motor all of which has to be turned on during the test.

3.2.2.2 The motor control

This section as its name implies controls the motor. When mounting the specimens into the machine, the motor has to be controlled manually. The motor speed part is used for this purpose. By changing the direction and the speed of the movement upwards or downwards, the operator arranges the moving upper joint in a way that the specimen can be pinned between the joints. After the placement of specimen, zero load cell button is used for the load.

3.2.2.3 The test control mode

The main purpose of the test control mode is loading state which enables the user to choose the testing mode. The jugging mode, conditioning mode and direct tension mode are enabled for the user to choose. At jogging mode the user can manually control the motor in order to mount the specimen as described previously. By choosing the conditioning mode, the pre-conditioning sequence will start. Finally, at the end of the pre-conditioning mode, the user starts the direct tension test by choosing the direct tension mode.

The preconditioning stage over part informs the end of preconditioning stage by blinking. It is worth mentioning that the program does not allow the user to switch to the direct tension mode before the preconditioning stage over part gives the green light. Apart from these, the elapsed time box and a file directory window for setting the saving path for the data file are in the test control mode section.

3.2.2.4 The displacement control

This section is for adjusting the input parameters for the displacement. One of the crucial steps before starting the experiment is that setting the LVDTs to zero after installing them into the aluminum bracket. As the experiment begins the compressor starts cooling the chamber from room temperature which is often around 20^{o}C to set temperature of 5^{o}C. The shrinkage of the specimen gives negative readings to the LVDTs, in the meantime the shrinkage of the extension bars give positive readings. The software subtract the shrinkage of extension bars from LVDT readings in order to eliminate error.

Two input boxes are also provide vital input parameters for specimen cross section area and gage length. The cross section area of each specimen is measured from three different points relatively from the top, from the middle and from the bottom of the specimen and the average of them is entered in squared millimeters. The software takes this area and the readings from the load cell uses them to calculate the stresses. Last but not least part of this section is gage length which is constant for all specimens. The brackets for mounting the LVDTs are glued to the specimens at two points with a specific template. The distance between the centers of these two points is 98.5 mm. The software calculates the strain by dividing the elongation readings from the LVDTs by the gage length and shows in micro-strain (μs). That being said the micro-strain is one millionth of a strain.

3.2.2.5 The load control

In this section, the operator can see live results of measured load, stress and total strain while conducting the test. As it is mentioned earlier, the software measures the load through the load cell, calculates stress by dividing the load with the cross section area and calculates the strain by using LVDTs and gage length. The preconditioning load on the other hand which is -5.25 Kg for all specimens that being tested, is for ensuring the specimen hangs freely through the entire preconditioning phase. Total weight of specimens and steel plates which is roughly 10 kilograms taken in order to assure freedom at both hands against gravitational pull. The speed of the direct tension test can be controlled with strain rate. Given input values will determine the amount of micro-strain on the specimen in a minute. The motor increases or decreases the actuator's speed in a way that the amount of desirable micro-strain levels can be achieved after 60 seconds.

3.2.2.6 The temperature data

At this final section, desired preconditioning time and temperature is arranged. In this thesis work, 5^{o}C of temperature and three hours of preconditioning time are considered in order to ensure the specimen reaches thermal equilibrium. Other sections show the five different RTD readings four of which on the surface of the specimen and one inside the dummy. The average temperature of five readings can be also seen.

3.3 Sample preparation

In this chapter a detailed explanation of selecting mixture design and test variables, compacting the mixtures into the slabs, cutting out the beam specimens from the slabs and measuring the properties of beam specimens will be given. The samples were prepared by Qadir (2010) for his thesis work. Several specimens were statistically designed and prepared in the laboratory, some of which is used in his effort to understand low temperature cracking. Afterwards some of the excess specimens was used by Arabzadeh (2015) in thermal fatigue cracking. Remaining specimens from their studies were used in this study. That being said the specimens have been kept in the laboratory for five years, from which age hardening is provided in a natural way without of course traffic load. This study is unique in this way since there has been no other study that considers the aging in a natural way apart from the work have done by Arabzadeh (2015).

3.3.1 Selection of the materials

Two types of aggregate, i.e., limestone and basalt, were selected and provided from an asphalt plant located in Ankara to assure the design requirements. In addition to aggregates, two types of bitumen binder, modified and unmodified, were provided by the Turkish General Directorate of Highways (TGDH). The properties of this two essential materials used in the study are given in Table 3.1 and 3.2.

Table 3.1 The basic properties of aggregates.

Properties	Aggregates	
	Limestone	Basalt
Specific gravity	2.75	2.93
Average absorption, %	1.45	1.00
LA abrasion value, %	28	15

Table 3.2 The basic properties of asphalt binder.

Properties	Asphalt	
	50-70	71-100
Penetration (0.1 mm)	54	73
Specific gravity	1.025	1.034

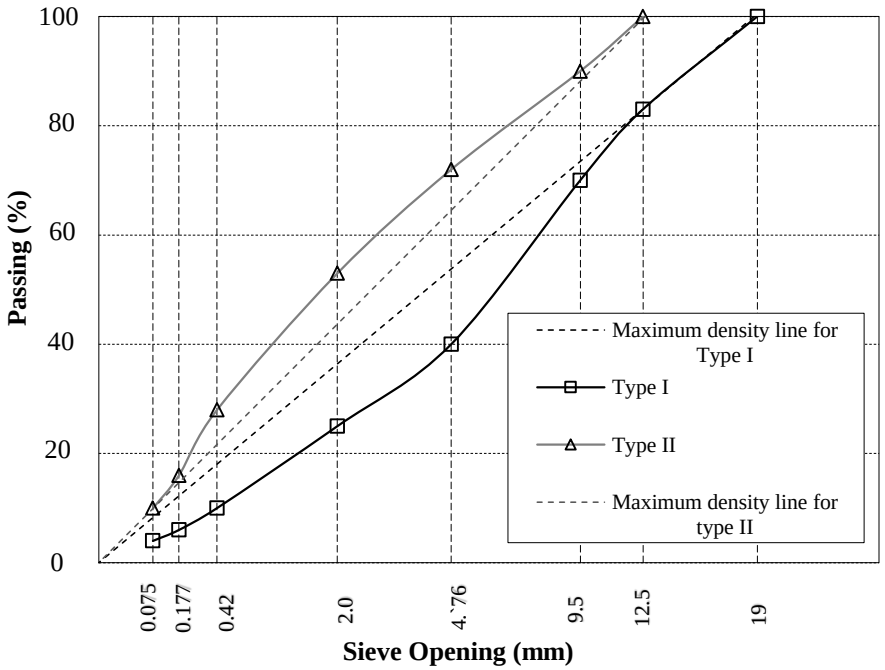

Figure 3.6 Selected aggregate gradation according to the standards of TGDH (Qadir, 2010).

The grading guidelines for the specimens were selected from TGDH specification book (2006), (Qadir, 2010). TGDH states that wearing course can be made of either coarse or fine graded aggregates. Consequently, two types of aggregate gradation were selected. Type I represents coarse gradation and Type II represents fine gradation, both which are plotted on a 0.45 gradation chart in Figure 3.6.

3.3.2 Superpave mixture design

One of the key factors in sample preparation was the asphalt content. While the selection of asphalt binder grade, aggregate gradation, and asphalt content taken into account with the TGDH standards, finding the optimum asphalt content was achieved by Superpave method. Superpave is the mixture design method that can be used as an alternative to Marshall mix design. Selection of asphalt binder grade, aggregate gradation, and asphalt content are parts of Superpave design, yet in this study they were considered under TGDH standards (Qadir, 2010).

According to Superpave mix design procedures, 4% of air voids content has to be achieved at the optimum asphalt content. With this purpose in mind, Qadir (2010) prepared three samples for every combination in order to find the optimum asphalt content. Then samples put in an oven for three hours for short term aging and compacted in a Servopack gyratory compactor. The Superpave mix design standards are presented in Table 3.3 (Qadir, 2010). AASHTO T 166 and AASHTO T 209 codes were used to calculate the bulk specific gravity values and theoretical maximum density values respectively. After finding the optimum asphalt content, Qadir (2010) calculated and summarized in Table 3.4 the values of voids filled with asphalt (VFA), voids in mineral aggregates (VMA), and the required weight for each 16 combinations. According to AASHTO standards it is possible to have some deviations in air voids contents. To compensate this variability, assumed a tolerance limit of ±5% (Qadir, 2010).

Table 3.3 Superpave mix design parameters (AASHTO T 312; Qadir, 2010).

Design parameters	Selected values
Number of Gyrations (N_{des})	100
Cumulative traffic assumed	3-10 million
Mixing temperature	165°C
Compaction temperature	145°C
Air void content selected for design	4%

Table 3.4 Summary of the sixteen mixture combinations (Qadir, 2010).

No.	Aggre-gate	Asphalt type	Modifi-cation	Grad-ation	Optimum AC %	Air voids %	Weight required (Kg)
1	B	57	Z	F	5.0	4.0	20.90
2	B	57	Z	C	4.4	4.0	20.93
3	B	57	S	F	5.2	4.0	20.21
4	B	57	S	C	4.8	3.6	20.71
5	B	71	Z	F	5.3	4.0	20.63
6	B	71	Z	C	4.5	3.9	20.35
7	B	71	S	F	5.4	4.0	20.87
8	B	71	S	C	5.0	3.9	21.07
9	F	57	Z	C	4.5	3.9	22.41
10	F	57	Z	F	5.3	4.0	22.14
11	F	57	S	C	5.0	4.0	22.14
12	F	57	S	F	5.5	4.0	22.09
13	F	71	Z	C	4.8	4.0	21.8
14	F	71	Z	F	5.4	4.0	22.46
15	F	71	S	C	5.5	4.0	21.92
16	F	71	S	F	5.1	3.9	22.5
AASHTO 2001 Criteria				12.5 mm (Maximum size of aggregate)			
VMA (%)				14			
VFA (%)				65-75			

Symbol used: Aggregate Type: L-Limestone, B-Basalt; Gradation: C-Coarse, F-Fine; Modification: Z-No Modification, S-SBS Modification; AC Type: 57- 50/70 Asphalt Grade, 71- 71/100 Asphalt Grade; AC Content: O-Optimum, OP- Optimum+0.5, OM- Optimum-0.5.

3.3.3 Sample preparation for direct tension tests

The TSRST testing setup requires beam specimens; in order to make these beam specimens, at first slabs were prepared according to the sixteen different combination of design variables in Table 3.4 and then they were cut into beam pieces. The rest of these beams after Qadir (2010) and Arabzadeh (2015) were used in this thesis work. The detailed procedure of the work done by Qadir (2010) is given in the following sections.

3.3.3.1 Preparation of slabs

Around 22-23 kg of aggregate and asphalt materials for each 72 samples (three samples for each 16 combinations) were prepared and mixed in the transportation laboratory of the Middle East Technical University. The lack of slab compactor in the laboratory led them to TGDH laboratory. After the three hours of short term aging of mix samples in the oven, they were compacted with French (LCPC) compactor into 50 x 18 x 10 cm dimensions.

3.3.3.2 Preparation of beam specimens

After the compaction, the slabs brought back to the laboratory. With a diamond saw machine two different sizes of beams, having dimensions 50 x 65 x 200 mm and 50 x 65 x 300 mm respectively, were cut out. The cross section of 50 x 65 was chosen for each of them to ensure that the effect of the aspect ratio on the response variables of the test is eliminated. (Vinson et al., 1989). Some of these specimens were used by Qadir (2010) for measuring the low temperature cracking and the glass transition temperature. The rest left in the laboratory for 5 years to ageing.

3.3.3.3 Sample preparation for direct tension tests

The specimens was waited five years in the laboratory while being aged but there are several steps to follow before making a specimen ready for testing. The first step of the preparation sequence is the aluminum fixtures which are used for holding the LVDTs. On the axes of each narrow side of the specimen two lines are drown respectively one longitudinal and one transversal. Next with using an aluminum frame, the plastic studs are attached on the specimen by epoxy. The aluminum frame has two holes on it of whose centers are separated by 98.5 cm from each other. By making sure the overlap between drawn lines and the lines on the aluminum frame, the alignment can be preserved. This alignment also means the alignment of aluminum fixtures, is very important and has to be neat in order to get an accurate strain data from the LVDTs. A specimen after this procedure can be seen from the Figure 3.7.

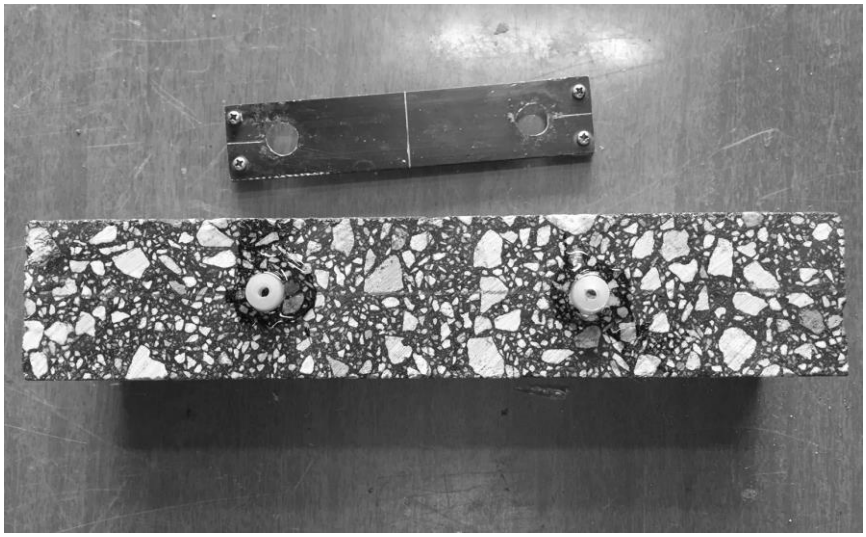

Figure 3.7 The specimen with plastic mounting studs

After gluing two studs on each narrow side of the specimen, it is time for mounting loading platens. Apart from the importance of the alignment of the aluminum fixtures the mounting of the specimens between steel plates is the turning point of the experiment. The work has been done in this step has to be splendid, otherwise the eccentricity may result in drastic moments and premature failure. In this regard first two lines are drawn at the top and at the bottom of the specimen similar to the procedure for the plastic studs. This lines are used for determining the center of the cross section of the specimen. Next a circular ring with a 15 mm of outside diameter, is glued on the center of both ends in order to achieve an accurate alignment of the specimens and the loading plates (Figure 3.8).

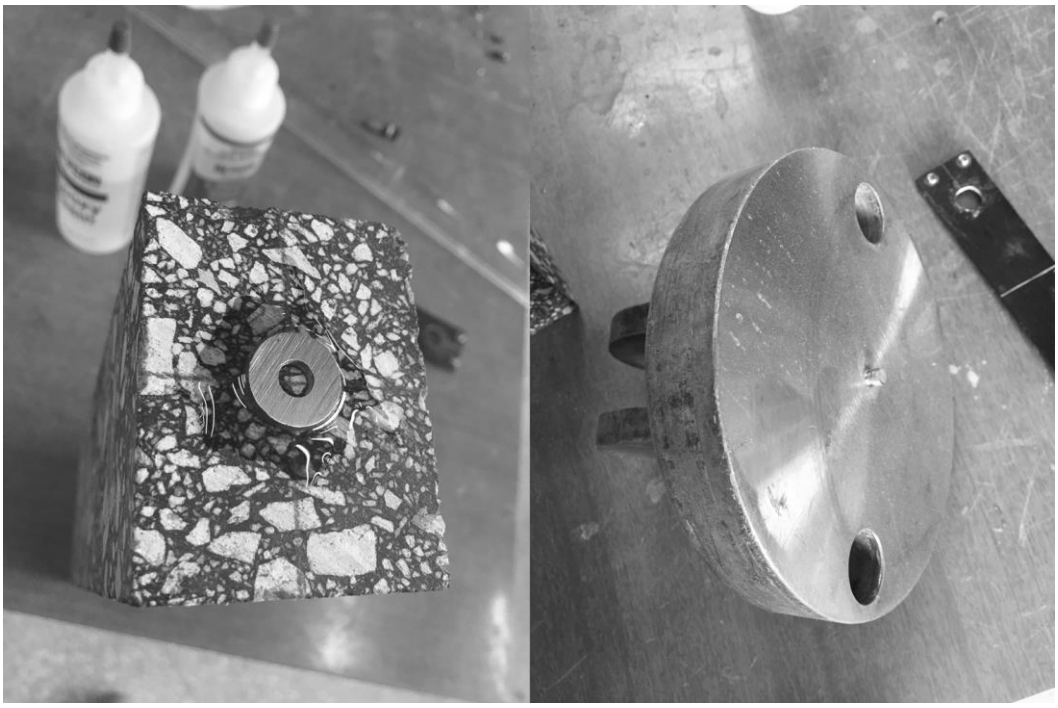

Figure 3.8 Aligning the specimen and the loading pates with a circular ring.

Final step is gluing the specimen between loading plates. The epoxy Sikadur®-31 which can sustain 40 - 60 MPa of tensile strength is used for this purpose. Against the asphalt's 5.0 - 5.5 MPa of typical tensile strength the epoxy would be sufficient. First the bottom plate fixed to the board and some epoxy is applied on the plate. Than the specimen placed on the top of the bottom plate by ensuring the interlock between circular rings and protrusion of plate. Same procedure is also done with the top plate. More epoxy is than spread all around the specimen and platens for increasing the adhesion surfaces. Two steel bars are attached into the holes located each side of the plates. While the specimen is kept on the board for 24 hours to dry, these bars provides axial alignment (Figure 3.9). It is worth mentioning that before every step that involves epoxy use, the surfaces have to be cleaned with acetone and trichloroethylene from residuals.

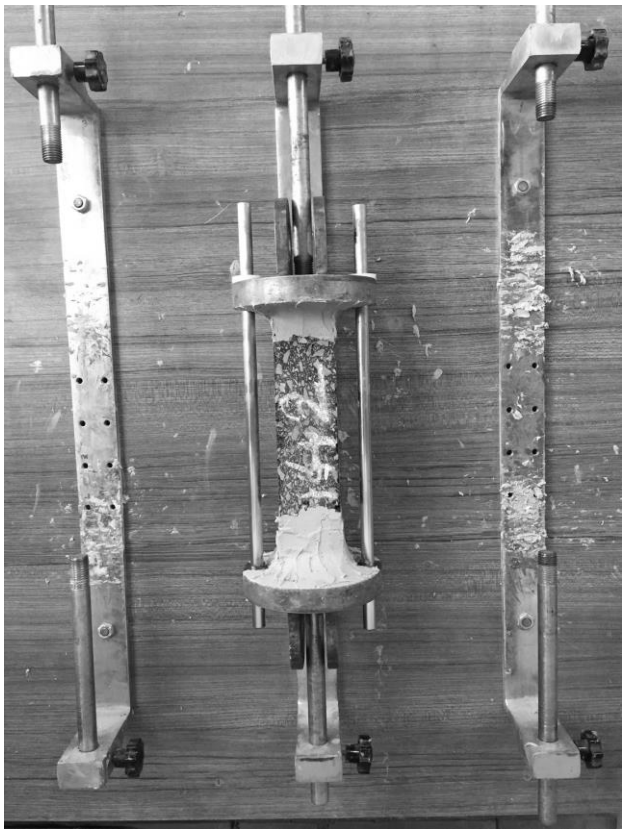

Figure 3.9 A specimen left for drying.

Table 3.5 Properties of the tested specimens.

NO	Sample ID	Aggregate type	Gradation	AC type	Modification	AC content
1	41	L	C	57	Z	OM
2	42	L	C	57	Z	OM
3	43	L	C	57	Z	OM
4	221	L	C	71	Z	OM
5	222	L	C	71	Z	OM
6	262	L	F	71	S	OM
7	263	L	F	71	S	OM
8	271	L	C	71	S	O
9	272	L	C	71	S	O
10	273	L	C	71	S	O
11	311	L	F	71	S	OM
12	343	L	F	71	S	OP
13	361	L	F	71	S	OM
14	362	L	F	71	S	OM
15	363	L	F	71	S	OM
16	393	B	C	57	Z	OP
17	401	B	C	57	S	OM
18	402	B	C	57	S	OM
19	403	B	C	57	S	OM
20	441	B	F	57	Z	OM
21	442	B	F	57	Z	OM
22	491	B	C	57	S	OM
23	492	B	C	57	S	OM
24	501	B	F	57	S	O
25	503	B	F	57	S	O
26	541	B	F	57	S	OM
27	542	B	F	57	S	OM
28	631	B	C	71	S	O
29	671	B	C	71	S	OM
30	701	B	F	71	S	OP

Symbol used: Aggregate Type: L-Limestone, B-Basalt; Gradation: C-Coarse, F-Fine; Modification: Z-No Modification, S-SBS Modification; AC Type: 57- 50/70 Asphalt Grade, 71- 71/100 Asphalt Grade; AC Content: O-Optimum, OP- Optimum+0.5, OM- Optimum-0.5.

3.4 Laboratory testing of the specimens

After the sample preparation the beams are ready for testing. First they are mounted inside the TSRST machine using pins and then two LVDTs are attached to the aluminum fixtures with screws. Since the direct tension tests would be applied, the LVDTs' points pushed to minus absolute in order to provide enough magnitude for extension. RTDs are than attached with tape, four for each side of the specimen and one for inside of the dummy.

After that, 3 hours of preconditioning phase at 5^{o}C is initiated. When it is over, the specimens are pulled with 100 micro-strain per minute rate until the failure occurs. Until the end of the experiment measured strains, loads, and the average temperature of the moment are recorded and stored in a text file with one second interval. At the end of the experimental period, 30 specimens were tested against direct tension test.

.

CHAPTER 4

RESULTS AND DISCUSTION

4.1 Introduction

In this chapter the results of analysis of the design of experiment is described in details. The effects of the input parameters on the output response data were investigated with the statistical analysis of variance (ANOVA) and presented in the following chapters.

4.2 Mixture design variables for ANOVA

The beam specimens used in this study were made ready by Qadir (2010) in the laboratory and the leftovers from Qadir's (2010) and Arabzadeh's (2015) thesis work were subjected to direct tension tests. In order to identify the specimens a system of coding was developed with the following design variables: Aggregate type: B for basalt and L for limestone; aggregate gradation: C for coarse aggregate and F for fine aggregate; asphalt grade: 57 (between 50 and 70) and 71 (between 70 and 100) for the asphalts with penetration (0.1 mm) values of 54 and 73 respectively; modifier: S for SBS modifier and Z for without any modifier; asphalt content: O for optimum asphalt content, O+ for 0.5% more than optimum asphalt content, and O- for 0.5% less than optimum asphalt content. For example, the code of BC57SO- corresponds to the specimen having basalt aggregate, coarse gradation, 54 of asphalt penetration, with SBS modifier and 0.5% less than the optimum asphalt content. More or less the same design variables were considered in this study as well apart from asphalt modifier. Since the SBS modifier was meant to change the grade of the asphalt, it was considered under the asphalt

grade, generating two additional levels of variables. In the ANOVA analyses, two levels of aggregate type, two levels of aggregate gradation, four levels of asphalt grade, and finally three levels of asphalt content have been considered (Table 4.1). A total of 30 proper specimens were tested with different combinations of these variables. However, due to the lack of sufficient number of specimens, the complete block design could not be implemented. Some specimens had one replicate while others had up to six (Table 4.2).

Table 4.1 Experimental design variables.

Design variables	Levels	No. levels
Aggregate Type	Limestone, Basalt	2
Gradation	Coarse, Fine	2
Asphalt Grade	(57-Z), (71-Z), (57-SBS), (71-SBS)	4
Modifier	Zero, SBS	0
Asphalt Content	Optimum, Optimum + 0.5%, Optimum - 0.5%	3

Table 4.2 Tested specimens and their number of replicates.

Specimen code	Number of replicates	Specimen code	Number of replicate
BC57SO-	5	BF71SO+	1
BC57ZO+	1	LC57ZO-	3
BC71SO	1	LC71SO	3
BC71SO-	1	LC71ZO-	4
BF57SO	2	LF71SO-	4
BF57SO-	2	LF71SO+	1
BF57ZO-	2		

4.3 Analysis of variance (ANOVA) for direct tension tests

Direct tension loads were applied to each prismatic specimens. After mounting the specimens into the TSRST machine, 100 μs/min strain rate was used to each specimen until the failure. The strain controlled experiments were conducted with a constant temperature of 5^{o}C. By using the data recorded through the testing period, stress versus strain graphs were plotted and analyzed in Matlab®. Such a plot is illustrated in Figure 4.1. As the tension loads are applied to each specimen, the stress levels start to build up until a certain point. At this point the stress at its peak and the value called peak stress point, which was considered one of the design outcomes. As the strain levels keep increasing, the stress starts to drop and eventually the specimen breaks. Afterwards, the toughness is calculated as the total area underneath the graph from zero to breakage. In the ANOVA analyses the outcome responses were peak stress and toughness.

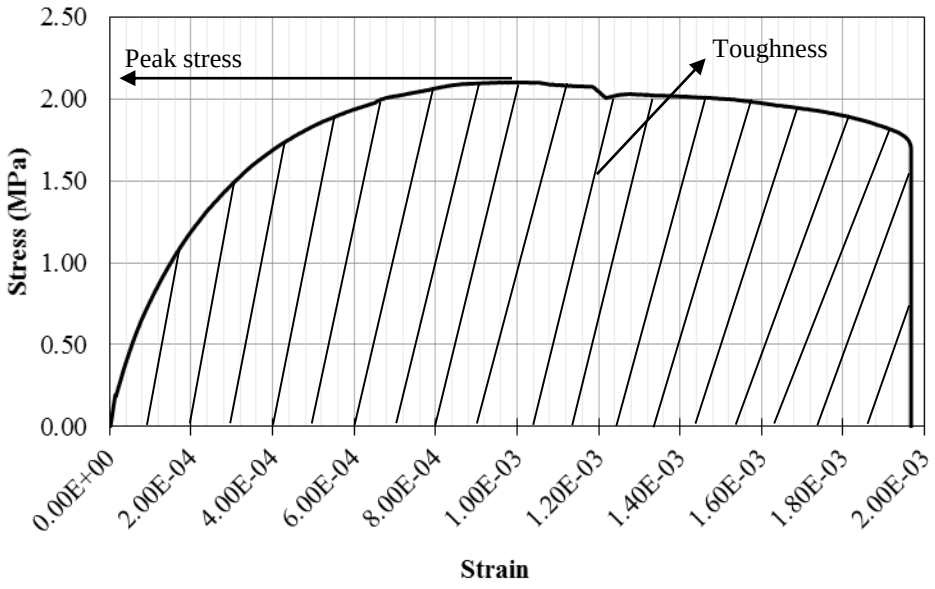

Figure 4.1 The data of applied strain on one of the samples and resulted stress.

4.3.1 Analysis for peak stress

One of the substantial parameter can be gathered from the stress-strain diagram is the peak stress. The maximum amount of stress that a material can withstand under tension or compression, is a measure of material's strength. 30 specimens were tested against direct tension test and from the stress versus strain graphs the maximum amount of the stresses for each specimen were calculated with a simple Matlab® code.

Test results have an average of 1.7 MPa with a 0.7 MPa of standard deviation (Table 4.3). Additionally, the maximum peak stress value (2.6 MPa) achieved from a specimen with limestone and the minimum one (0.2 MPa) corresponded to a specimen with basalt aggregate. Furthermore the average peak stresses for every design parameter were calculated from different replications (Table 4.4).

Table 4.3 Statistics of peak stress.

Statistical parameter	Value (MPa)
Average	1.7
Standard deviation	0.7
Maximum	2.6
Minimum	0.2

The statistical analysis of variance for the peak stresses is given in Table 4.5. With a confidence level of 95% ($p<0.05$) the ANOVA results indicate that aggregate gradation is the most significant factor for peak stress having a probability nearly equal to zero followed by asphalt content and asphalt grade. On the other hand, the effect of aggregate type is insignificant since the p-value of 0.0899 is bigger than the confidence interval of 5%.

Table 4.4 Peak stress results from the experiment.

Design Parameters	**Levels**	**Symbol**	**Average** (MPa)	**Standard deviation** (MPa)	**Median** (MPa)
Aggregate type	Basalt	B	1.352	0.771	1.618
	Limestone	L	2.050	0.304	2.047
Gradation	Coarse	C	1.997	0.344	2.029
	Fine	F	1.256	0.816	1.283
Asphalt grade	50-70	57Z	1.591	0.603	1.894
	71-100	71Z	2.357	0.268	2.393
	50-70+SBS	57S	1.226	0.865	1.481
	71-100+SBS	71S	1.910	0.308	1.727
Asphalt content	Optimum-0.5%	O-	1.807	0.692	2.047
	Optimum	O	1.236	0.628	1.605
	Optimum+0.5%	O+	1.883	0.219	1.827

Table 4.5 ANOVA results for the peak stresses.

Model parameters	**F**	**Probability Prob>F**
Aggregate type	3.15	0.0899
Gradation	39.46	0.0000
Asphalt grade	5.49	0.0057
Asphalt content	14.11	0.0001

The effect of gradation on the peak stress responses for each 13 unique combinations specimens is illustrated in Figure 4.2. The whole results for 30 specimens can be found in the appendix section of the thesis. The findings indicate that coarse gradation outperforms fine gradation. As it can be seen from the Figure 4.2, the specimens with the coarse gradation have higher average peak stresses than the ones with fine graded. For instance the specimen BC57SO- experienced a drastic decrease in its peak stress from 1.9 MPa to 0.3 MPa when the gradation changed from coarse to fine only.

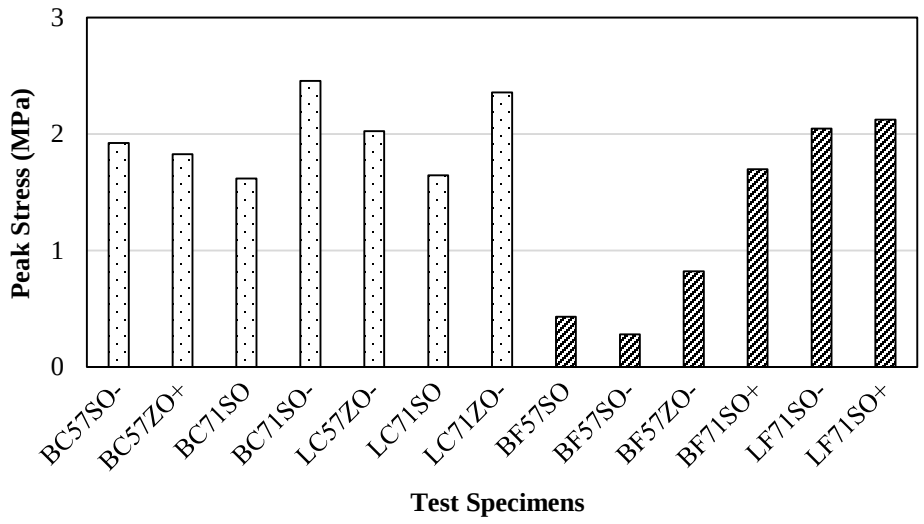

Figure 4.2 The average peak stresses for different types of specimens grouped by gradation.

Asphalt content was one of the important design variables affecting the peak stresses. Figure 4.3 shows the average peak stress values for 13 different specimen combinations ranked by their asphalt content. Highest average peak stress values with the lowest standard deviation were achieved from the specimens having optimum + 0.5% asphalt content.

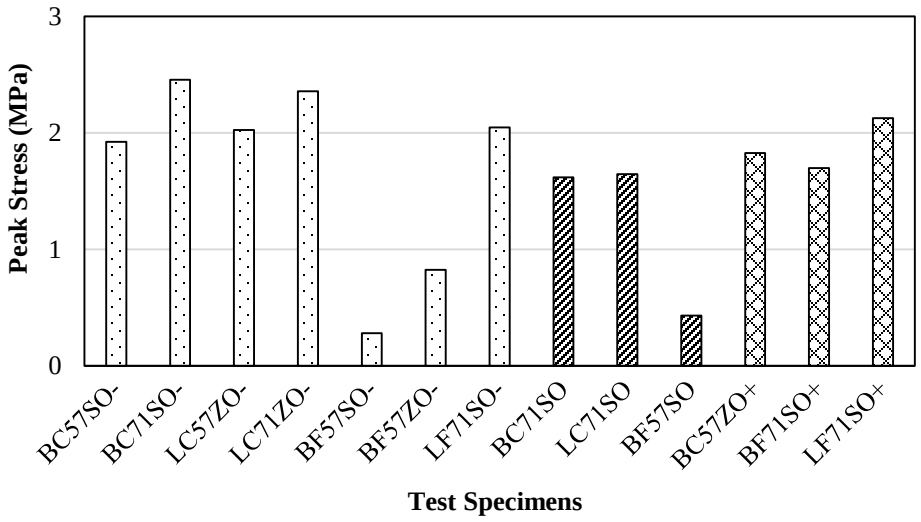

Figure 4.3 The average peak stresses for different types of specimens grouped by asphalt content.

Another significant factor is the asphalt grade. The results of ANOVA showed with a 0.0057 probability the effect of the four different asphalt grades on the peak stress is significant. The 71-100 graded specimens have generally higher stress values than 50-70 graded ones (Figure 4.4). On the other hand SBS modification caused negative effect by decreasing the peak stresses of both 50-70 and 71-100 graded specimens.

Even though the average peak stresses are seem to be higher for the specimens with limestone aggregate (Figure 4.5), the ANOVA analysis showed the effect of the aggregate type on the peak stress is insignificant.

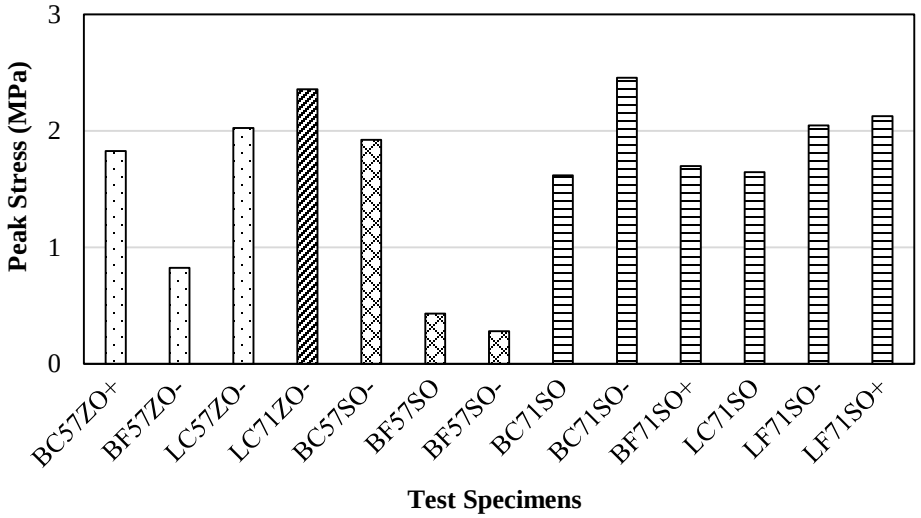

Figure 4.4 The average peak stresses for different types of specimens grouped by asphalt grade.

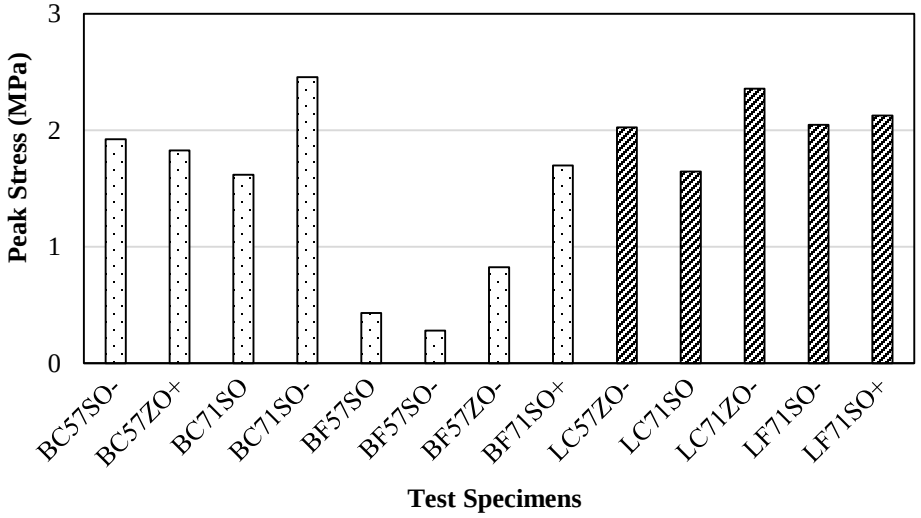

Figure 4.5 The average peak stresses for different types of specimens grouped by aggregate type.

4.3.2 Analysis for toughness

Toughness, commonly expressed in terms of the amount of energy that a material can absorb, is a measure of a material's resistance to fracture. Tough materials can absorb a considerable amount of energy and plastically deform before fracturing. Rather than being a single property, toughness is a combination of strength and ductility. A material with high strength and high ductility will have more toughness than a material with low strength and high ductility. Therefore, a good way of measuring toughness is to calculate the area under the stress versus strain curve from a tensile test such as direct tension test.

In this thesis work, the toughness of the asphalt mixtures were calculated from the area underneath the stress-strain curves as units of energy per volume. Analysis of the experiment resulted in an average of 1941.633 J*m-3 toughness (Table 4.6). While the maximum of them was achieved from a specimen having limestone aggregate and coarse gradation as 4593.800 J*m-3, with 35.500 J*m-3 the minimum toughness was found from specimens with basalt aggregate and fine gradation.

Table 4.7 shows the average results of each design variable. It is worth mentioning that the replications for each design variable were not equal. The appropriate 30 specimens were selected and tested among the available ones. That being said some variables had more samples than the others. The replication numbers for each design variable combination is given in Table 4.2.

Table 4.6 Statistics for toughness.

Statistical parameter	Value ($J*m^{-3}$)
Average	1941.633
Standard deviation	1367.150
Maximum	4593.800
Minimum	35.500

Table 4.7 Toughness results from the experiment.

Design Parameters	Levels	Symbol	Average ($J*m^{-3}$)	Standard deviation ($J*m^{-3}$)	Median ($J*m^{-3}$)
Aggregate type	Basalt	B	1263.6	1384.806	507.4
	Limestone	L	2619.7	984.320	2474.2
Gradation	Coarse	C	2496.1	1234.413	2589.0
	Fine	F	1110.0	1146.842	509.5
Asphalt grade	50-70	57Z	2081.8	1371.485	2380.6
	71-100	71Z	1876.8	701.118	2059.6
	50-70+SBS	57S	1203.3	1593.435	230.2
	71-100+SBS	71S	2492.8	1209.521	2113.1
Asphalt content	Optimum-0.5%	O-	1868.8	1239.866	1811.1
	Optimum	O	2322.3	1915.731	2665.4
	Optimum+0.5%	O+	1690.2	1403.210	1684.2

Table 4.8 ANOVA results for the toughness.

Model parameters	F	Probability Prob>F
Aggregate type	6.6	0.0175
Gradation	16.41	0.0005
Asphalt grade	2.69	0.0710
Asphalt content	0.02	0.9803

The toughness results were evaluated for finding the significant mixture design variables. The probability values from the statistical analysis of variance is presented in Table 4.8. As it can be seen from the ANOVA results, the gradation is the most significant factor for toughness with 95% of confidence interval followed by aggregate type.

In Figure 4.6 the average toughness for all different specimen combinations is illustrated. Apart from the two combinations, toughness values are generally higher for the specimens with course gradation than for those with fine gradation.

The effect of aggregate type as is also understood from the Figure 4.7 is definite since the probability is much lower than the confidence level (0.0175<0.05). According to the experiment results the limestone aggregate outperforms the basalt. The average toughness values are much greater with limestone aggregate.

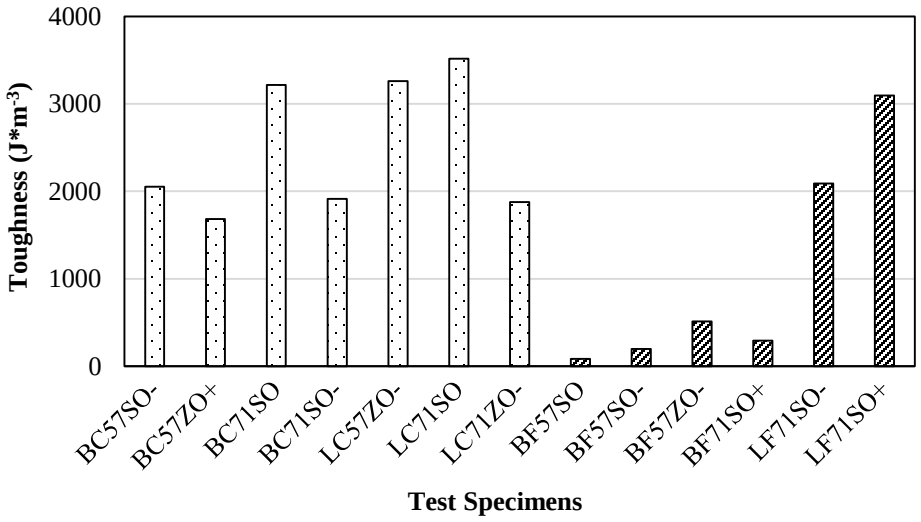

Figure 4.6 The average toughness for different types of specimens grouped by gradation.

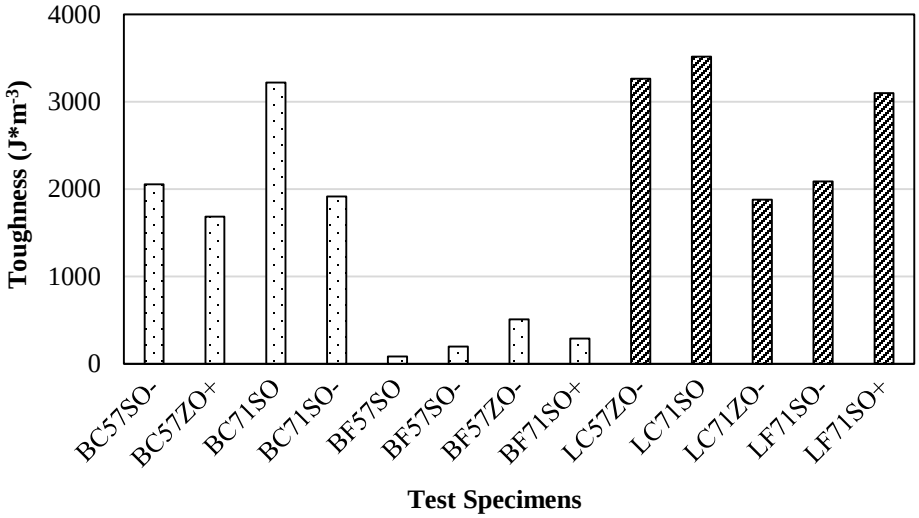

Figure 4.7 The average toughness for different types of specimens grouped by aggregate type.

The statistical analysis of variance indicated that with a 0.0710 probability the effect of asphalt grade on the toughness results is insignificant. In Figure 4.8 the average toughness values regarding to four different asphalt grade are illustrated. For the asphalt binder with penetration of 73 (0.1mm) the average toughness reaches to its peak value.

Additionally, ANOVA results showed that there is no significant effect of asphalt content on the specimen toughness. Three different asphalt content ,i.e., optimum, optimum + 0.5%, optimum - 0.5% were used in the experiment, and toughness results for these asphalt contents are given in the Figure 4.9. For the specimens having optimum asphalt content the average toughness is achieved at its peak value. Neither increasing the asphalt content nor decreasing it were resulted in better results in the terms of mixture toughness.

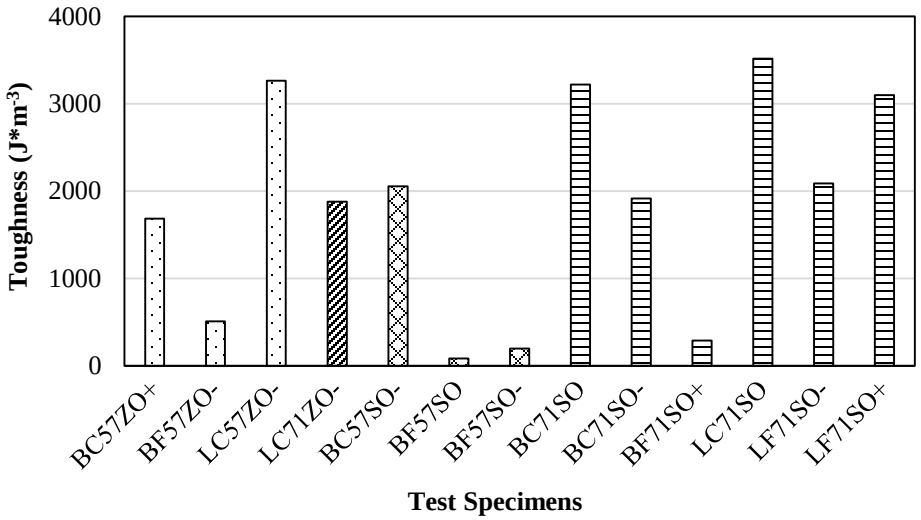

Figure 4.8 The average toughness for different types of specimens grouped by asphalt grade.

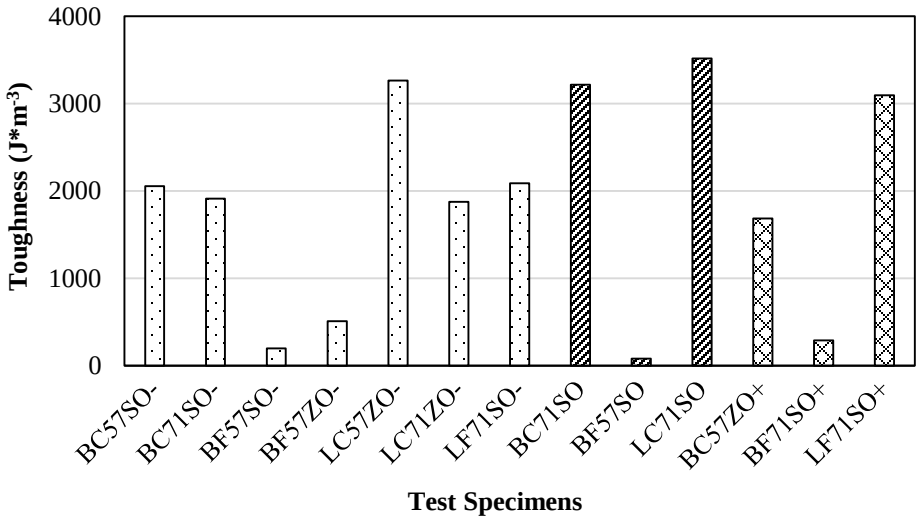

Figure 4.9 The average toughness for different types of specimens grouped by asphalt content.

4.4 Comparison of the direct tension test results

As it was stated in the previous chapters, Qadir (2010) prepared the prismatic beam specimens and performed various tests for fracture strength using the TSRST equipment to investigate the low temperature behavior of asphalt concrete samples. In the isolated chamber the specimens were kept stationary as the temperature decreases steadily. The two dependent variables of that study were the fracture strength and the fracture temperature, for which the former accounts for the maximum stress level that the specimen can hold while the latter indicates the temperature at which the fracture occurs, respectively.

Table 4.9, the results from the analysis of variance are given. According to the ANOVA results aggregate type and asphalt content seem to be the dominant factors in terms of both fracture strength and fracture temperature with the lowest probability value of nearly zero. For the fracture strength, while the gradation was found to be a significant design variable with a probability slightly higher than 0.05, the effect of asphalt grade did not show a significant effect. Moreover, results did not yield a significant effect of gradation and asphalt grade on the fracture temperature (Qadir, 2010).

In his thesis work, Arabzadeh (2015) applied cyclic loads on the same specimens using the same TSRST system. The required number of cycles for 50% reduction in stiffness compared to its initial value were calculated for each specimen. However, in terms of time and economy, instead of waiting for that long, the 50% reduction in stiffness was extrapolated from the linear portion of the log-log scale data by using a power model (Arabzadeh, 2015). The slope of the linear portion of the log-log scale data was also one of the design outcomes.

ANOVA results from thermal fatigue tests were given in Table 4.10 (Arabzadeh, 2015). Among the design variables used, while aggregate type and asphalt content showed significant effect on %50 reduction in stiffness, gradation and asphalt grade were not found to be significant factors for the stiffness. For the slopes of the fitted lines aggregate type seems to be the most dominant factor with a probability value slightly above the confidence interval of 5% as does the asphalt content. According to the Arabzadeh's (2015) results, the effect of gradation was not also a significant factor.

Table 4.9 ANOVA results from low temperature cracking tests (Qadir, 2010).

Design variable	Fracture strength	Fracture temperature
Aggregate type	0.000	0.000
Gradation	0.061	0.325
Asphalt grade	0.222	0.140
Asphalt content	0.000	0.000

Table 4.10 ANOVA results from thermal fatigue tests (Arabzadeh, 2015).

Design variable	%50 reduction in stiffness	Slopes of the fitted linear lines
Aggregate type	0.0539	0.0027
Gradation	0.5288	0.3330
Asphalt grade	0.5844	0.0845
Asphalt content	0.0237	0.0611

Table 4.11 ANOVA results from direct tension tests.

Design variable	Peak stress	Toughness
Aggregate type	0.0899	0.0175
Gradation	0.0000	0.0005
Asphalt grade	0.0057	0.0710
Asphalt content	0.0001	0.9803

The results of analysis of variance on the basis of direct tension tests were given in Table 4.11. Considering the ANOVA results from three different experimental studies, aggregate type seems to be a very important design variable and has a major influence on thermal behavior of asphalt mixture. Two different aggregate type, i.e., limestone and basalt, were used in three different experimental study, and the ANOVA results showed the significance of the aggregate type with very low probabilities except the one from peak stresses. That being said, there exists a partial similarity between the ANOVA results from low temperature cracking tests, thermal fatigue tests, and direct tension tests in response to aggregate type.

While the gradation was not considered an important factor for the thermal mixture tests because of its relatively higher probabilities than the confidence interval, for the direct tension tests it has great impact on the test results with very low probabilities. The ANOVA results for gradation indicate that the direct tension tests have failed to correlate well with thermal mixture tests.

It was clear from the ANOVA results that asphalt grade has no influence on any experimental results apart from the peak stresses. As can be seen from Table 4.9 and Table 4.10, the results of low temperature and thermal fatigue tests in response to asphalt grade are resemble each other, yet from the direct tension tests only half of the results were consistent. Similar conclusions can also be made for the asphalt content as well. The ANOVA results showed the coherence between experimental studies apart from the toughness results obtained from the direct tension tests.

The average experimental results from low temperature cracking tests (Qadir, 2010) and the direct tension tests were given in Figure 4.10, 4.11, 4.12 and 4.13. It is worth mentioning that the number of replications for each specimen was different in both study; because of this the average values are illustrated in the following graphs.

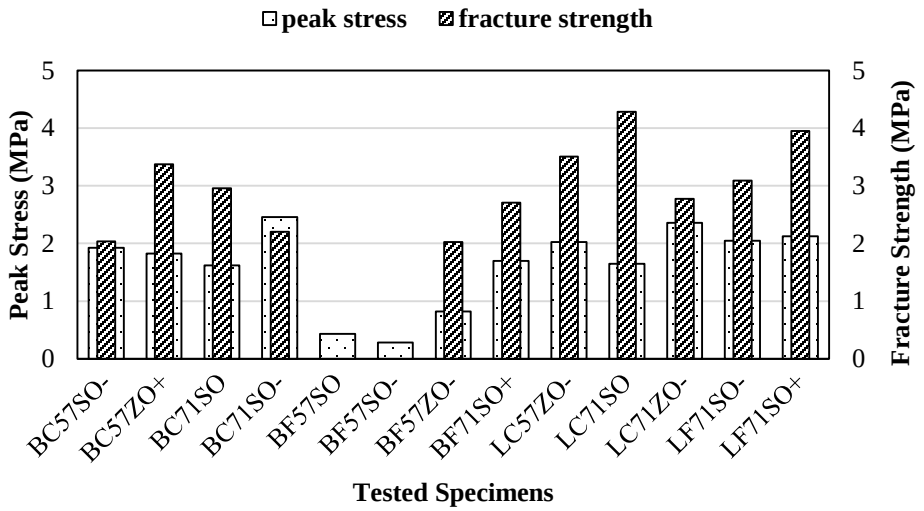

Figure 4.10 Comparison of average peak stress and fracture strength.

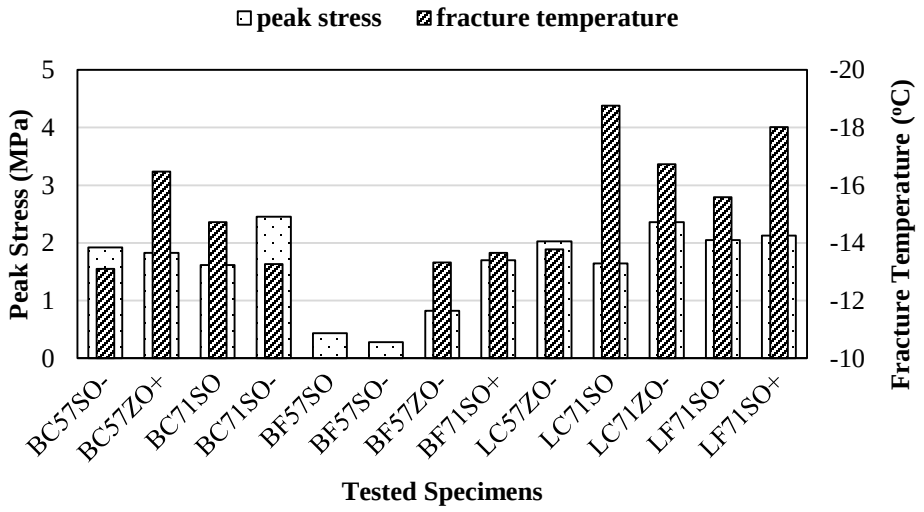

Figure 4.11 Comparison of average peak stress and fracture temperature.

Average peak stress results are compared with fracture strength and fracture temperature in Figure 4.10 and Figure 4.11. The specimens with limestone aggregate tend to have higher strength than those with basalt aggregate. Although there is a consistency between the peak stresses and thermal strength test results for a few of specimens, an overall coherence between these experimental results yet do not exist.

Figure 4.12 and Figure 4.13 illustrate the toughness results versus fracture strength and fracture temperature. It is clear from the figures that the test results for each specimen vary each other, and on the basis of the test results, the correlations between direct tension test, thermal fatigue test and low temperature cracking test failed. The reason might be because of the fact that the direct tension test represents a fast loading mode and fails to simulate the real temperature fluctuations, which are much slower.

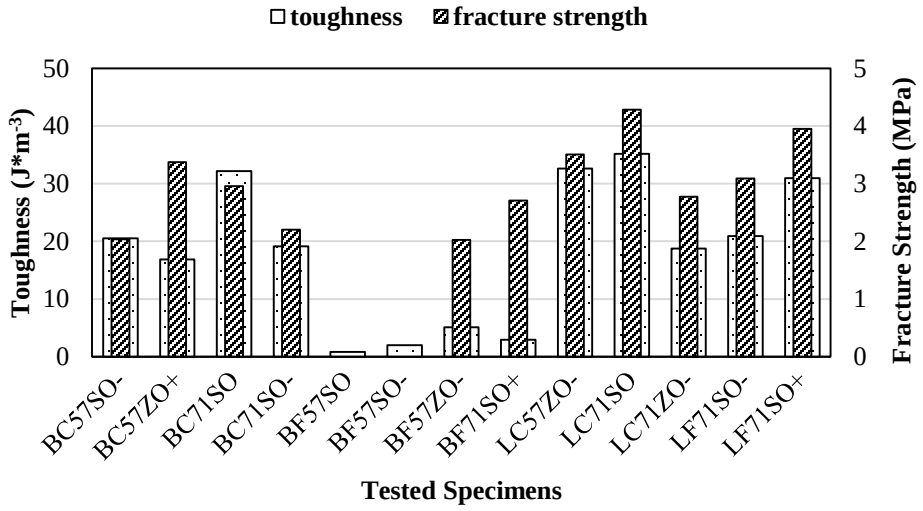

Figure 4.12 Comparison of average toughness and fracture strength.

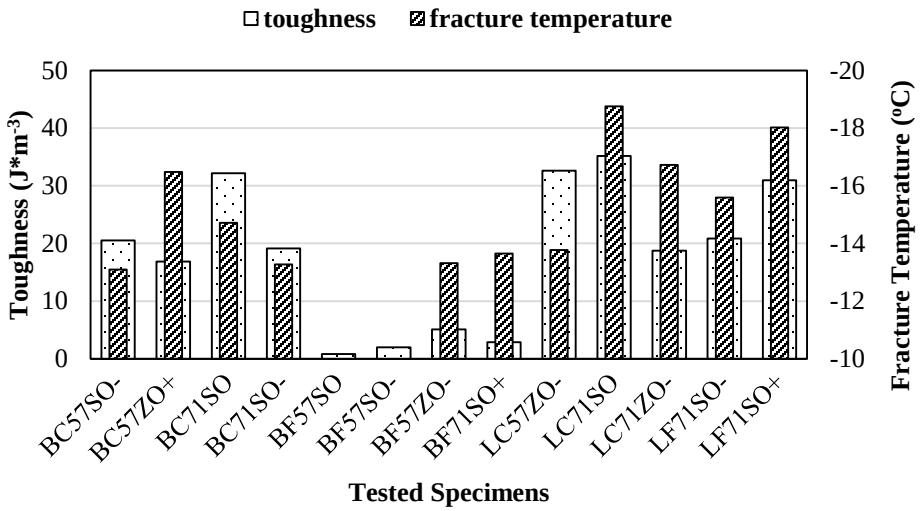

Figure 4.13 Comparison of average toughness and fracture temperature.

CHAPTER 5

CONCLUSIONS AND RECOMMENDATIONS

5.1 Introduction

In this chapter, the findings of this study are summarized. Recommendations were included to help further studies. It should be emphasized that the technique, materials, test procedures and conditions used in this study are unique and summarized findings may differ from other studies.

5.2 Conclusions

Direct tension tests were applied to 30 prismatic beam specimens using TSRST test setup. Maximum stress and toughness values were calculated for each specimen. Statistical analysis of variance were conducted in order to see the effect of the input parameters on the output response variables. In the ANOVA, mixture design variables, i.e., aggregate type, gradation, asphalt grade, and asphalt content, were treated as input parameters. Finally, the comparisons were made to see the correlations between the direct tension tests and the other thermal performance tests. The findings of this study can be summarized as follow:

- The effect of the aggregate type on the peak stress was not been validated. Although the mixtures with limestone aggregate tend to have higher tensile strength than those with basalt, the ANOVA analysis showed there is no significant difference between the peak stresses' of the mixtures regardless of their aggregate type.

- The gradation was proven to be a very important factor in terms of tensile strength of the asphalt mixtures. The mixtures having coarse gradation outperformed the ones with fine gradation with their peak stress values.
- Asphalt grade had a strong influence on the tensile strength. The asphalt binders with higher penetration values had higher peak stresses than ones with lower penetration values. The SBS modification, on the other hand, had adverse effect, resulting in lower peak stress values for both types of asphalt binder.
- The impact of the asphalt content on the peak stress turned out to be very important and the highest average peak stress values with the lowest standard deviation were achieved from the specimens with optimum+0.5% asphalt content.
- In contrast to the peak stress, the ANOVA results revealed the remarkable effect of aggregate type on the toughness results. It seems that specimens with limestone aggregate have higher energy absorption capacities than the specimens with basalt aggregate. The reason can be explained by the differences in the characteristics of the two aggregate types, i.e., surface texture, aggregate shape, etc.
- The effect of gradation on the toughness turned out to be definite. Similar to the peak stress, specimens with coarse gradation outperform the ones with fine gradation.
- ANOVA results indicated that the effect of asphalt grade on toughness results is insignificant.
- The impact of asphalt content on toughness was not found to be significant.
- The ANOVA results from the three different studies have indicated that there is no a clear correlation between the direct tension tests and the other thermal performance tests, i.e., low temperature cracking tests and thermal fatigue tests.

5.3 Recommendations

The following recommendations can be made for future studies:

- Based on the findings the correlation between direct tension tests and the other thermal tests does not exist. This should be further investigated by using a larger specimen set.
- The SBS modification did not show any beneficial effects on the tensile strength of the mixtures. Thus, either the amount of the modifier should be increased or its type should be changed in the experimental program.

REFERENCES

Al-Qadi, I. L., Hassan, M. M., & Elseifi, M. A. (2005). Field and Theoretical Evaluation of Thermal Fatigue Cracking in Flexible Pavements. *Transportation Research Board*, 87-95.

Anderson, O., K., & Epps, J. A. (1983). *Asphalt Concrete Factors Related to Pavement Cracking in West Texas.* AAPT.

Apeagyei, K. A., Dave, V. E. & Buttlar, W. G. (2008). Effect of Cooling Rate on Thermal Cracking of Asphalt Concrete Pavements. *Journal of the Association of Asphalt Paving Technologists, 41,* 383-423.

Arabzadeh, A. (2015). *The Influence of Different Mixture Design Variables on Thermal Fatigue Cracking of Asphalt Concrete Pavements* (Master's thesis, Middle East Technical University, Ankara, Turkey).

Bahia, H. U., & Anderson, D. A. (1993). Glass Transition Behavior and physical hardening of Asphalt Binders. *Journal of the Association of Asphalt Paving Technologies, 62-93,* 93-129.

Breen, J. J., & Stephens, J. E. (1967). The Glass Transition and Mechanical Properties of Asphalt. *Annual Conference of Canadian Technical Asphalt Association.*

Carpenter, S.H., Lytton, R. L., & Epps, J. A. (1974). *Environmental Factors Relevant to Pavement Cracking in West Texas.* Texas Transportation Institute.

Carpenter, H., S., & Lytton, R. L. (1977). *Thermal Pavement Cracking in West Texas.* Texas Transportation Institute.

Carpenter, & H., S. (1983). *Thermal Cracking in Asphalt Pavements: an Examination of Models and Input Parameters.* USA CRREL.

Epps, A. L. (1999). An Approach to Examine Thermal Fatigue in Asphalt Concrete. *Journal of the Association of Asphalt Paving Technologists,* 319-348.

Fabb, T. R. J. (1974). The Influence of Mix Composition, Binder Properties and Cooling Rate on Asphalt Cracking at Low Temperature. *AAPT, 43,* 285-331.

FHWA courses. (1998).

Forough, S. A., Nejad, F. M., & Khodaii, A. (2013). A Comparative Study of Temperature Shifting Techniques for Construction of Relaxation Modulus Master Curve of Asphalt Mixes. *Construction and Building Materials, 53,* 74-82.

Gerritsen, A. H., & Jongeneel, D. J. (1988). *Fatigue Properties of Asphalt Mixes under Conditions of Very Low Loading Frequencies.*

Glaoui, B., Van de Ven, M., et al. (2011). Thermal Fatigue with Freeze-Thaw Cycles of Polymer Modified Bitumen. *Journal of Applied Sciences, 11(6),* 1012-1018.

Gonzalez, J. M., Canet, J. M., Oller, S., & Miro, R. (2006). A Viscoplastic Constitutive Model with Strain Rate Variables for Asphalt Mixtures-Numerical Simulation. *Computational Materials Science, 38,* 543-560.

Haas, R. (1973). A Method for Designing Asphalt Pavements to Minimize Low-temperature Shrinkage Cracking. *RR-73-I,* Asphalt Institute.

Haas, R., Meyer, R., Assaf, G., & Lee, H. (1987). A Comprehensive Study of Cold Climate Airport Pavement Cracking. *Journal of Association of Asphalt Paving Technologists, 56,* 198-245.

Haas, R., & Topper, T. (1969). Thermal Fracture Phenomena in Bituminous Surfaces. *Special Report No. 101,* Highway Research Board, Washington, D.C.

Hamzah, M. O., Kakar, M. R., Quadri, S. A., & Valentin, J. (2013). Quantification of Moisture Sensitivity of Warm mix asphalt Using Image Analysis Technique. *Journal of Cleaner Production, 68*, 200-208.

Ho, S. & Zanzotto, L. (2005). The Low Temperature Properties of Conventional and Modified Asphalt Binders Evaluated by the Failure Energy and Secant Modulus from Direct Tension Tests. *Materials and Structures, 38*, 137-143.

Huang, B., Li, G., & Mohammad, N. L. (2003). Analytical Modelling and Experimental Study of Tensile Strength of Asphalt Concrete Composite at Low Temperatures. *Composites: Part B 34*, 705-714.

Huang, Y. H. (2004). *Pavement Analysis and Design.* Pearson.

Isacsson, U., & Zeng, H. (1996). Low-Temperature Cracking of Polymer-Modified Asphalt. *Materials and Structures, 31,* 58-63.

Jackson, N. M. (1992). *Analysis of Thermal Fatigue Distress of Asphalt Concrete Pavements* (Doctoral thesis, Oregon State University).

Jackson, M. N., & Vinson, T. S. (1996). Analysis of Thermal Fatigue Distress of Asphalt Concrete Pavements. *Journal of the Transportation Research Board,* 43-49.

Jung, D. H. & Vinson, T. S. (1994). Low-Temperature Cracking: Binder Validation. *Report for A-003A of the Strategic Highway Research Program (SHRP).*

Jung, D. H. & Vinson, T. S. (1994). Low-Temperature Cracking: Test Selection. *Report for A-003A of the Strategic Highway Research Program (SHRP).*

Keliewer, J. E., & Zeng, H. (1996). Aging and Low Temperature Cracking of Asphalt Concrete Mixtures. *Journal of Cold Regions Engineering, 10,* 134-148.

Lee, Q. S., Van Bameveld, A., Corbett, M. A. (2009). Low Temperature Cracking Performance of Superpave and Cold in-Place Recycled Pavements in Ottawa-Carleton.

Lee, S., Mun, S., & Kim, Y. R. (2011). Fatigue and Rutting Performance of Lime-Modified Hot-mix Asphalt Mixtures. *Construction and Building Materials, 25,* 4202-4209.

Lee, S., Baek, C., & Park, J. (2012). Performance-based mix Design of Unmodified and Lime-Modified Hot mix Asphalt. *Can. J. Civ. Eng., 39,* 824-833.

Marasteanu, M., Zofka, A., Turos, M., et al., (2007). Investigation of Low Temperature Cracking in Asphalt Pavements National Pooled Fund Study 776. *Minnesota Department of Transportation, Research Services MS 330, St. Paul, MN 55155.*

Mun, S., & Lee, S. (2010). Determination of the Fatigue-Cracking Resistance of Asphalt Concrete Mixtures at Low Temperatures. *Cold Regions Science and Technology, 61,* 116-124.

Nam, K. & Bahia, H. U. (2009). Effect of Modification on Fracture Failure and Thermal-Volumetric Properties of Asphalt Binders. *Journal of Materials in Civil Engineering, 21(5),* 198-209.

Nam, K. (2005). *Effects of Thermo-Volumetric Properties of Modified Asphalt Mixtures on Low-Temperature Cracking* (Doctoral dissertation, University of Wisconsin-Madison).

Qadir, A. (2010). *Investigation of Low Temperature Cracking in Asphalt Concrete Pavements* (Doctoral thesis, Middle East Technical University, Ankara, Turkey).

Pellinen, T. K., & Xiao, S. (2006). Stiffness of Hot mix Asphalt. *Joint Transportation Research Program, SPR-2644,* Final Report, FHWA/IN/JTRP- 2005/20.

Roberts, F., Kandhal, P. S., Brown, E. R., & Lee, D. Y. (1996). *Hot Mix Asphalt Materials, Mixture Design and construction.* Lanham, Maryland: Research and Education Foundation.

Schmidt, R. J., & Santucci, L. E. (1966). *A Practical Method for Determining the Glass Transition Temperature of Asphalt and Calculation of Their Low Temperature Viscosities. Proc., AAPT, 35*, 61-90.

Sebaaly, P. E., Lake, A. & Epps, J. (2002). Evaluation of Low-Temperature Properties of HMA Mixtures. *Journal of Transportation Engineering, 128(6),* 578-586.

Shen, W. & Kikrner, D. J. (2001). Thermal Cracking of Viscoelastic Asphalt-Concrete Pavement. *Journal of Engineering Mechanics 127,* 700-7009.

Shahin, M., & McCullough, B. F. (1972). Prediction of Low-Temperature and Thermal Fatigue Cracking in Flexible Pavements, *Research Report 123·14, Austin, Texas: Center for Highway Research.*

Sugawara, T., & Moriyoshi A. (1984). Thermal Fracture of Bituminous Mixtures. Proceedings of the Paving in Cold Areas, *Mini-Workshop,* 291-320.

Underwood, B. S., & Kim, Y. R. (2013). Effect of Volumetric Factors on the Mechanical Behavior of Asphalt Fine Aggregate Matrix and the Relationship to Asphalt Mixture Properties. *Construction and Building Materials, 49,* 672-681.

Vinson, T. S., Janoo, V. C., & Haas, R. G. (1989). Low Temperature and Thermal Fatigue Cracking. *Summary Report for A-003A of the Strategic Highway Research Program (SHRP).*

Wang, W., Mo, Y., He, H., & Zeng, H. (2011). Aging Effects on Pavement Performance of Asphalt Mortar. *Advanced Materials Research, 150-151*, 247-251.

Wysong, Z. D. (2004). *Development and Comparison of the Asphalt Binder Cracking Device to Directly Measure Thermal Cracking Potential of Asphalts* (Master's thesis, Ohio University).

Xie, J., Xiao, Y., Wu, S., & Huang, J. (2011). Research on Fracture Characteristic of Gneiss Prepared Asphalt Mixture with Direct Tensile Test. *Construction and Building Materials, 28*, 476-481.

Xinjun, L., Marasteanu, O. M., Kvasnak, A., et al. (2010). Factors Study in Low-Temperature Fracture Resistance of Asphalt Concrete. *Journal of Materials in Civil Engineering, 22(2),* 145-152.

Yoo, P. J., & Al-Qadi, I. L. (2013). Pre- and Post-Peak Toughening Behaviors of Fiber-Reinforced Hot-mix Asphalt Mixtures. *International Journal of Pavement Engineering, 15:2*, 122-132.

Yoo, P. J., & Kim, K. (2014). Thermo-plastic Fiber's Reinforcing Effect on Hot-mix Asphalt Concrete Mixtures. *Construction and Building Materials, 59*, 136-143.

Zeng, G., Yang, X., Yin, A., & Bai, F. (2014). Simulation of Damage Evolution and Crack Propagation in Three-Point Bending Pre-Cracked Asphalt Mixture Beam. *Construction and Building Materials, 55*, 323-332.

Zhaohui, S., Yu, Q., Yu, B., Zhu, G. & Ma, J. (2014). The Effect of Asphalt and Aggregate Gradation on the Low-temperature Performance of Asphalt Mixtures for Intermediate and Underlying Course. *Applied Mechanics and Materials, 505-506,* 251-254.

APPENDIX A

DIRECT TENSION PLOTS

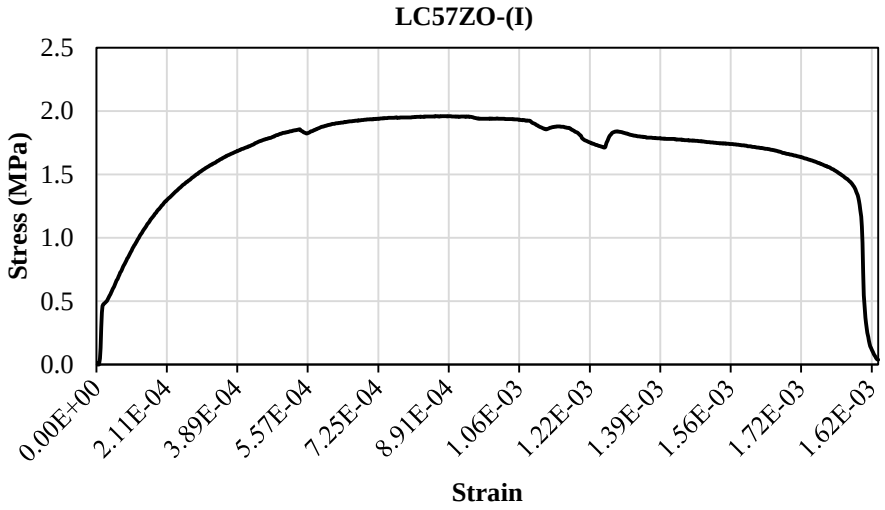

Figure A.1 Direct tension plot of tested samples.

Symbols used:

Aggregate Type: L-Limestone, B-Basalt; Gradation: C-Coarse, F-Fine; AC Type: 57-50/70 Asphalt Grade, 71-71/100 Asphalt Grade; Modification: Z-No Modification, S-SBS Modification; AC Content: O-Optimum, O+- Optimum+0.5, O--Optimum-0.5.

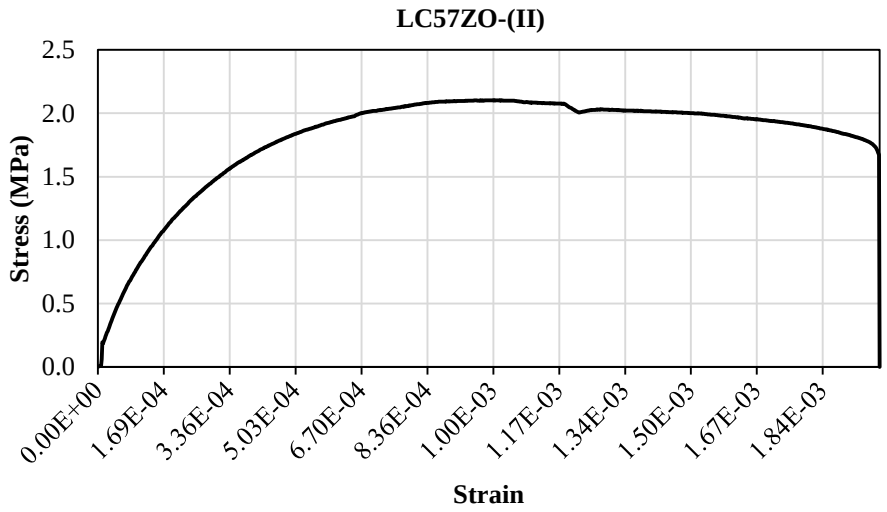

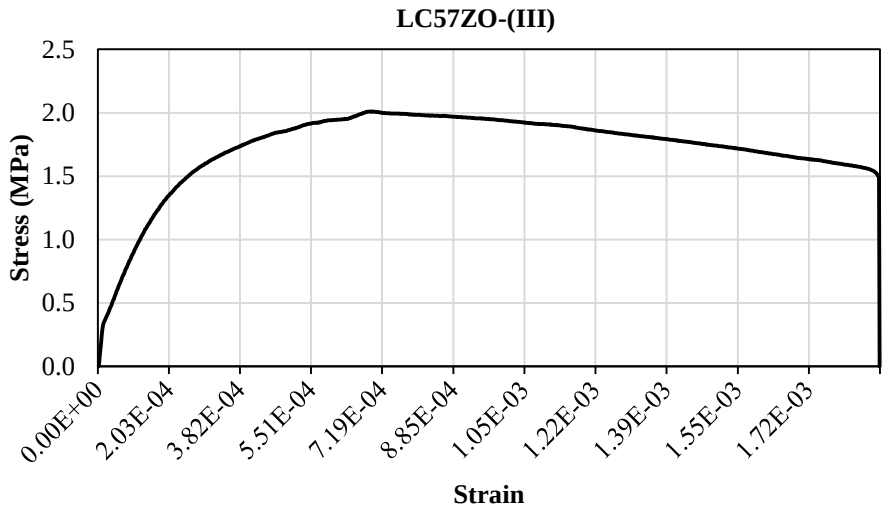

Figure A.1 (continued)

Symbols used:

Aggregate Type: L-Limestone, B-Basalt; Gradation: C-Coarse, F-Fine; AC Type: 57-50/70 Asphalt Grade, 71-71/100 Asphalt Grade; Modification: Z-No Modification, S-SBS Modification; AC Content: O-Optimum, O+- Optimum+0.5, O--Optimum-0.5.

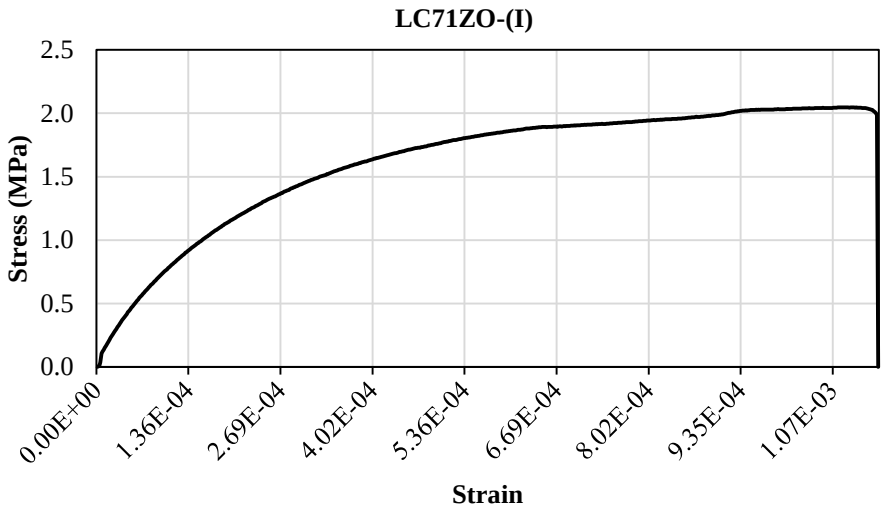

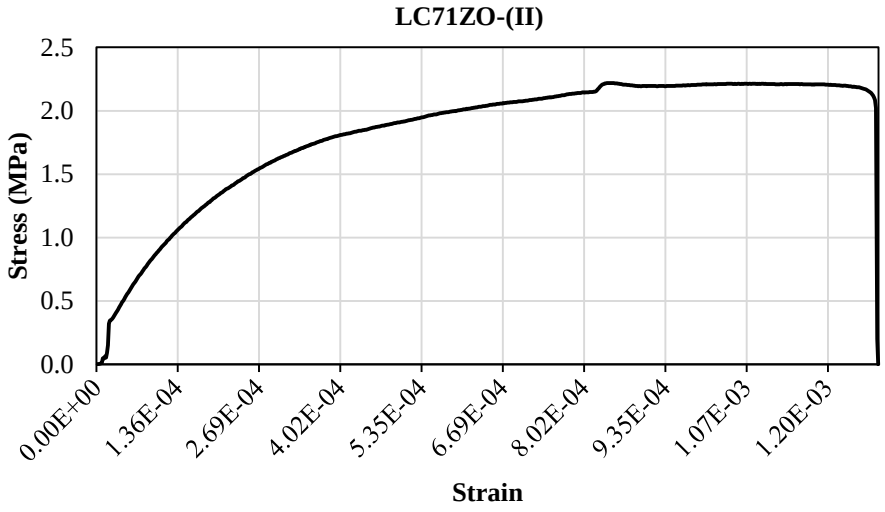

Figure A.1 (continued)

Symbols used:

Aggregate Type: L-Limestone, B-Basalt; Gradation: C-Coarse, F-Fine; AC Type: 57-50/70 Asphalt Grade, 71-71/100 Asphalt Grade; Modification: Z-No Modification, S-SBS Modification; AC Content: O-Optimum, O+- Optimum+0.5, O--Optimum-0.5.

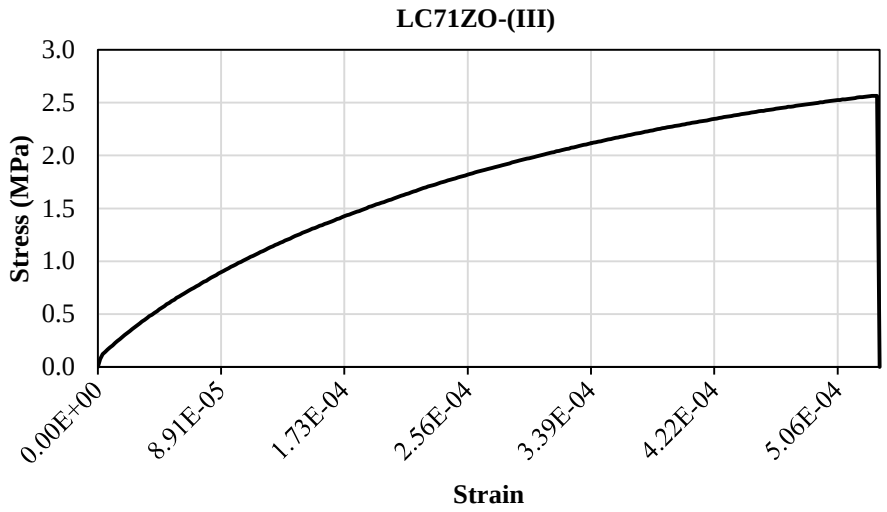

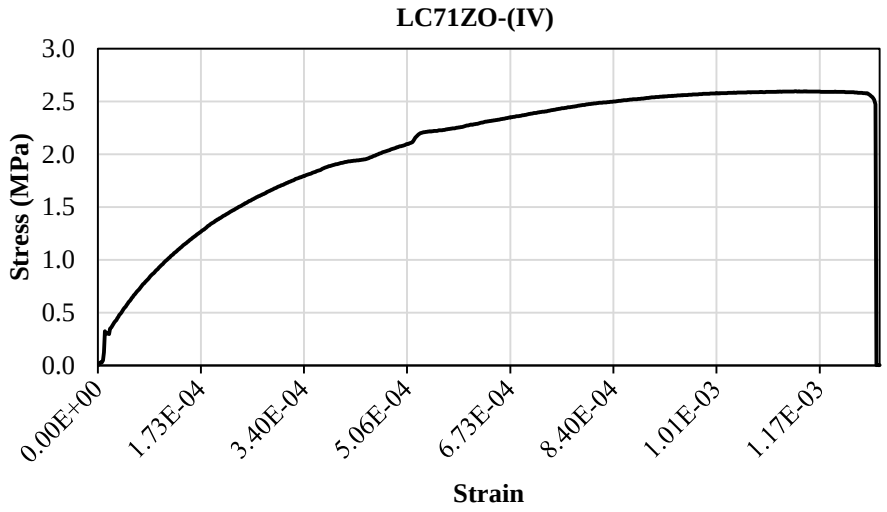

Figure A.1 (continued)

Symbols used:

Aggregate Type: L-Limestone, B-Basalt; Gradation: C-Coarse, F-Fine; AC Type: 57-50/70 Asphalt Grade, 71-71/100 Asphalt Grade; Modification: Z-No Modification, S-SBS Modification; AC Content: O-Optimum, O+- Optimum+0.5, O--Optimum-0.5.

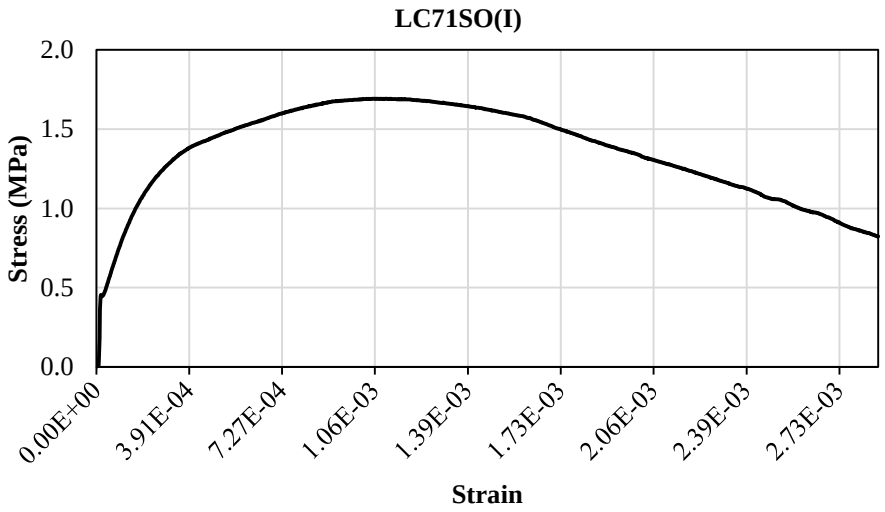

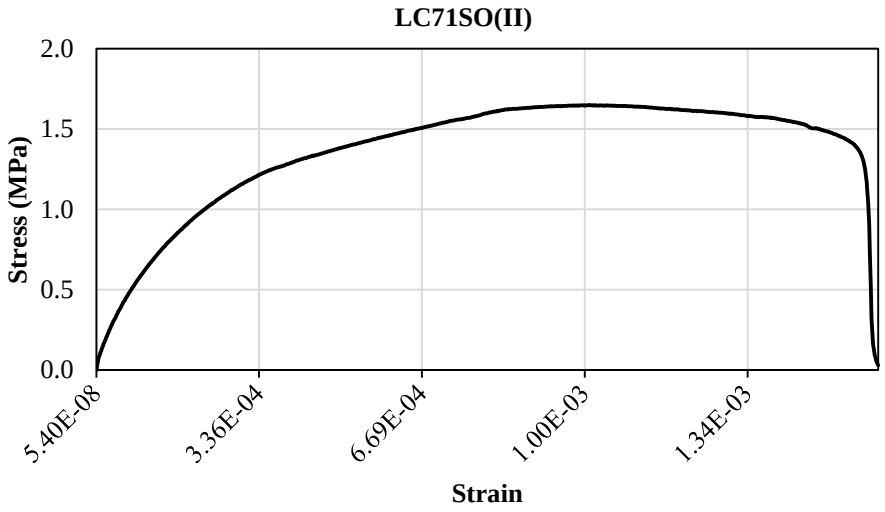

Figure A.1 (continued)

Symbols used:

Aggregate Type: L-Limestone, B-Basalt; Gradation: C-Coarse, F-Fine; AC Type: 57-50/70 Asphalt Grade, 71-71/100 Asphalt Grade; Modification: Z-No Modification, S-SBS Modification; AC Content: O-Optimum, O+- Optimum+0.5, O--Optimum-0.5.

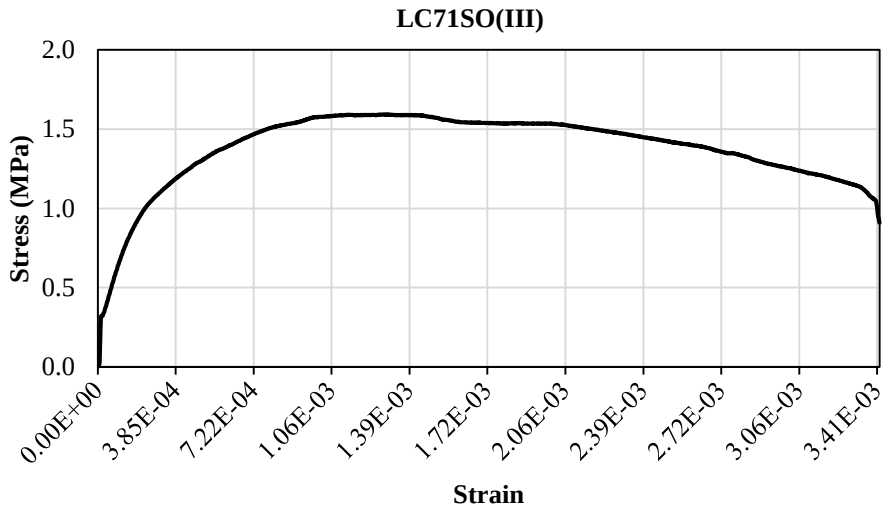

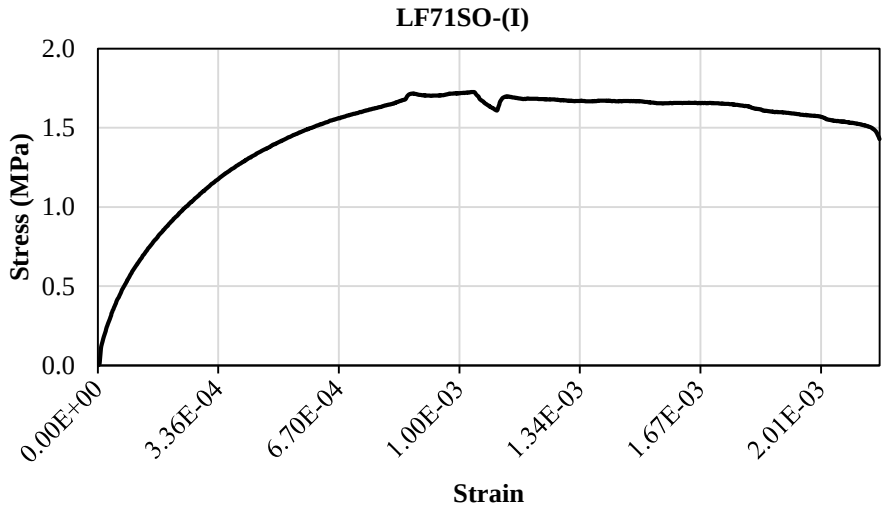

Figure A.1 (continued)

Symbols used:

Aggregate Type: L-Limestone, B-Basalt; Gradation: C-Coarse, F-Fine; AC Type: 57-50/70 Asphalt Grade, 71-71/100 Asphalt Grade; Modification: Z-No Modification, S-SBS Modification; AC Content: O-Optimum, O+- Optimum+0.5, O--Optimum-0.5.

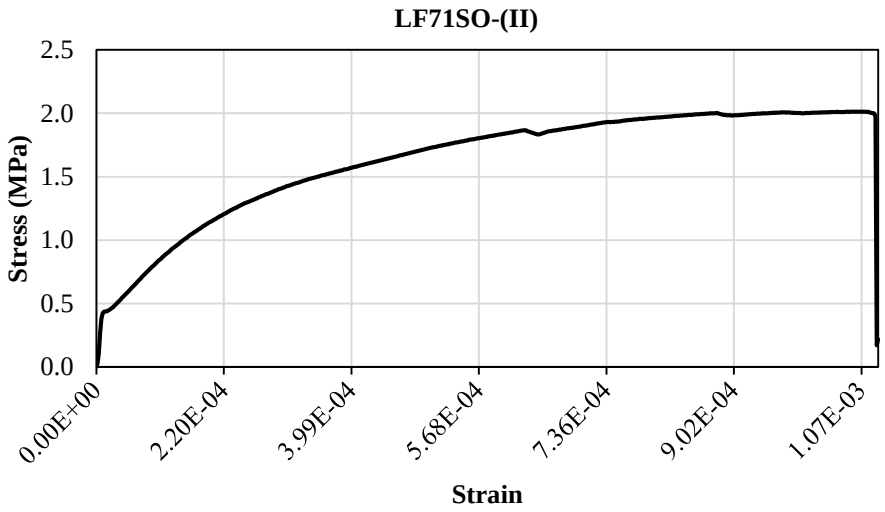

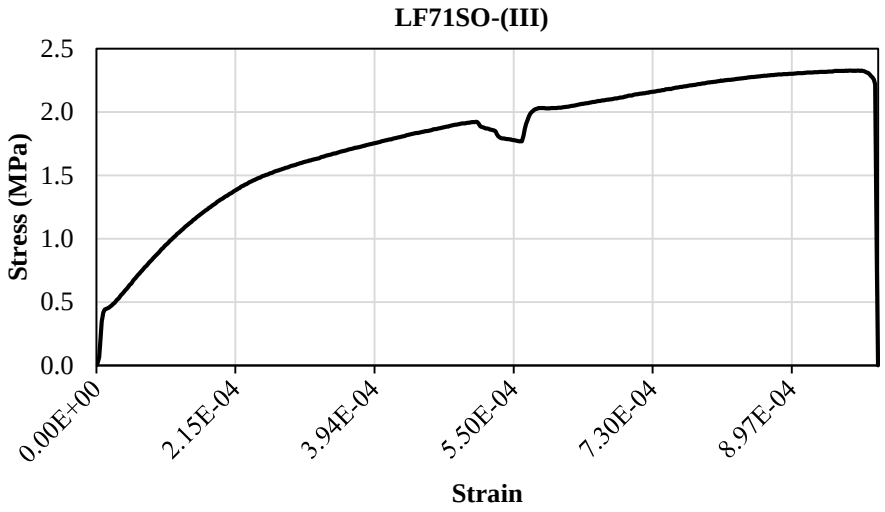

Figure A.1 (continued)

Symbols used:

Aggregate Type: L-Limestone, B-Basalt; Gradation: C-Coarse, F-Fine; AC Type: 57-50/70 Asphalt Grade, 71-71/100 Asphalt Grade; Modification: Z-No Modification, S-SBS Modification; AC Content: O-Optimum, O+- Optimum+0.5, O--Optimum-0.5.

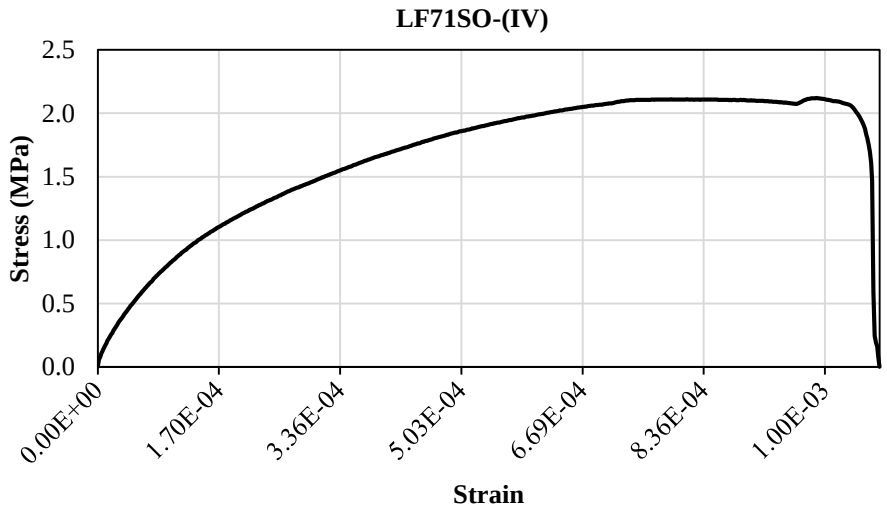

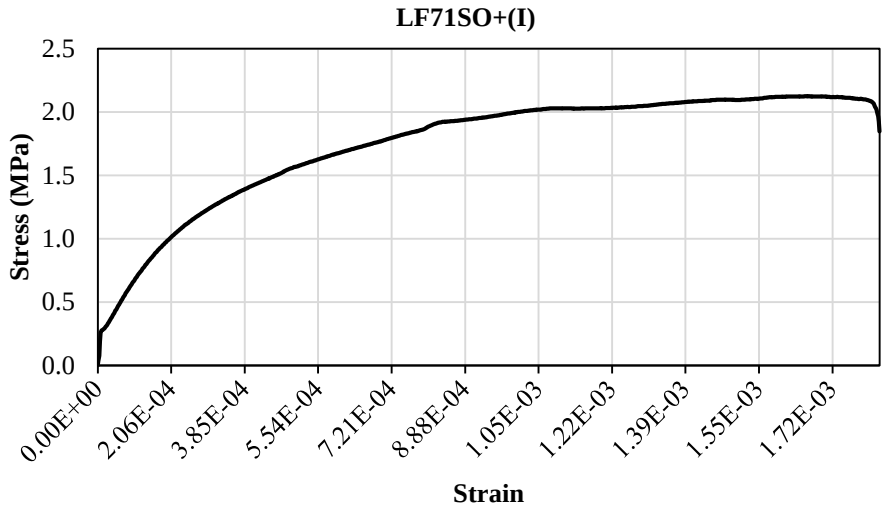

Figure A.1 (continued)

Symbols used:

Aggregate Type: L-Limestone, B-Basalt; Gradation: C-Coarse, F-Fine; AC Type: 57-50/70 Asphalt Grade, 71-71/100 Asphalt Grade; Modification: Z-No Modification, S-SBS Modification; AC Content: O-Optimum, O+- Optimum+0.5, O--Optimum-0.5.

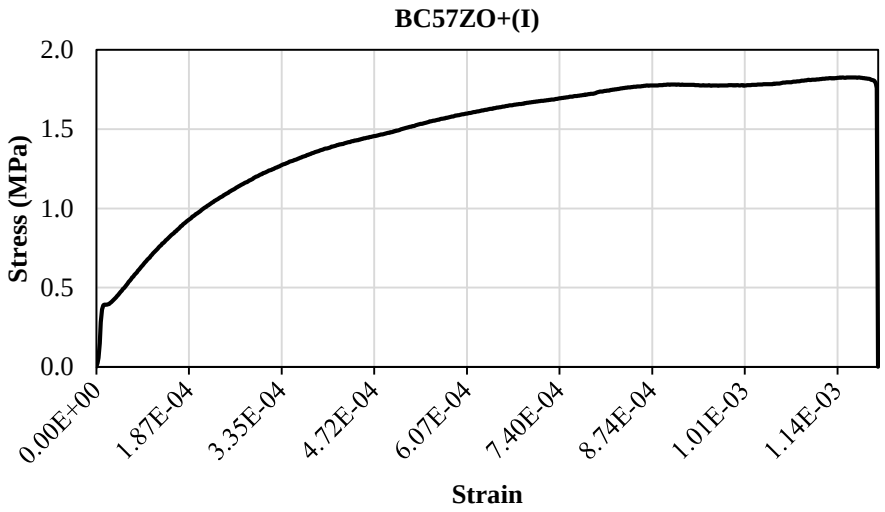

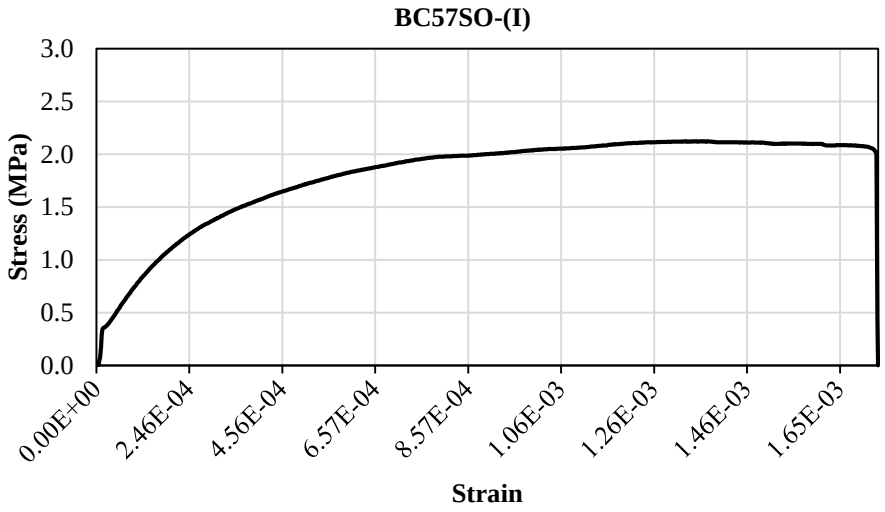

Figure A.1 (continued)

Symbols used:

Aggregate Type: L-Limestone, B-Basalt; Gradation: C-Coarse, F-Fine; AC Type: 57-50/70 Asphalt Grade, 71-71/100 Asphalt Grade; Modification: Z-No Modification, S-SBS Modification; AC Content: O-Optimum, O+- Optimum+0.5, O--Optimum-0.5.

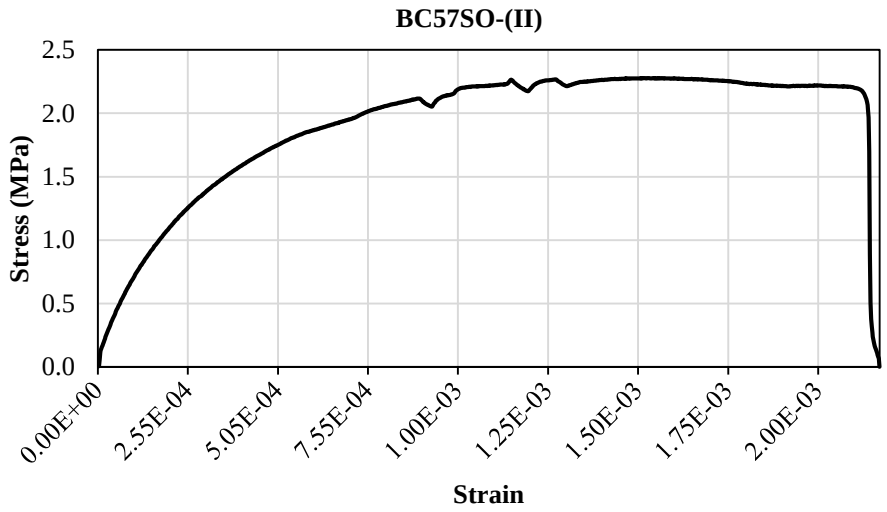

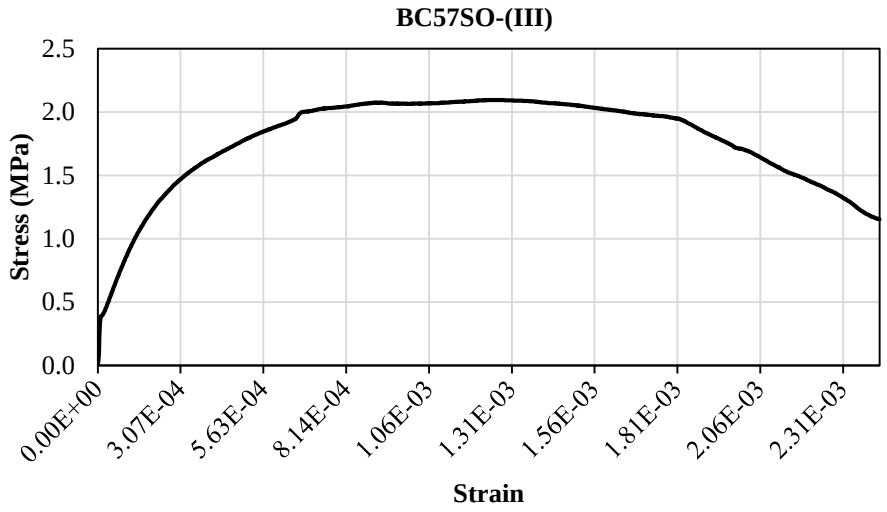

Figure A.1 (continued)

Symbols used:

Aggregate Type: L-Limestone, B-Basalt; Gradation: C-Coarse, F-Fine; AC Type: 57-50/70 Asphalt Grade, 71-71/100 Asphalt Grade; Modification: Z-No Modification, S-SBS Modification; AC Content: O-Optimum, O+- Optimum+0.5, O--Optimum-0.5.

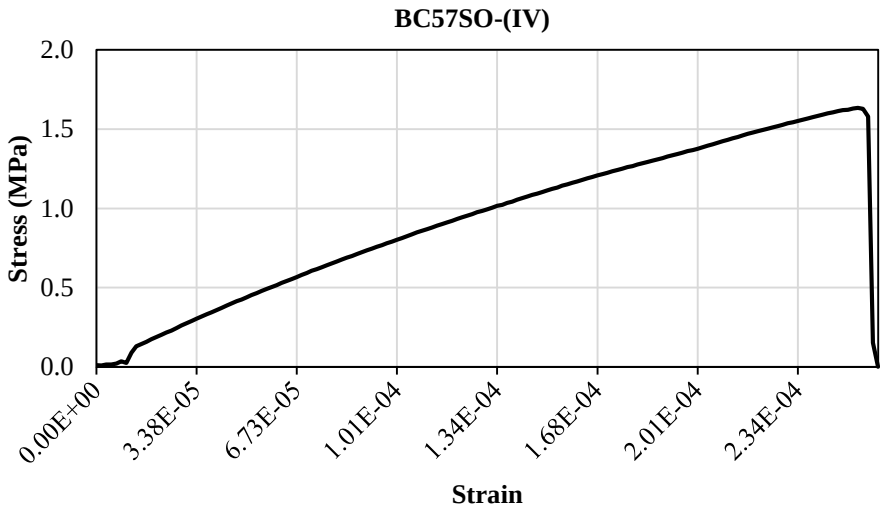

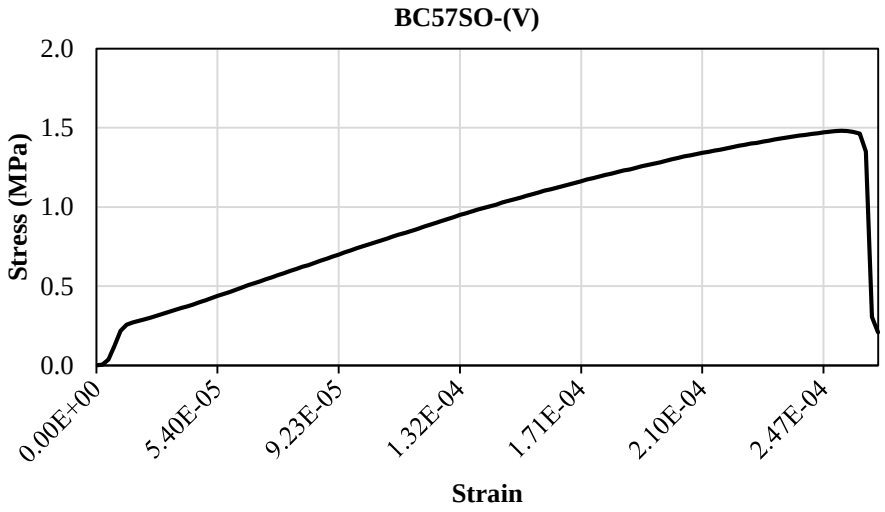

Figure A.1 (continued)

Symbols used:

Aggregate Type: L-Limestone, B-Basalt; Gradation: C-Coarse, F-Fine; AC Type: 57-50/70 Asphalt Grade, 71-71/100 Asphalt Grade; Modification: Z-No Modification, S-SBS Modification; AC Content: O-Optimum, O+- Optimum+0.5, O--Optimum-0.5.

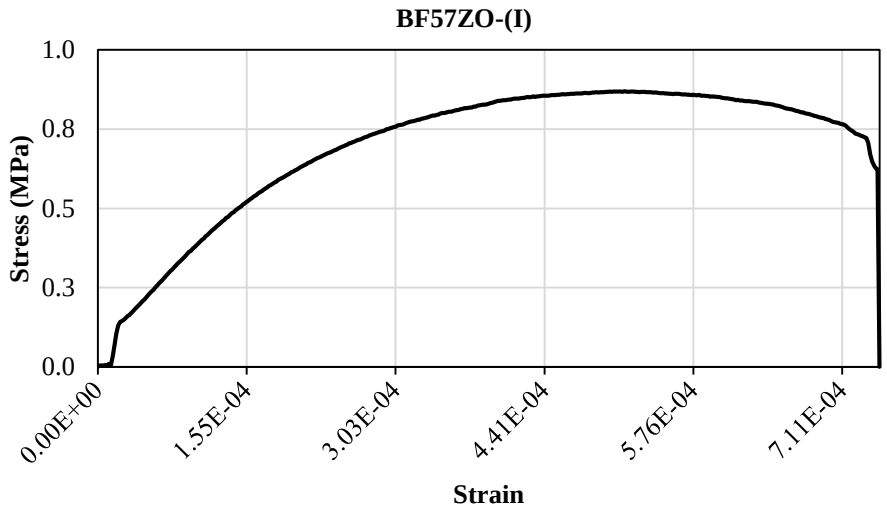

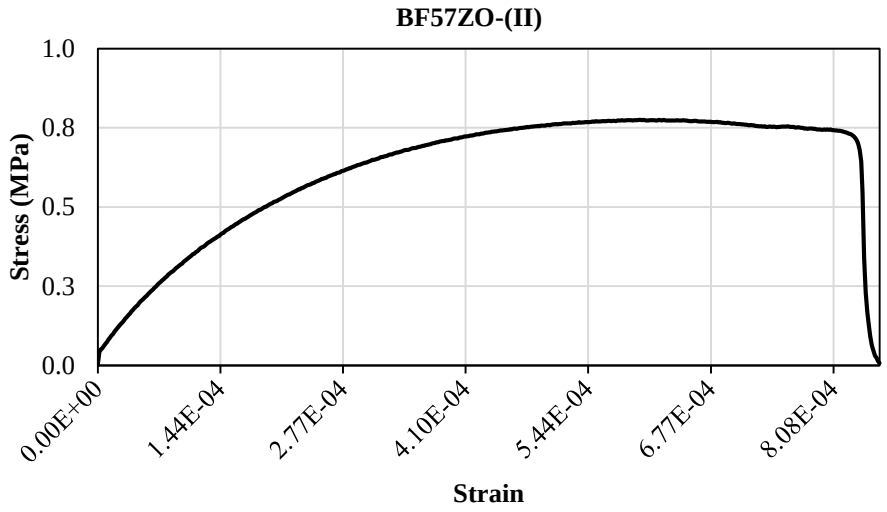

Figure A.1 (continued)

Symbols used:

Aggregate Type: L-Limestone, B-Basalt; Gradation: C-Coarse, F-Fine; AC Type: 57-50/70 Asphalt Grade, 71-71/100 Asphalt Grade; Modification: Z-No Modification, S-SBS Modification; AC Content: O-Optimum, O+- Optimum+0.5, O--Optimum-0.5.

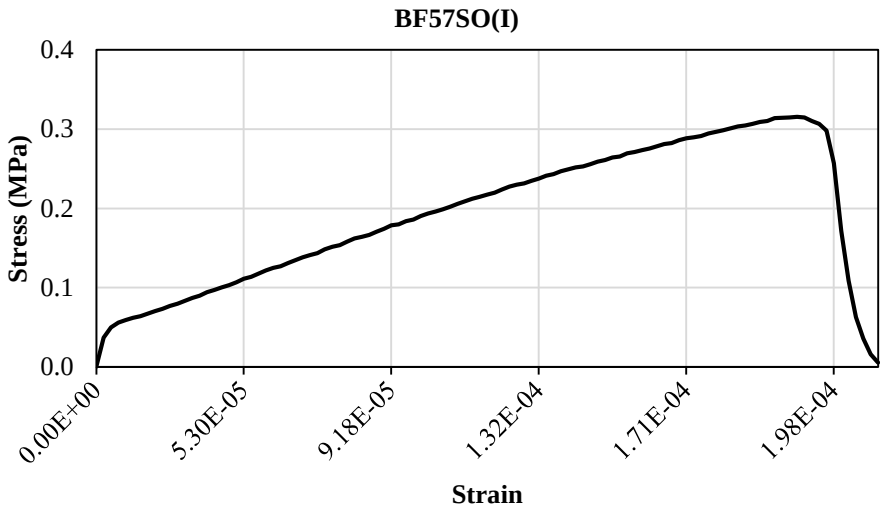

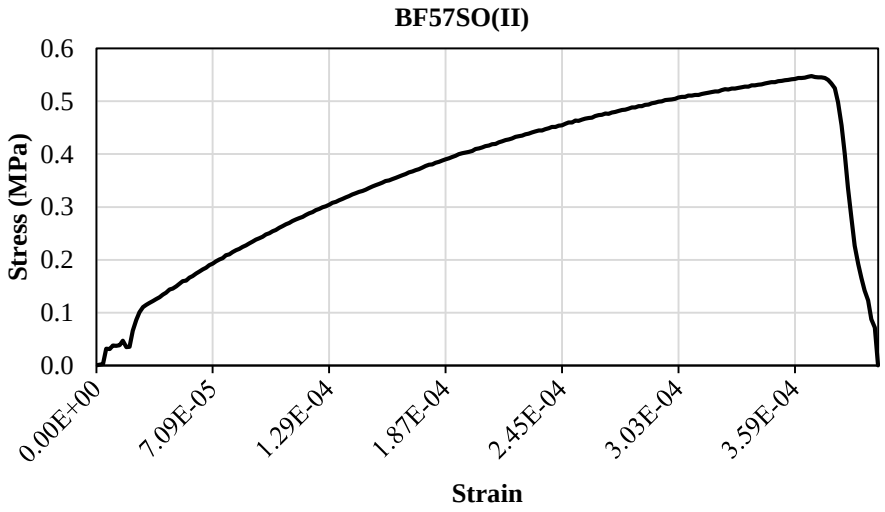

Figure A.1 (continued)

Symbols used:

Aggregate Type: L-Limestone, B-Basalt; Gradation: C-Coarse, F-Fine; AC Type: 57-50/70 Asphalt Grade, 71-71/100 Asphalt Grade; Modification: Z-No Modification, S-SBS Modification; AC Content: O-Optimum, O+- Optimum+0.5, O--Optimum-0.5.

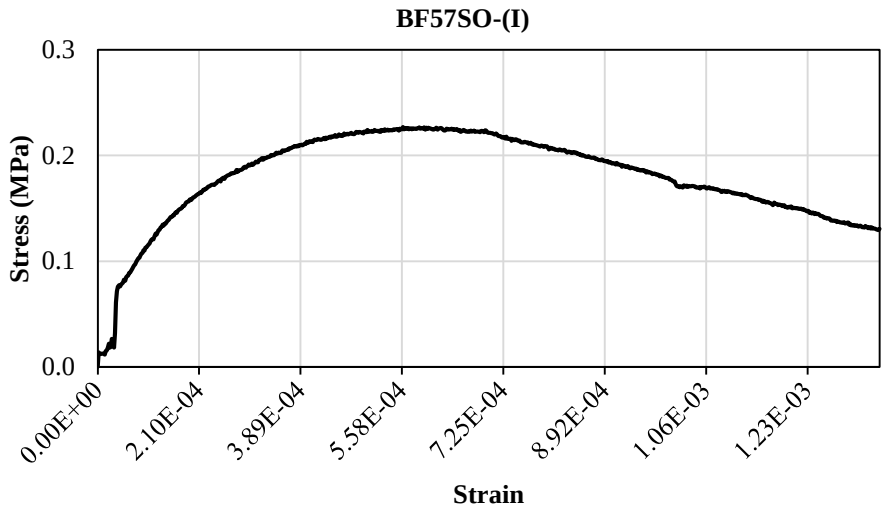

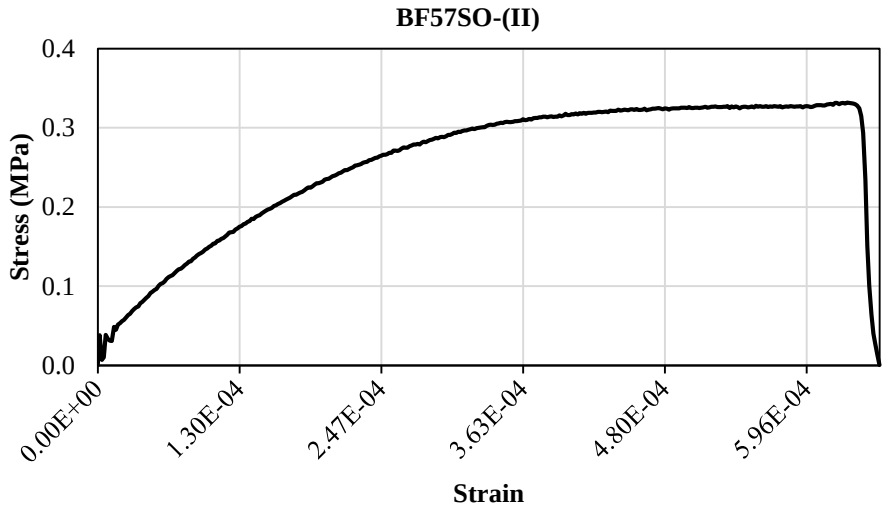

Figure A.1 (continued)

Symbols used:

Aggregate Type: L-Limestone, B-Basalt; Gradation: C-Coarse, F-Fine; AC Type: 57-50/70 Asphalt Grade, 71-71/100 Asphalt Grade; Modification: Z-No Modification, S-SBS Modification; AC Content: O-Optimum, O+- Optimum+0.5, O--Optimum-0.5.

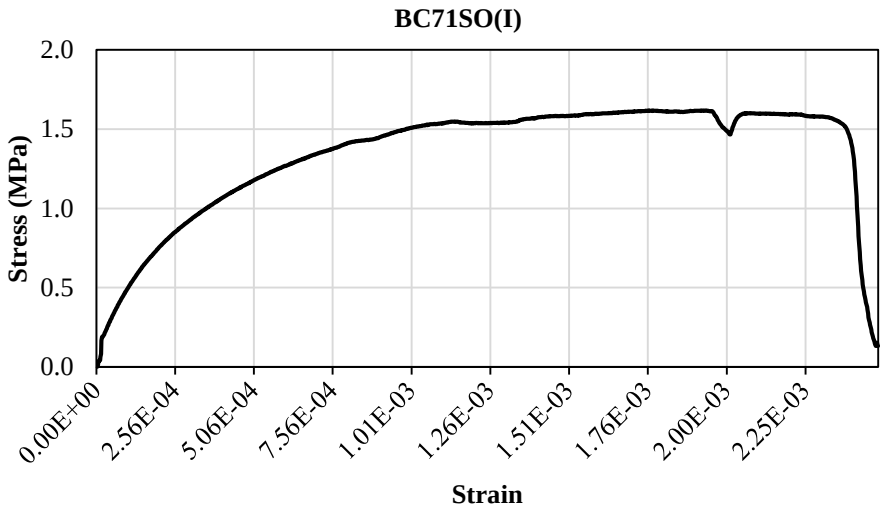

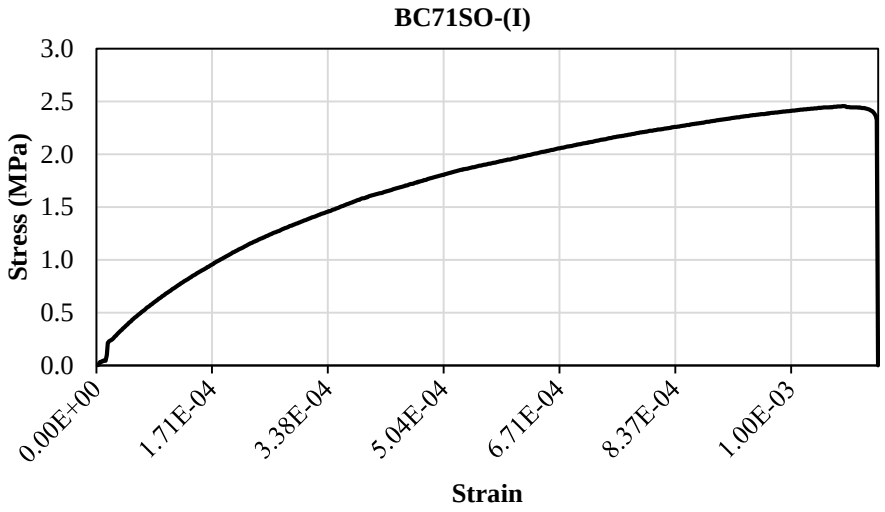

Figure A.1 (continued)

Symbols used:

Aggregate Type: L-Limestone, B-Basalt; Gradation: C-Coarse, F-Fine; AC Type: 57-50/70 Asphalt Grade, 71-71/100 Asphalt Grade; Modification: Z-No Modification, S-SBS Modification; AC Content: O-Optimum, O+- Optimum+0.5, O--Optimum-0.5.

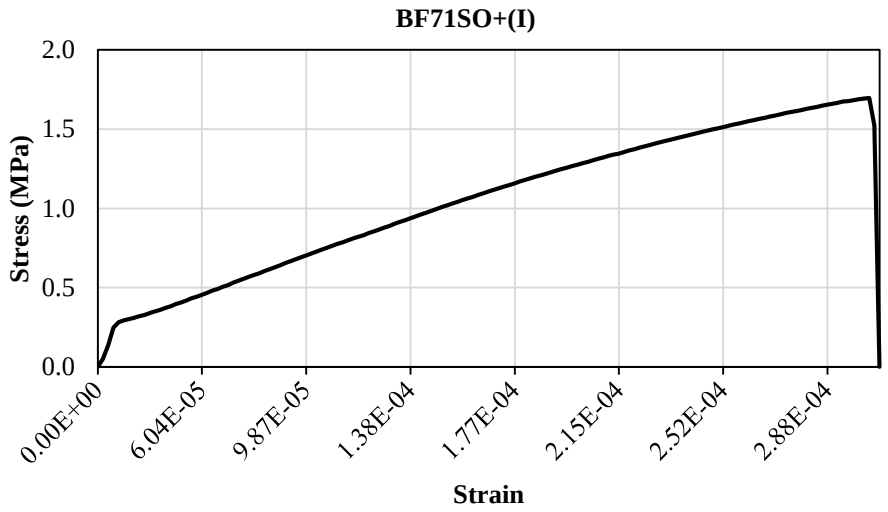

Figure A.1 (continued)

Symbols used:

Aggregate Type: L-Limestone, B-Basalt; Gradation: C-Coarse, F-Fine; AC Type: 57-50/70 Asphalt Grade, 71-71/100 Asphalt Grade; Modification: Z-No Modification, S-SBS Modification; AC Content: O-Optimum, O+- Optimum+0.5, O--Optimum-0.5.

APPENDIX B

THE EFFECT OF DIFFERENT MIX DESIGN VARIABLES ON THE RESPONSES FOR EACH 30 SPECIMENS

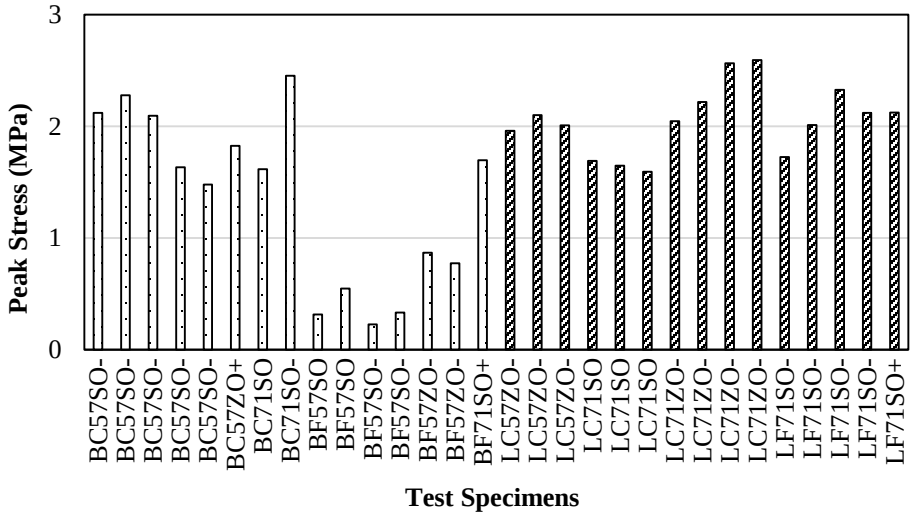

Figure B.1 The measured peak stress values for all the specimens grouped according to aggregate type.

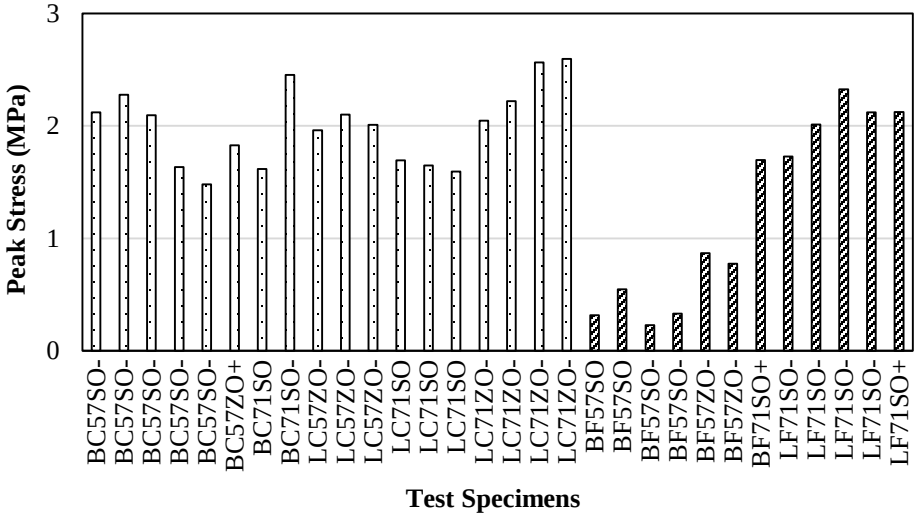

Figure B.2 The measured peak stress values for all the specimens grouped according to gradation.

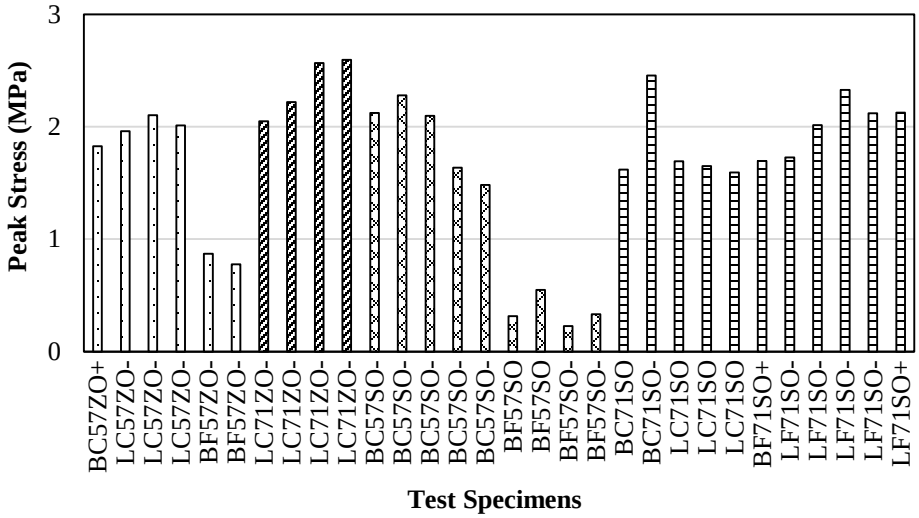

Figure B.3 The measured peak stress values for all the specimens grouped according to asphalt grade.

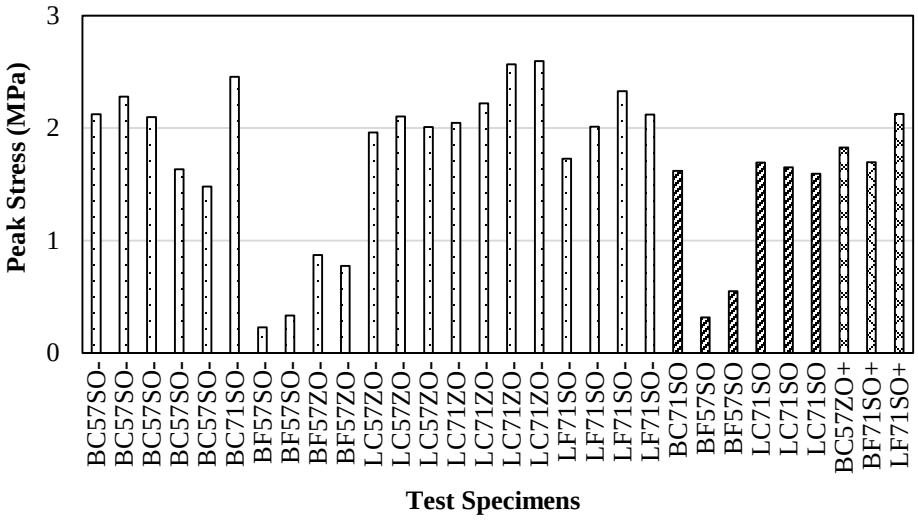

Figure B.4 The measured peak stress values for all the specimens grouped according to asphalt content.

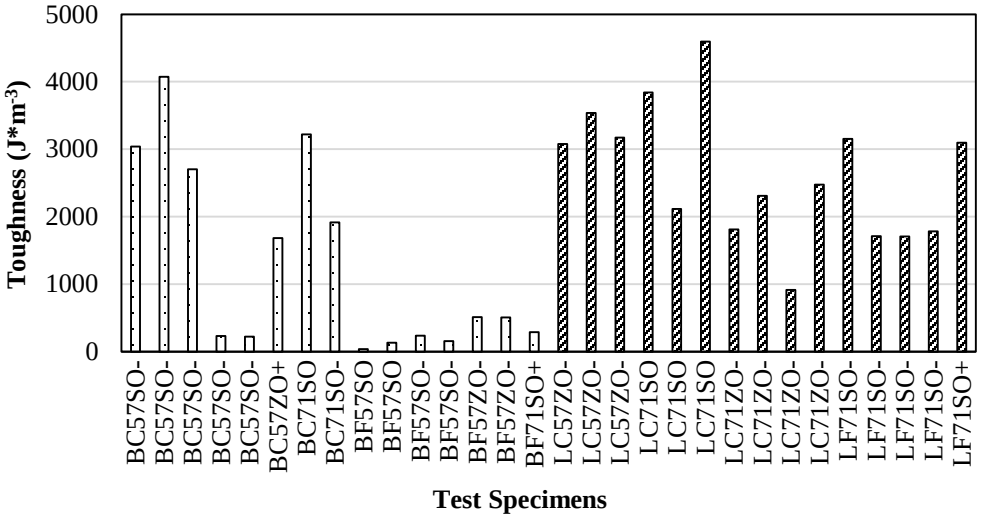

Figure B.5 The measured toughness values for all the specimens grouped according to aggregate type.

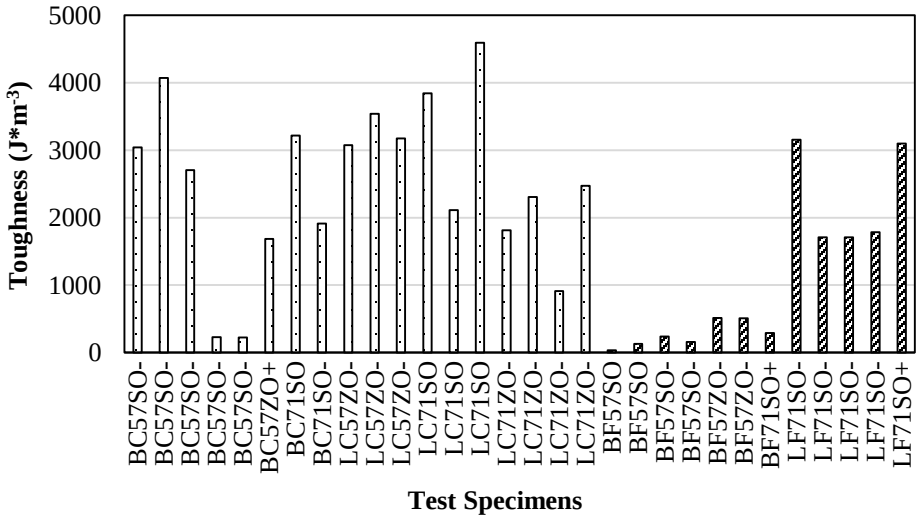

Figure B.6 The measured toughness values for all the specimens grouped according to gradation.

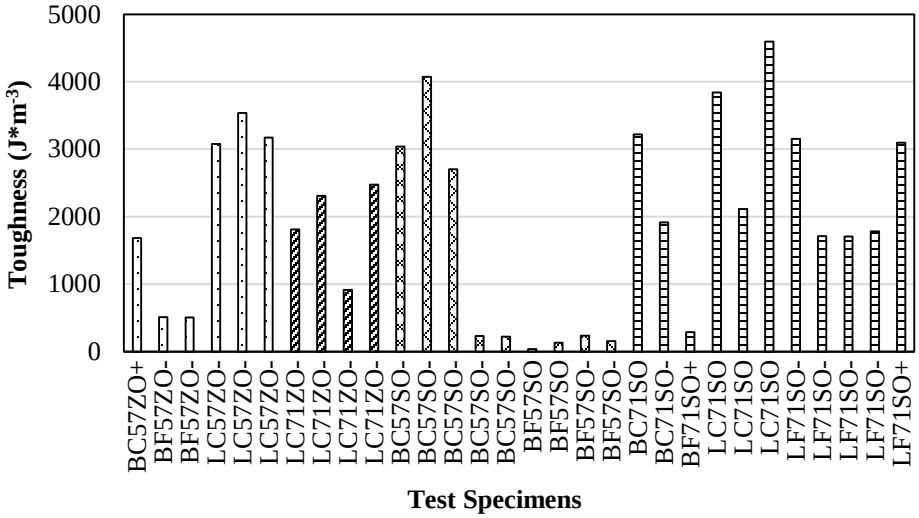

Figure B.7 The measured toughness values for all the specimens grouped according to asphalt grade.

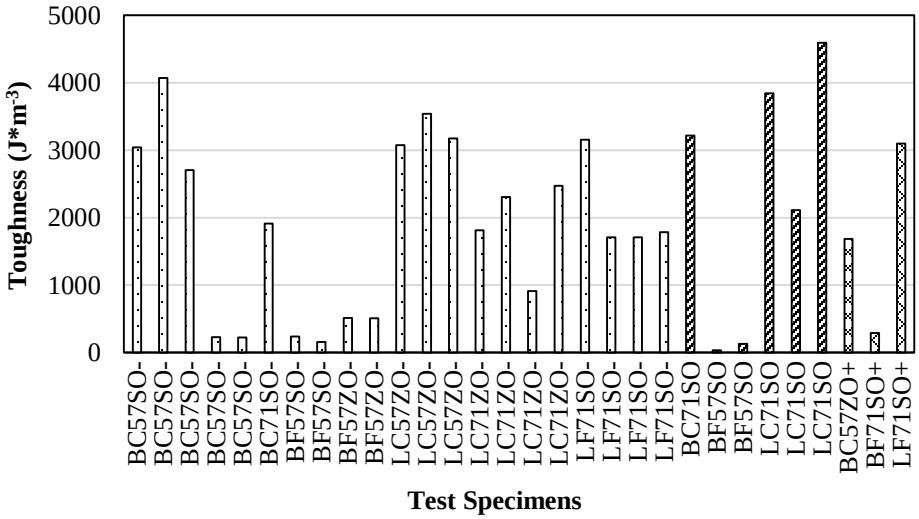

Figure B.8 The measured toughness values for all the specimens grouped according to asphalt content.

Symbols used:

Aggregate Type: L-Limestone, B-Basalt; Gradation: C-Coarse, F-Fine; AC Type: 57-50/70 Asphalt Grade, 71-71/100 Asphalt Grade; Modification: Z-No Modification, S-SBS Modification; AC Content: O-Optimum, O+- Optimum+0.5, O--Optimum-0.5.

APPENDIX C

SOFTWARE MANUALS

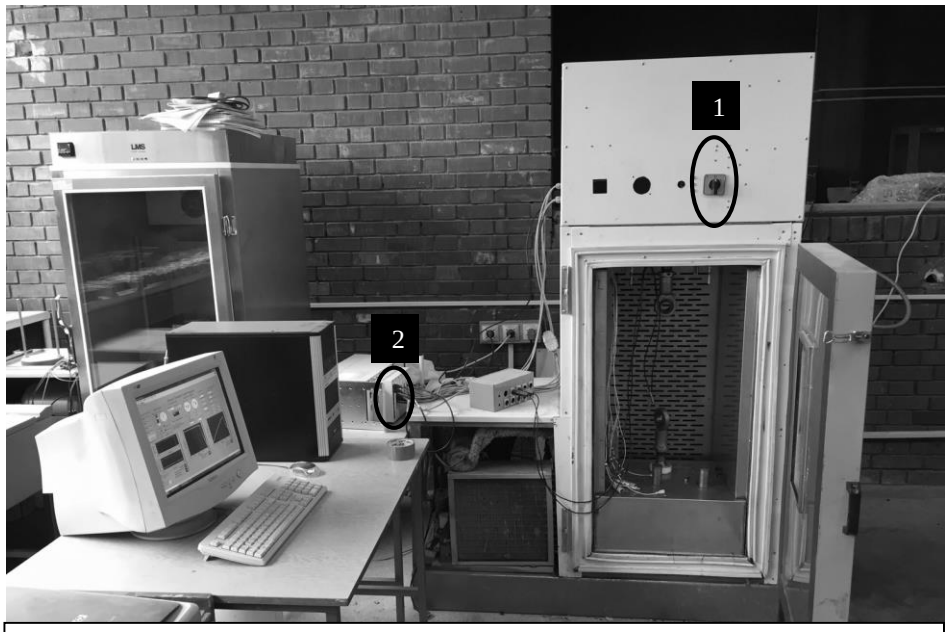

1. First thing is to open the TSRST switch on.
2. For turning on the data acquisition system, press this button.

Figure C.1 Software manuals.

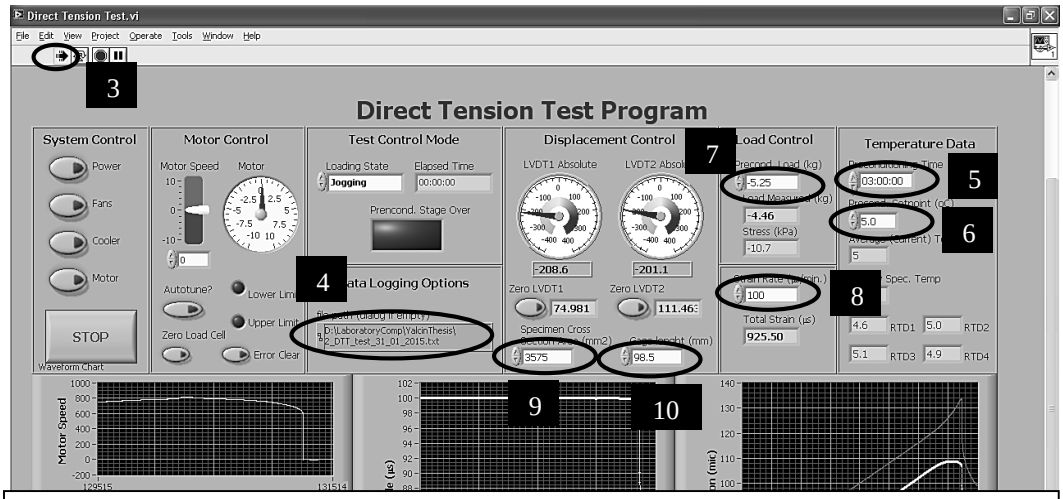

3. Press this button to start the software.
4. Define a destination for the file in which the data will be recorded.
5. Set a time for the pre-conditioning.
6. Set a temperature at which the pre-conditioning will be applied.
7. Set a load at which the pre-conditioning will be applied (Half of the total specimen weight as compressive).
8. Enter the speed of the DTT as strain rate.
9. Input the pre-measured cross section of the specimen that being tested as millimeter square.
10. Input the average length of the steel bars.

Figure C.1 (continued).

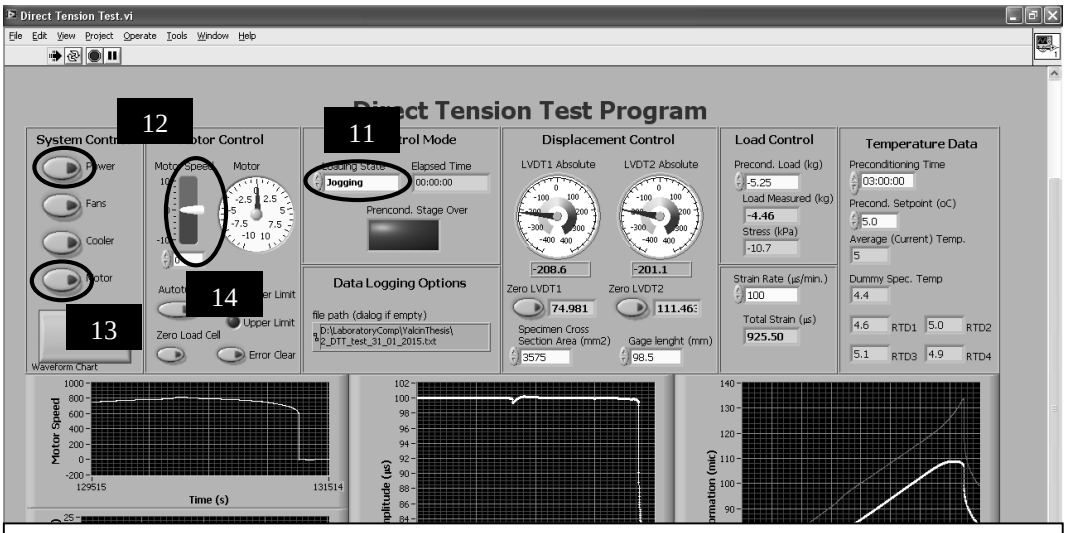

After the step 10, the specimen has to be hanged between the loading bars from the top.
11. Turn the motor into the "Jogging" mode.
12. Press the "Power" button and wait for the second click sound.
13. Turn on the motor.
14. Slide this button to change the speed and the direction of motor rotation, so that you can adjust the distance between the two universal joints. Then, you can connect the bottom plate to the lower universal joint using a pin. In addition you must attach all of the sensors after the mounting stage.

Figure C.1 (continued).

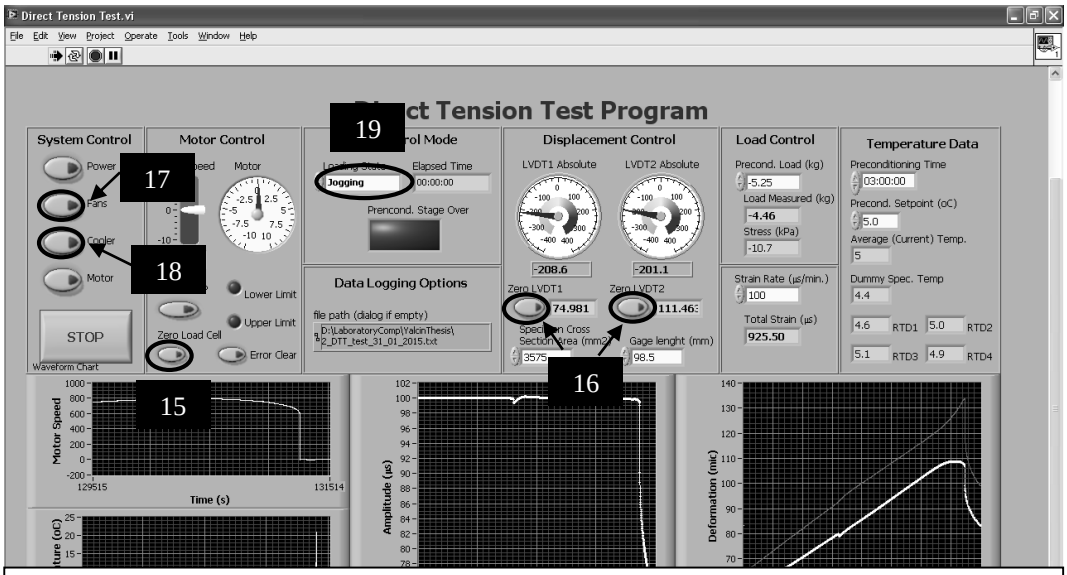

After mounting the specimen and placing all the sensors:
15. Click this button to zero the load cell.
16. Click these two buttons to zero the LVDTs.
17. Turn on the fans by clicking this button.
18. Turn on the cooler by clicking this button.
19. Set the motor to the pre-conditioning mode.

Figure C.1 (continued).

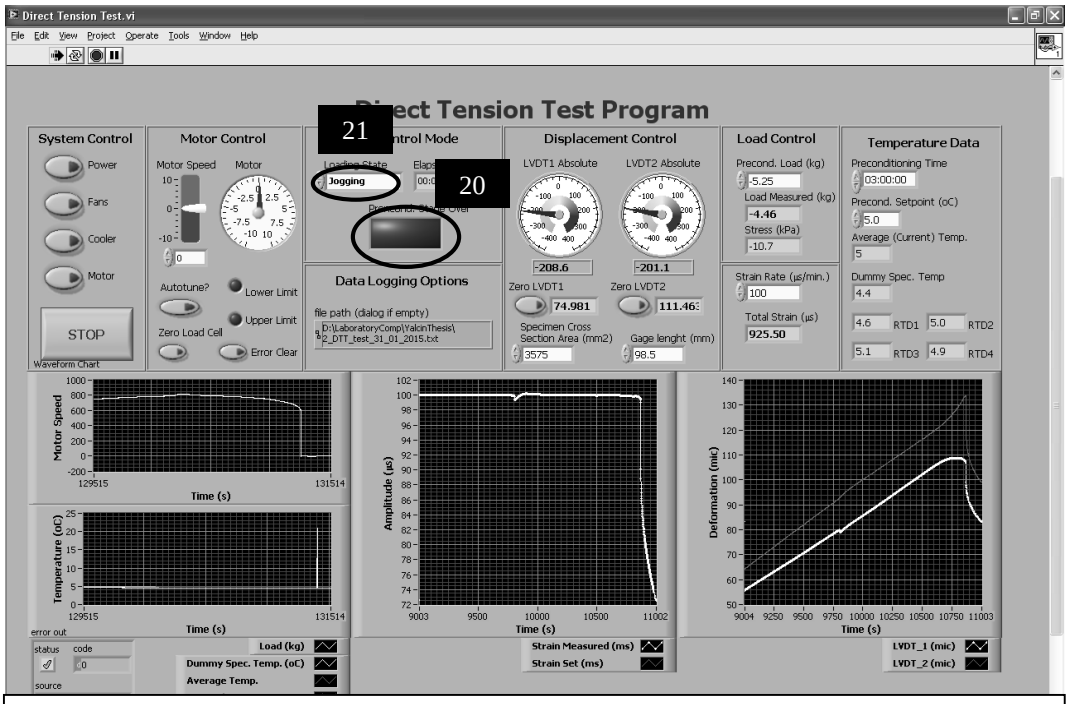

20. When the pre-conditioning stage is over, this green light will start to blink.
21. Set the motor to the "Direct Tension" mode in order to start the experiment.

Figure C.1 (continued).

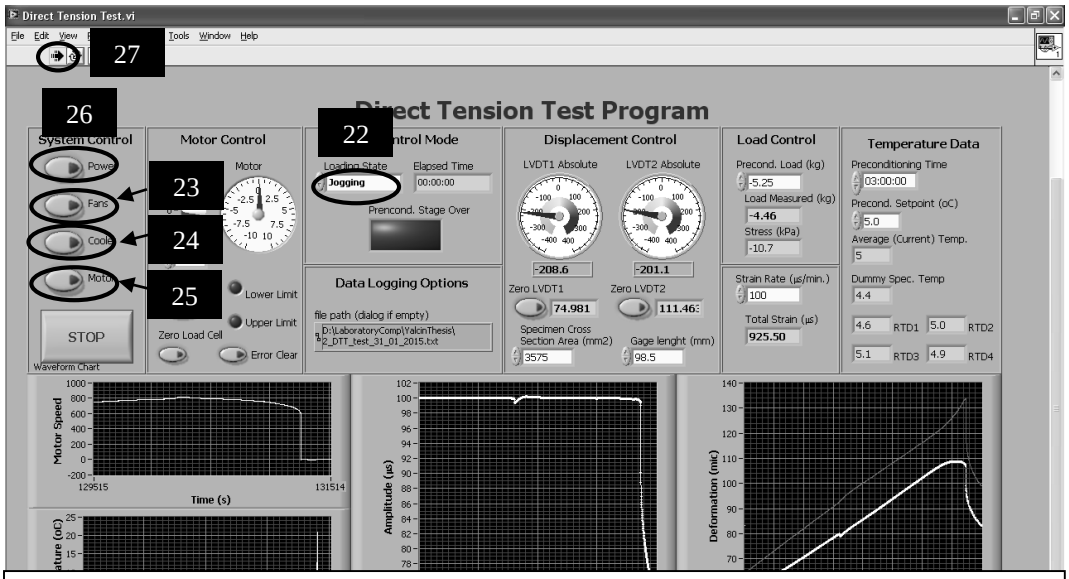

22. Once the experiment finishes turn motor into jogging mode.
23. Turn off the fans.
24. Turn off the cooler.
25. Turn off the motor.
26. Turn off the power.
27. Turn off the software.

Do not forget to turn off the TSRST and data acquisition system after removing the specimen

Figure C.1 (continued).